Czech Technical University in Prague
Faculty of Electrical Engineering

Doctoral Thesis

November 2014 *Michal Vlk*

Czech Technical University in Prague
Faculty of Electrical Engineering
Department of Radioelectronics

A Novel Method of Noise Reduction in the Low-frequency Parametric Amplifier

Doctoral Thesis

Michal Vlk

Prague, *November 2014*

Ph.D.Programme: Electrical Engineering and Information Technology

Branch of study: *Acoustics*

Supervisor: *Doc. Ing. Petr Skalický, CSc.*

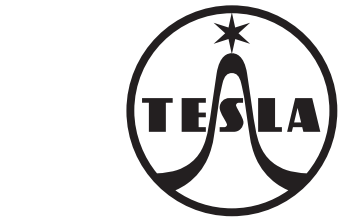

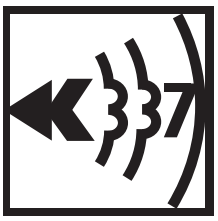

AKADEMIE VĚD
ČESKÉ REPUBLIKY

IG ASCR

Contents

List of Figures

Acknowledgements

I would like to thank several people who encouraged me to white this thesis. In order of time - the oldest first.

- To my first boss Ing. Zdeněk Krumphanzl of TESLA Hloubětín who motivated me to study analogue discrete in-time systems for signal processing based on universal ICs. Measurement systems designed by him were used in the transmitter centres over all the eastern globe.
- To Prof. Zdeněk Škvor who (as former head of the Scientific Council) advised me study at the faculty and answered all my questions on topics of electroacoustics. He served as a real mentor for me since I have met him for the first time.
- To Ass.-Prof. Petr Skalický who let me do laboratory work during my four years at the Faculty
- To Dr. Pavel Hejda- director of the Institute of Geophysics who let me move my laboratory to the Budkov Observatory and work there for the last three years and who encouraged me to finish the work.
- To Dr. Jaroslav Tauer who language edited the thesis
- And to all ladies of my life for realy good food and other good things.

Summary

This thesis concerns low-frequency parametric amplifiers. These systems have been widely used in power electronics since semiconductors replaced it. Today, they are used only in systems where the low 1/f noise corner is the main interest. The schematic diagrams of these systems are still in the style of 1960. Several methods are presented to improve electronic circuits and also the noise property of parametric amplifier circuits and allow using the power of todays personal computers used as data-loggers.

- The method of singular elements can significantly simplify circuit analysis. It gained popularity in the late 1970s because monolithic integrated circuits do not allow coils to be used inside the structure. Here, this method is used as a tool to analyse a simplified circuit of the input amplifier to improve its property as an electronic idler cooling element and to improve its stability.
- Switched MOS power amplifiers with external commutation are discussed and used as a source of the pump signal with wery low output impedance.
- The software radio is used to process parametric amplifier idler signals. Since the idler signal is at intermediate frequency, the system 1/f noise is not affected by the 1/f noise of DC amplifier or A/D converter. A linear envelope detector is used instead of a phase-sensitive detector which eliminates the sensitivity of the spurious phase-drift which occurs in ferroresonant pump circuits and tuned idler circuits.
- Plesiochronnous signal processing is used to eliminate the need of a synchronised oscillator as an A/D converter frequency source if the data sampling rate must be synchronised to the global time - source.

The use of these techniques is illustrated on two case studies: high-frequency condenser microphone and second harmonic fluxgate.

Résumé

Práce pojednává o zlepšení šumových vlastností nízkofrekvenčních parametrických zesilovačů. Tyto systémy byly používány před nástupem polovodičů ve výkonové elektrotechnice, v současné době se používají jen v systémech s velkými nároky na 1/f šum. Obvodová řešení takových systémů se od šedesátých let mnoho nezměnila. V práci předkládám několik přístupů k modernizaci obvodových schémat, které by zlepšily parametry a umožnily využít výkonu současné výpočetní techniky v roli akvizičního systému.

- Metoda singulárních elementů, která dovoluje výrazně zjednodušit analýzu zejména idealizovaných obvodů, dosáhla maxima své popularity v sedmdesátých letech dvacátého století z důvodu masového nástupu analogových monolytických integrovaných obvodů, které nemohou mít ve své struktuře skutečné cívky. Zde je tato metoda použita pro syntézu vstupního zesilovače speciálních vlastností - tedy nefiltračního obvodu.

- Spínané výkonové zesilovače osazené tranzistory MOS s vnějšími komutačními obvody ve spojení s oscilátorem s velkou fázovou čistotou umožňují snížit vliv budicích obvodů na celkový šum soustavy jednak zmenšením tlumicího odporu a jednak zvětšením reaktančního výkonu pumpovacího zdroje.

- Digitální zpracování signálu na kmitočtu idleru umožňuje využít optimalizací známých v konsturukci mezifrekvenčních zesilovačů a odstranit vliv 1/f šumu A/D převodníku.

- Plesiochronní zpracování signálu umožňuje použít volně běžící oscilátor bezprostředně u A/D převodníku, což zjednodušuje konstrukci a snižuje fázový šum hodin převodníku.

Použití těchto technik je ilustrováno na dvou studiích: vysokofrekvenčním kondenzátorovém mikrofonu a indukčnostním magnetometru.

Preface

This thesis is based on the research started in 2005 in the former "Division of AM transmitters" of the TESLA company the purpose of which was to construct a new type of power stage for solid-state transmitters. After dissolution of the division in 2007, the author continued in developing switched power amplifiers for different applications: for applications in low-frequency parametric amplifiers, used as non-electric quantity sensors - microphones as a full-time Ph.D. student in the Department of Radio-electronics of the Faculty of Electrical Engineering of the Czech Technical University in Prague (FEE CTU). During this time, the analogue part of the capacitor bridge with preamplifier was improved using semi-symbolical methods of circuit analysis and synthesis of the circuits with nullators and norators. The results of this method is circuit diagram of capacitor microphone whose functiality was proved by laboratory sample. The main idea of this design (damping of the capacitor bridge by reactance feedback) was granted a national patent. On finishing the full-time Ph.D. studies in 2011, the author joined the Geomagnetic Department of the Institute of Geophysics of the Academy of Science of the Czech Republic (IG ASCR), and continued with the application of the switched PA and special low-noise preamplifiers for the magnetic amplifier used in measuring the geomagnetic field: triaxial fluxgate. The result of the work, carried out during period is the variometer, used as hot-swap equipment with the possibility of 1Hz data output. This variometer is based on a spare set of NAROD ring-core fluxgate coils which were left intact and, therefore, the design is very conservative.

Introduction

This doctoral thesis should be called “Variation on a Topic by Radeka”, because Radeka (1974) used the synthetic resistor in a low-noise circuit about forty years ago. Synthetic elements are not widely used in modern constructions, although vintage electroacoustic equipment is full of it (i.e. the first high-quality tape recorder TELEFUNKEN K7 of the 1940s). Now nearly forgotten. These circuits cannot be divided into parts with voltage input and voltage output; they must be analysed as a whole. The method of singular elements, developed in the early 1970s as a filter synthesis tool in the electr(on)ic circuit theory, may be applied to semi-symbolical analysis of not only the said electronic circuits, but also to a wider class of circuits used as electrical analogies of acoustic system sand to transduction phenomena themselves in their naturally non-linear form (used as the base for parametric amplification). Electro-acoustics, which historically describes the system through borders of acoustical - mechanical - electrical domains, will be expanded to describe the system through broads of electrical - magnetostatical domain to describe magnetic amplifier in the form of the fluxgate sensor. The magnetic amplifier is studied here not only as a model of data processing of a high-frequency digital microphone. It is also studied as an example of describing the coupling of electrical systems via on principle non-linear magnetostatic system. And this system is studied and treated in the same way as an electro-acoustic system. The author believes that the electro-acoustic approach can be used in future for amplifiers at the molecular level - MASERs. The circuits presented in the thesis are based on long-term experimental works and the described circuits are the best which the author has found for the given application.

The purposes of this study are:

1. The application of the method of singular circuit elements to solving problems of special linear circuits used to improve the noise property of low-frequency parametric amplifiers which are difficult to replace by other technologies.

2. The application of the method of software radio to solving problems of processing signals digitised at the idler frequency, which leads to solving problems with 1/f noise of A/D converters.

3. The application of switched solid-state power amplifiers to lower noise dragged to the pumping circuit of low-frequency parametric amplifiers.

4. The application of the method of plesiochronous data acquisition to solving problems of the metastable state in buffered UNIX-based loggers.

1 Electronic Circuits

1.1 Linear noiseless electronic circuits

Assume electronic circuit as a closed graph of twopoles. Each standard twopole (fig. 1.1) can be described as an operational function[1] of the circuit variable.

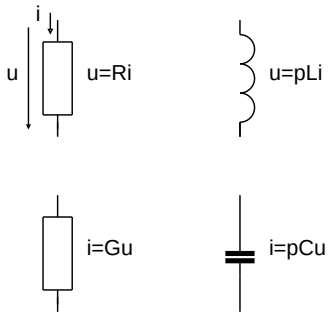

Figure 1.1: Standard circuit elements

It is natural to enlarge the set of twopoles by two singular elements: the norator and nullator (fig. 1.2). This allows us to deal with active and passive multibranches via its equivalent schemes.

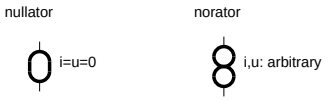

Figure 1.2: Singular circuit elements

In this thesis we shall use exclusively the method of circuit determinant. This method allows us to concentrate circuit algebraics at one point, which finds correspondence between the circuit graph and mathematical formula. This correspondence is generally known as ‘the circuit determinant’. The method is simple for passive electric circuits and has been known since nineteenth century due to Feussner (1904). For graphs with singular elements, rules are not so straight (Parten, 1972) Author decided to use a non-direct method to obtain the circuit determinant based on the extended sparse tableau.

The network (fig. 1.3) is a set of nodes $\mathcal{N}$ and branches $\mathcal{B}$

Node represents a volume of infinite conductivity. Practically, it is a metallurgic connection of circuit elements. The branches represent circuit elements. In real electronic circuits, there are elements with two wires (diodes), three wires (triodes), etc. We shall limit ourselves only to two-wire linear elements: regular - impedances and singular - nullators and norators (Vágó, 1985). The singular elements occur in the circuit in pairs (nullator-norator) called

[1] Product of operator p creates with summation so called convolution ring. It is natural generalisation of the Ohm's law for reactive elements. See (Yoshida, 1984)

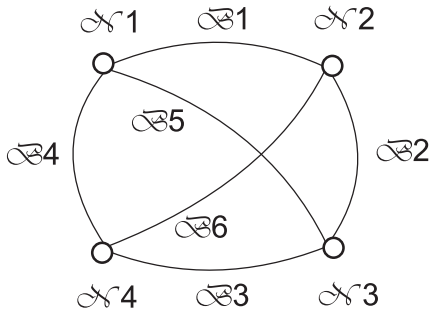

Figure 1.3: Graph of the circuit

nullors. This does not means that every particular nulator is paired with a particular norator, but only that the numbers of nullators and norators are the same. The network with branches on which elements are placed on is called a circuit (fig. 1.4).

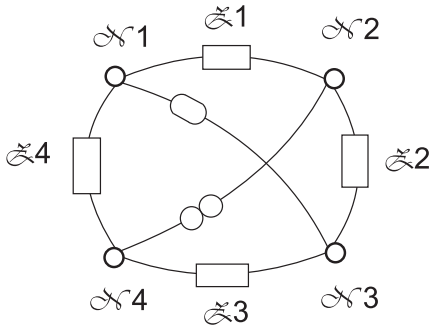

Figure 1.4: Electronic circuit

Singular elements have the interesting property that Kirchhoff voltage and current laws hold in the circuit outside them (fig. 1.5). This fact can be useful in setting up equations of the lumped circuits including non-linear elements and nullors (Moos, 1983) or in the future for solving very general distributed networks, which have nullors in an infinitesimal part of the circuit - nullor fields. This kind of system can be extremely useful in analysing of microwave systems.

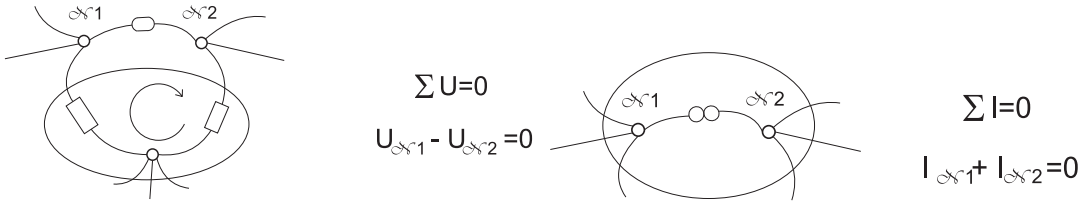

Figure 1.5: Properties of singular elements

Mapping from the set of elements to the set of nodes of the circuit is called the incidence matrix. We will use an oriented incidence matrix (Guillemin, 1953). The orientation of the matrix will be established artificially so that the node with the higher number of one branch has the plus sign. Also the node with the lowest number (reference node) will vanish from the matrix. We shall introduce the convention that the elements in the incidence matrix are ordered as regular first, then nullators and last the norators.

The incidence matrix of the circuit in fig. 1.4 is:

$$\begin{bmatrix}\mathbf{A}_r & \mathbf{A}_0 & \mathbf{A}_8\end{bmatrix} = \begin{bmatrix}1 & -1 & 0 & 0 & 0 & -1\\ 0 & 1 & -1 & 0 & 1 & 0\\ 0 & 0 & 1 & 1 & 0 & 1\end{bmatrix} \tag{1.1}$$

The extended sparse tableau can be created from the incidence matrix and circuit elements in the folowing way:

$$\begin{bmatrix}\mathbf{1} & \mathbf{0} & \mathbf{0} & \mathbf{0} & \mathbf{0} & \mathbf{0} & -\mathbf{A}_r^T\\ \mathbf{0} & \mathbf{1} & \mathbf{0} & \mathbf{0} & \mathbf{0} & \mathbf{0} & -\mathbf{A}_0^T\\ \mathbf{0} & \mathbf{0} & \mathbf{1} & \mathbf{0} & \mathbf{0} & \mathbf{0} & -\mathbf{A}_8^T\\ \mathbf{0} & \mathbf{0} & \mathbf{0} & \mathbf{A}_r & \mathbf{A}_0 & \mathbf{A}_8 & \mathbf{0}\\ \mathbf{0} & \mathbf{1} & \mathbf{0} & \mathbf{0} & \mathbf{0} & \mathbf{0} & \mathbf{0}\\ \mathbf{0} & \mathbf{0} & \mathbf{0} & \mathbf{0} & \mathbf{1} & \mathbf{0} & \mathbf{0}\\ \mathbf{Y} & \mathbf{0} & \mathbf{0} & \mathbf{Z} & \mathbf{0} & \mathbf{0} & \mathbf{0}\end{bmatrix} \begin{bmatrix}\mathbf{U}_b & \mathbf{I}_b & \mathbf{U}_n\end{bmatrix} = \begin{bmatrix}\mathbf{0}\\ \mathbf{0}\\ \mathbf{0}\end{bmatrix} \tag{1.2}$$

Here $\mathbf{Y}$ and $\mathbf{Z}$ are diagonal matrices of regullar circuit element imitances. (Whether element have impedance operational model, corresponding element in admittance matrix is 1). The determinant of the sparse tableau is the determinant of the circuit graph (Fakhfakh, 2012). Using of the sparse tableau instead of the other methods, i.e. the admittance matrix, has the advantage that it exists for every circuit. This is very important in analysing simplified circuit where other methods, i.e. numerical solving in SPICE software, fail or need additional elements (usually resistors) to converge. Another advantage of the sparse tableau is that every tableau cell contains no more than one element. It simplifies programming this method. The author's program in ANSI-C language for symbolical solution of circuits using this method is listed in Appendix B. Resulting formulas can be manipulated by any computer algebra system to more convenient form of " low-entropy " (Vorperian, 2002) which deals with using operator "parallel" $A\|B = \frac{1}{\frac{1}{A}+\frac{1}{B}}$ if possible. Using this operator with the simple formula tell us how the formula can be realized with the circuit.
Let us clarify this method on analysing of the simple oscillator in fig. 1.6.

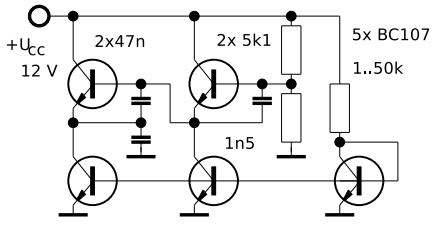

Figure 1.6: Two-transistor oscillator

A simple model of the transistor can be treated as one nullator - norator pair with transconductance (fig. 1.7). In reality, transistor transconductance depends on the actual DC current flowing through the device. A model, in which the transconductance has a fixed value $g_m \approx 40 I_c$ is said to be linearized.

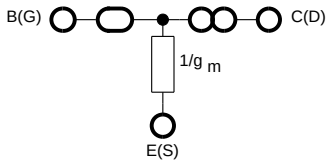

Figure 1.7: Simple linear transistor

When we redraw this scheme in fig. 1.6 with the linearized model of the transistor, we get an AC linearized model of the oscillator (fig. 1.8).

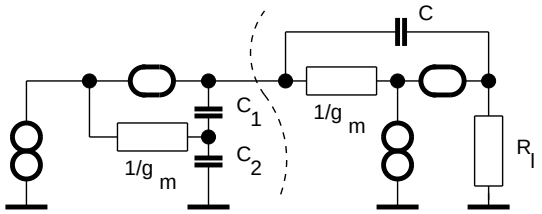

Figure 1.8: Linearized oscillator

We can split this circuit into the left and right part, and analyse the input impedance of the two parts separately. The input impedance (Braun, 1990) of the circuit in the branch we are interested in is the ratio of two determinants, where the numerator determinant contains this circuit with the added parallel connection of the nullator and norator to the branch we are dealing with, and the denominator determinant contains this circuit without change.

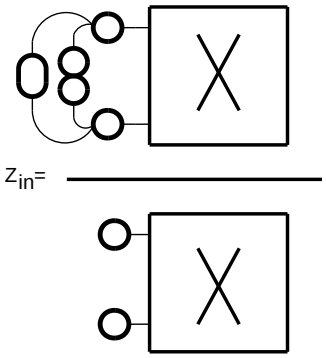

Figure 1.9: Input impedance

The input impedance of the left part is:

$$Z_{inl} = \frac{1}{p(C_1 \| C_2)} + \frac{g_m}{p^2 C_1 C_2} \tag{1.3}$$

Which can be understood as a series combination of a capacitor and "Double capacitor" or "Frequency-Dependent Negative Resistor" (Gouriet, 1950) with impedance:

$$Z = \frac{1}{p^2 D} \tag{1.4}$$

The input impedance of the right part is:

$$Z_{inr} = \frac{1 + \frac{1}{pR_l C}}{\frac{1}{R_l} + \frac{g_m}{pR_l C}} \tag{1.5}$$

If the second term in the numerator is small enough, the formula simplifies to:

$$Z_{inr} = R_l \| \frac{pR_l C}{g_m} \tag{1.6}$$

which can be understood as a parallel combination of a resistor and inductor.

Since there is no problem in converting parallel to series circuits at one frequency of interest, it is possible to convert $R + D$ to $R \| D$. The equivalent circuit then has one of the following forms:

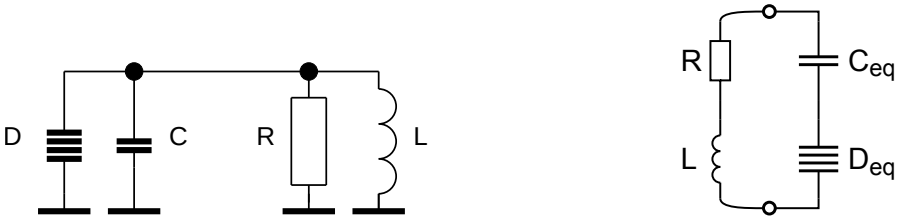

Figure 1.10: Two forms of resonant circuit

and the condition of oscillation is the Thomson rule:

$$LC = RD = \omega^{-2} \tag{1.7}$$

Due to the elementary property of operational calculus:

$$p^2 = -\omega^2 \tag{1.8}$$

The circuit has become an oscillator, but despite the schematic diagram in fig.1.6 does not look like an oscillator, because there is no easily visible feedback. But deeper analysis can find it. We can see that this structure can be easily formed by the parasitic elements in amplifiers. Practical construction problems, connected with parasitically formed synthetic elements, are often solved by ad-hoc methods which result in suboptimal performance.
The circuit in the right-hand part of fig. 1.10 can be used with an ordinary inductor: this produces Colpitts oscillator. Since the Thompson rule prescribes the quality of the inductor, this kind of oscillator woks well at high frequencies. At lower frequencies it is better to use a series LC circuit instead of pure L. This kind of oscillator is called Gouriet (1950) oscillator. If the oscillator has to be retuned in a wide range, i.e. one octave, two additional capacitors are added to form a Vackar (1960) circuit:

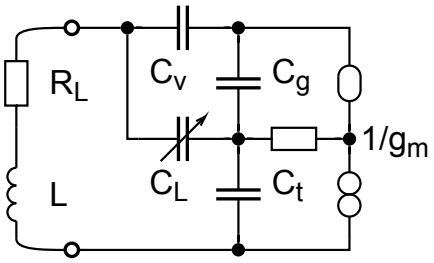

Figure 1.11: Vackar oscillator

The input impedance (seen by the inductor) of Vackar circuit is:

$$Z_{in} = \frac{1}{p(((C_v \| C_g) + C_L) \| C_t)} + \frac{g_m}{p^2 C_L C_g C_t (C_L \| C_g \| C_v)} \tag{1.9}$$

Ideal operational amplifiers can be modelled as an grounded nullator - grounded norator pair [1] Circuit with operational amplifier (Fig. 1.12) can be redrawn to nullator/norator model in Fig. 1.13.

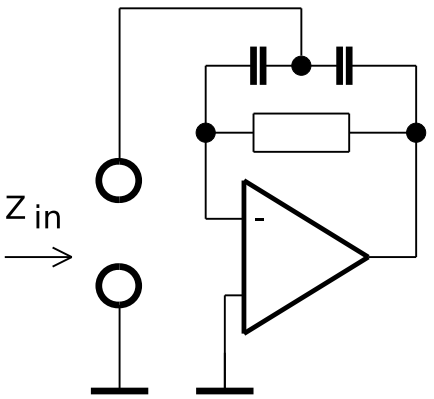

Figure 1.12: Leaky FDNR realisation with operational amplifier

[1] Model of operational amplifiers with floating nullator are used sometimes. It leads to false opinion, that plus and minus terminals of operational amplifiers can be swapped and this false opinion is taken as "proof" that using of singular elements has no sense. Let us have follower with swapped input terminals.

Nullator - norator model leads to negative impedance converter, which assumes output impedance of the circuit with normal operational amplifier negative and then unstable.

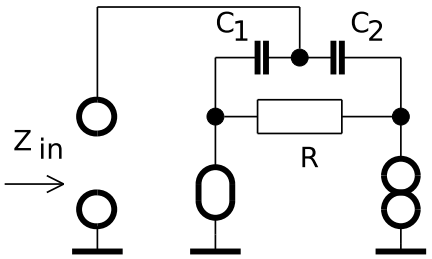

Figure 1.13: Model of leaky FDNR

Its input admittance is:

$$Y_{in} = p(C_1 + C_2) + p^2 RC_1C_2 \tag{1.10}$$

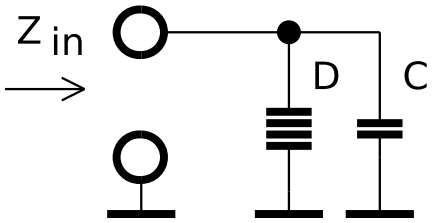

Figure 1.14: Leaky FDNR

By substitution ($s = 1/p$) in 1.10 and transformation ($Y' = sY$) in fig. 1.12 we get different circuit with input admittance:

$$Y_{in}^{'} = (C_1 + C_2) + RC_1C_2/s \tag{1.11}$$

This circuit represents ideal inductor with parallel leak resistor. This device will be used as basic building block of the filter - amplifier in the fig. 3.31. [1].

1.2 Noise in electronic circuits

Theory of circuit noise has a background in thermodynamics. Here it is claimed, that noise power in a circuit in thermodynamic equilibrium is a absolute function of its thermodynamic temperature and frequency. The power on resistor is $P = 4kT$ [2] and then:

$$\overline{u^2} = 4kTR \qquad \overline{i^2} = 4kTG \tag{1.12}$$

where $k = 1.3804410^{-23}$ J/K is the Boltzmann constant, T[K] is the thermodynamic temperature and R[Ohm]/G[S] is the resistance / conductance of the element. If the resistor

[1] Operational amplifiers are multistage amplifiers and their stability is determined by internal frequency compensation, usually by simple "dominating" pole. Parts used in this work (OP07, OP27, TL072) are compensated to unity gain and feedback network must achieve this unity in limit of HF frequency. The simplest way to achieve this is to add small capacitor between output and inverting input of the amplifier. In the circuit discussed above, this condition is granted when high-quality capacitors are used in the feedback network (TGL33965, F&G KSM 4G , Electel KS50). These parts uses polystyrol (styroflex) film with indium metallurgical contacts and are not suitable for SMT. To solve this problem, manufacturers developed parts where this capacitor is part of its internal structure (OPA211, AD 797)

[2] In the microwave circuits quantuum correction must be also included.

is not in thermodynamic equilibrium, - i.e. the direct current is flowing through it, or, the resistor is not a physical device, but the property of some active element, equations 1.12 does not hold and we must include the technological noise factor γ (Dementjev, 1963), which is frequency dependent, usually by this rule (Motchenbacher et al., 1973):

$$\gamma(f) = \gamma_0 \left[1 + \frac{F_1}{f} + \left(\frac{f}{F_2} \right)^2 \right] \tag{1.13}$$

Equations 1.12 then becomes:

$$\overline{u^2} = 4kT\gamma(f)R \qquad \overline{i^2} = 4kT\gamma(f)G \tag{1.14}$$

The specification of γ for resistors is not a catalogue parameter (Vlk, 1-2005). It is known that for the resistors $\gamma_0 = 1$. The catalogue value of the resistor (as a device) is the so-called Noise Index:

$$NI = \frac{u_{nd}}{U_{dc}} \text{ [V/V/dec]} \tag{1.15}$$

Here u_{nd} is the additional noise voltage in one frequency decade and U_{dc} is the DC voltage at the resistor terminals. In practice, a value six orders higher is used:

$$NI = \frac{u_{nd}10^6}{U_{dc}} \text{ [}\mu\text{V/V/dec]} \tag{1.16}$$

Or in logarithmic units:

$$NI_{dB} = 20 \log_{10} \left(\frac{u_{nd}}{U_{dc}} 10^6 \right) \text{ [dB]} \tag{1.17}$$

Since the spectral density of the $1/f$ noise is:

$$\overline{u^2}(f) = \frac{K}{f} \tag{1.18}$$

The noise power between two frequencies will then be the integral of the formula above:

$$\overline{u^2}(f_1 ... f_2) = K \ln \left(\frac{f_2}{f_1} \right) \tag{1.19}$$

Since the catalogue values of NI are in decades, the ratio of frequencies is 10 and:

$$\overline{u^2}(\Delta f) = 2.303K \tag{1.20}$$

The spectral density of the resistor $1/f$ noise is then:

$$\overline{u^2} = \frac{NI^2 U_{dc}^2}{2.303f} \tag{1.21}$$

At the corner frequency, the value of the thermal and $1/f$ noise equals:

$$\frac{NI^2 U_{dc}^2}{2.303f} = 4kTR \tag{1.22}$$

If we assume that the low-frequency corner is the parameter of voltage at the resistor, we set:

$$F_1 = \phi U_{dc}^2 \tag{1.23}$$

And get:

$$\phi = \frac{NI^2}{9.212kTR}[\text{Hz/V}^2] \tag{1.24}$$

If we start with catalogue values, it is better to use the simplified formula:

$$\phi = \frac{10^{\frac{NI_{dB}}{10}}}{3.69 \cdot 10^{-8} R} \tag{1.25}$$

The noise indices of resistors of some technologies depend slightly on the resistor value. Since computing the noise factor includes division by the resistor value it may be possible that the noise factor ϕ of resistors of different values made with the same technology may have a smaller span. Typical noise of manufactured resistors is shown in the graph 1.15:

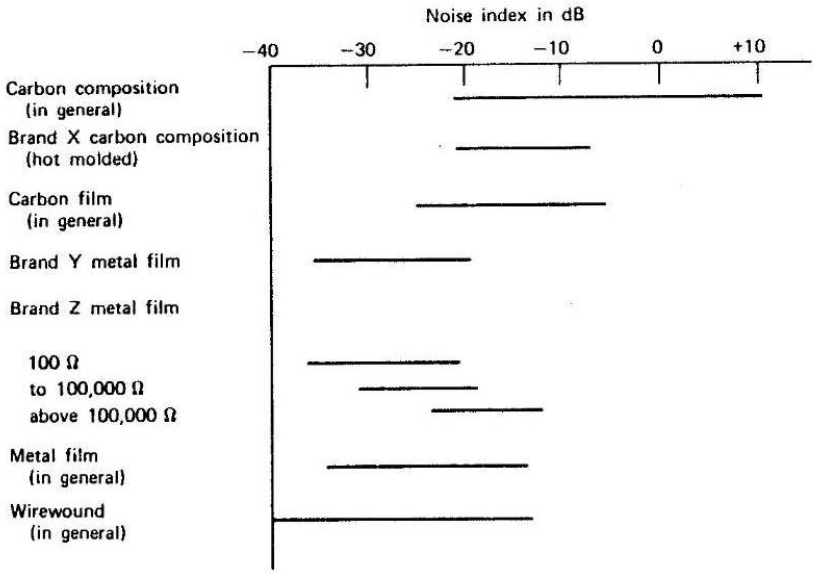

Figure 1.15: Noise of resistors (Motchenbacher et al., 1973)

The noise parameters of active circuits are slightly more complicated. The situation can be simplified by using a unilateral model in fig. 1.16, which has the same topology for all active devices, only the parameters of the devices change somewhat.

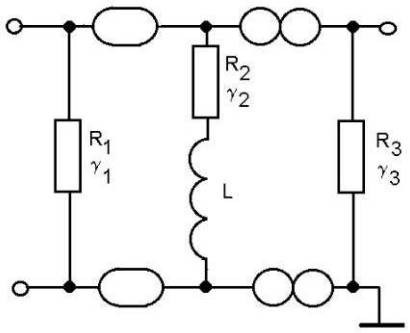

Figure 1.16: Noisy active element

Note that when the left-down input node is grounded, the nullor down transforms into short. The operational amplifier is the only element where this node has sense, otherwise, it is grounded. The next table (Vlk, 1-2005) summarizes the noise properties of several electronic devices. The values there are only for illustration, and precise values must be computed in every case for given DC operating point of the device from the catalogue data. Since modern devices are designed to shape transfer characteristics to a given purpose, i.e. linear or logarithmic amplification, theoretical formulas do not hold exactly for them.

Element	R_1	γ_1	R_2	γ_2	L	R_3	γ_3
Triode	$\frac{0.1}{I_g}$		$\frac{1}{K\sqrt[3]{I_a}}$	2.5		$\frac{1}{g_s D}$	
Pentode				$\frac{2.5+20I_s/S}{1+I_s/I_a}$			
JFET			$\frac{U_p}{2\sqrt{I_{ds}I_d}}$	0.66		$\frac{K}{\sqrt{I_d}}$	
BJT	$\frac{\beta}{40I_c}$	(0.2)	$\frac{1}{40I_c}$	(10)		$\frac{U_e}{I_c}$	
NE5534	$5 \cdot 10^4$	1.8	0.12	$6.8 \cdot 10^3$	$38 \cdot 10^{-6}$	$3 \cdot 10^3$	

Operational amplifier is described by model similar to the model of simple transistor. The only difference is that resistances of the equivallent circuit have very high noise factor in both input[1] and transconductance elements [2] These devices are not generaly suitable for input stages of ultra low noise amplifiers[3].

1.3 Low-noise electronic systems

A slightly simpiler circuit is a little more interesting.

[1] Input circuit of modern bipolar operational amplifiers are normally of "bias cancellation" type, what serves as an bootstrap. Hence, input impedance is made greater at the cost of input noise current enlargement (OP27)

[2] Transcon noise factor is determined by the input stage current. This can be modified in some types of "programmed" operational amplifiers (LM381)

[3] Recent advances in the semiconductor technology reduced low-frequency noise corner of so-called video operational amplifiers to infrasonic band. Example of this part is LME49990. These parts are not suitable for general using in low-noise audio - frequency systems, mainly because special grounding methodology (ground - plane layout) is recommended by the manufacturer, what is in contradiction with normally used star grounding Ott (1976). When these parts are used in non-appropriate layout, UHF frequency oscillations may occur. They can be detected sometimes by measurement of DC power consumption of the part and using human finger as "damping volume", or (better) by using HF voltmeter with random-sampling head i.e. HP3406.

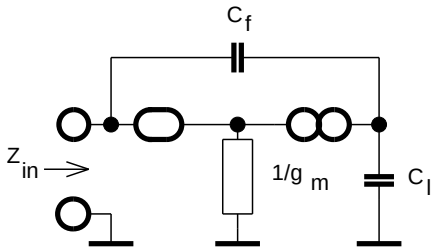

Figure 1.17: Amplifier

The input impedance of this circuit has the form:

$$Z_{in} = \frac{1}{p(C_l \| C_f)} \| \frac{C_f + C_l}{C_f g_m} \tag{1.26}$$

This is the parallel combination of resistor and capacitor. Let us see how noisy this resistor is. One description of noise in electronic circuits originates from the so-called technological noise quotient γ. This constant tell us how the element differs in noise temperature from the ordinary resistor:

$$\overline{i_n^2} = 4kT\gamma GB \tag{1.27}$$

Since electronic systems are not in thermodynamic equilibrium, this quotient tell us how the noise power of the "electronic resistor" differs from that of the resistor (the resistor can not exists as a device) in the thermodynamic equilibrium. To calculate how the noise factor of the synthetic element differs from the noise factor of the real element requires performing the energetic sum of current noises of all amounts from the noisy circuit elements. The situation in this case is simple: we have only one noisy element in the circuit, transistor transadmittance g_m. We must determine the current transfer from g_m to the input synthetic resistance. The current transfer computation can be transformed to input impedance computation by adding several circuit elements:

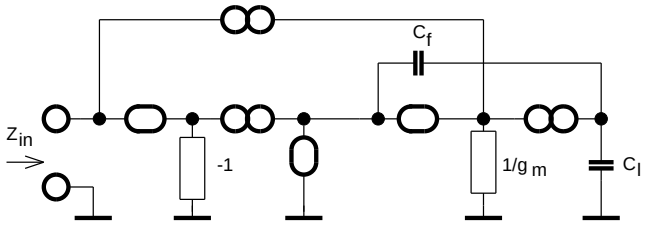

Figure 1.18: Current transfer to impedance circuit

After computation, the current transfer yields:

$$Z_{in} = \frac{C_f}{C_f + C_l} \tag{1.28}$$

The noise current at the input reads:

$$\overline{i_n^2} = (\frac{C_f}{C_f + C_l})^2 4kT\gamma_m g_m B \tag{1.29}$$

But the value of the input real conductance:

$$g_m' = \frac{C_f}{C_f + C_l} g_m \tag{1.30}$$

Comparison with formula 1.27 yields:

$$\gamma' = \gamma \frac{C_f}{C_f + C_l} \tag{1.31}$$

One can see, that the noise factor decreased by a large amount. If the noise factor is smaller than one, it has the same effect as cooling the circuit to a lower temperature, we may refer to it as electronic cooling (or cooled termination). Practically we are limited by other noise sources and also system headroom and cooling under $1/10$ of the ambient temperature has no sense.
As an example of practical application of this topology, the author describes the simple phonograph pick-up amplifier.

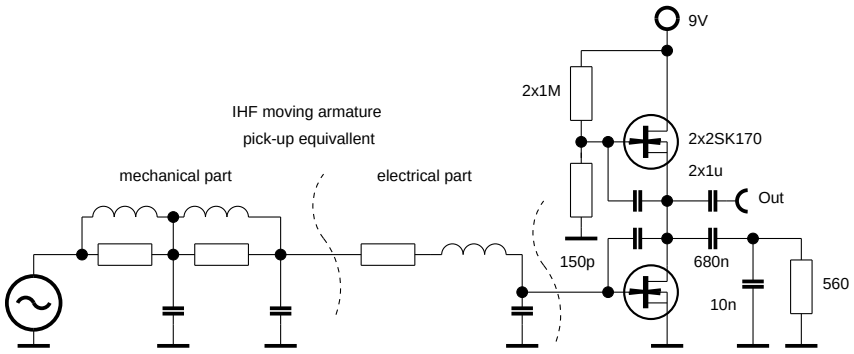

Figure 1.19: Pick-up amplifier

The moving armature pick-up (in the form of a moving magnet or moving permalloy cross) is the most common in low-end HiFi vinylite record players. The problem of this design are two resonances which lie in the higher part of the acoustical band due to the resonance of the needle with its gymbal and the groove material (Miller, 1950). These two mechanical resonances can not be damped from the electrical side. The only thing that can be done is to maintain the electrical resonance properly damped to linearize the overall frequency response. Damping the impedance by simple shunt resistor degrades noise performance of the system in the high-frequency part of the audio band (Sýkora, 1990). Sýkora used parallel resistance feedback to achieve cooled termination; his circuit in minimal form has three operational amplifiers. Our circuit is much simpler, it uses a single dynamically loaded transistor stage. This stage is loaded with a shunt RIAA corrector. This forms an integrator in the high-frequency band where cooled termination of the pick-up is needed. Enlarging of the Miller transistor capacity allow us to set the input resistance at the prescribed value.

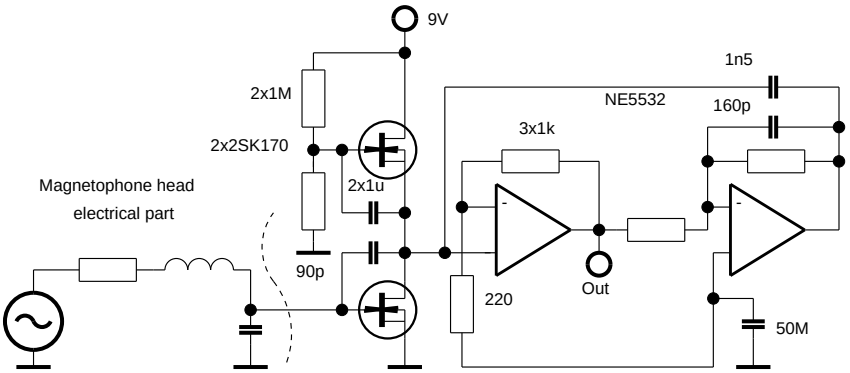

Figure 1.20: Tape-recorder preamplifier

It is possible to realise the loading capacitor via a feedback circuit. This solution is advantageous for tape-recorder preamplifier where the noise has a different character, and bad transient - intermodullation distortion (Otala, 1972) of the operational amplifier is not an issue.
Using cooled termination in baseband amplifiers is not as advantageous than using it in amplifiers which use amplification at pure reactance - parametric amplifiers.

1.4 Parametric Amplifiers

The basic form of the parametric amplifier (PARAMP)[1] used in the microwave frequency range has the form of one branch. This one branch is realised as a non-linear capacitor (varactor diode) to which pumping power (normally higher than amplified frequency) is coupled, and which has resonant loading at combinational frequencies of pump and signal of higher frequencies (so-called idlers). Input and output waves are decoupled by circulator.

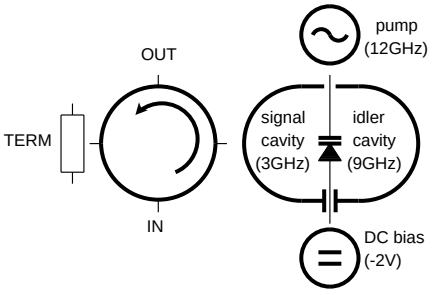

Figure 1.21: HF PARAMP

The theoretical behaviour of these circuits depends only on the energy conservation law, and is independent of their nonlinearity shape (Manley, 1956). It also holds that the reactance power rises with frequency which means that gain is proportional to the pump-to-signal frequency ratio. Microwave amplifiers have now been mostly replaced by HEMT transistor

[1] Mathematical tool for analysis of the parametric systems is Mathieu (1868) equation in form: $\ddot{y} + (a + 16q\cos 2x)y = 0$. Electronic systems are nonlinear- simply described by Van der Pol (1927) equation for oscillator with limited output amplitude in form: $\ddot{y} - \mu(1 - y^2)\dot{y} + y = 0$. Real parametric amplifier can be described by proper combination of both equations like this: $\ddot{y} - \mu(1 - y^2)\dot{y} + (1 - ry^2)(a + 16q\cos 2x)y = 0$

stages and there are only a few niches where survives i.e. radar input amplifiers (PARAMPs withstand high input overload)

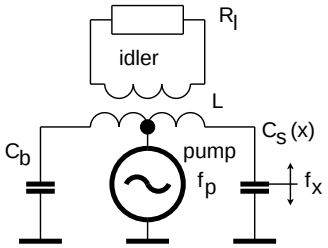

Figure 1.22: LF PARAMP

Low-frequency PARAMPs are now used exclusively for measuring DC and baseband non-electrical quantities such as distance (micrometer, seismometer, microphone, Atomic Force Microscope) or magnetic field (fluxgate or fluxset magnetometer, direct cross current meter). Another application is railway track circuit (Macoun, 1971) where high overload immunity is needed. Since lumped realisation of circulators leads to hybrids, it is better to use symmetrical configuration whenever possible.
Another common feature of LF PARAMS is, that the output signal lies outside the input band (in the so-called idler band). This has several advantages. The signal is not degraded by further down-conversion from idler to base frequency. The signal can be separated using a filter. The signal can be relatively in the narrow band and not in the base band, which simplifies the next stage that has the form of an IF amplifier with all its optimisations. Since damping with the idler band defines the bandwidth, using of the cooled termination enlarges the signal bandwidth without degrading the noise properties of the system.
Fig. 1.22 clearly indicates, that the only resistance in the circuit is the idler termination resistor, which is related to the quality factor as:

$$Q = R\sqrt{\frac{C}{L}} \tag{1.32}$$

Since the 3 dB bandwith of the system is directly connected with circuit Q:

$$BW = \frac{f_c}{Q} \tag{1.33}$$

The proper termination is determined by the required bandwidth and/or régime of the system . By using the cooled termination we can control these with small effect on the circuit noise performance.
Two examples of such systems were realised to confirm these assumptions. Please, note, that the design of the "transducer" or "sensor" itself is not within the scope of this study.
The first system is a condenser microphone in a high-frequency circuit. This circuit is widely used if the microphone can be affected by poor environmental condition as in location film shooting or making a TV report. The main purpose if designing of this circuit was to obtain the lowest possible noise performance of the electronics.
The second system is a ring-core fluxgate magnetometer. The main purpose of the design was to maintain the triaxial fluxgate sensor head intact and to start-up the system as soon as possible. From the point of view of design, this system is not optimal, but it is designed in modular manner, which allows easy repairs and future improvements.

2 High-frequency condenser microphone

2.1 Convergence of multimedial technology

In today information technology we use unified physical-logical layer to transfer, process and storage of all the real - world signals. It is now common that radio, television, telephones and many other equipments can be substituted by special programs in the computer connected to the computer network (INTERNET). This process is called convergence. Further generalization for the audio technology is, that all professional audio input and output equipments (microphones, speakers) could be viewed like computer network devices and special studio equipments (mixing consoles, audio effect processors and recorders) could be viewed as computer programs. Such that system would be free from dynamic and bandwidth limitation of today analogue systems. The barrier which is still not been overcame is analogue nature of electroacoustic transduction. In department of radioelectronics of the Czech Technical University in Prague research focused on analog to digital and digital to analog conversion based on transduction phenomenon have been started a couple years ago (Husník, 2003), (Kovář, 2004) ,(Motl, 2005). The goal of this part is to complement this research with transducers which does not work in base frequencies. Transducers constructed in this way does operation of spectral transposition and we will call them parametric transducers. Spectral transposition (under some circumstances (Manley, 1956)) is the origin of power gain, which is theoretically noiseless. This is especially useful for parametric microphones because it could works closer to theoretical noise minimum than other microphone types.

2.2 Condenser microphone as parametric elecroacoustic system

In typical[1] condenser microphone all acoustical system is concentrated to the part - capsule[2] Typical capsule is in fig. 2.1

[1] Somewhat different are line transducers, where body of the microphone creates acoustical waveguide to obtain high degree of sensitivity. Sometimes are to pressure capsule attached pieces in the form of a disc with a hole for capsule or short tube of capsule diameter - these members can modify high-frequency characteristics at the cost of directional characteristics

[2] Capsules in the studio microphones are usually replaceable as spare parts when microphone is repaired

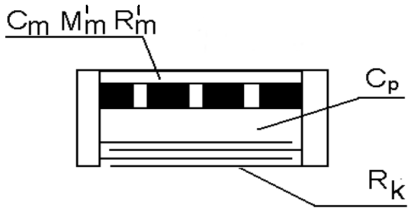

Figure 2.1: Microphone capsule

For modelling of the capsule, non-standard analogy is presented, where voltage equals the displacement and current equals the force. This analogy origins from energy equation of the electrostatic transduction, which is eq. 6.9 in the appendix A. At the mechanical side it resembles mobility analogy (Lenk, 1973). Difference is in operational form, that eleastor is modelled by resistor, mechanic resistor is modelled by capacitor[1] and inertor is modelled by a double capacitor, what directly resembles the second Newton law $f = ma = m\ddot{x}$ Electromechanical conversion is modelled by two arbitrary current sources (eqs. 6.12 and 6.13 in the appendix A) At the electrical side mutator is included serving as integrating gyrator which transforms charge to current[2] . The microphone creates one arm of a bridge, fed by symmetrical voltage source and loaded by a resistor matched by a series inductor. Reference arm of the bridge is shunt capacitor (fig. 2.2).

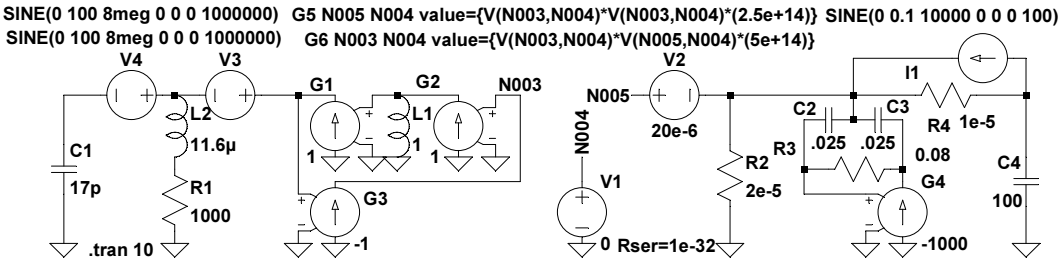

Figure 2.2: Model of HF condenser microphone

Because SPICE simulator does not allow using of singular circuit elements, we will use voltage-controlled current source (VCCS) to model unilateral voltage - to current converters (fig.1.16 with only R2). Tables to translate circuit blocks with singular elements to blocks with controlled sources are given in Kvasil (1981) and Vágó (1985). Typical transient simulation is in fig. 2.3

[1] It may cause problem in the noise simulation, but simulation of the acoustic resistor can be done via mutator loaded by resistor. There is one condition, that cascade of mutators (on the electrical side and the second on the mechanical side before resistors must be symmetrical (Vlk, 9-2008))

[2] This nonlinear model can be also used for modelling of capacitor microphone in regime with constant charge for evaluation of transducer-based nonlinear distortion. Frederiksen (1994) showed, that distortion of microphone increases with increasing of the load electric capacity what is in contradiction with Pastille (2001). Problematics is discussed in (Vlk, 5-2008)

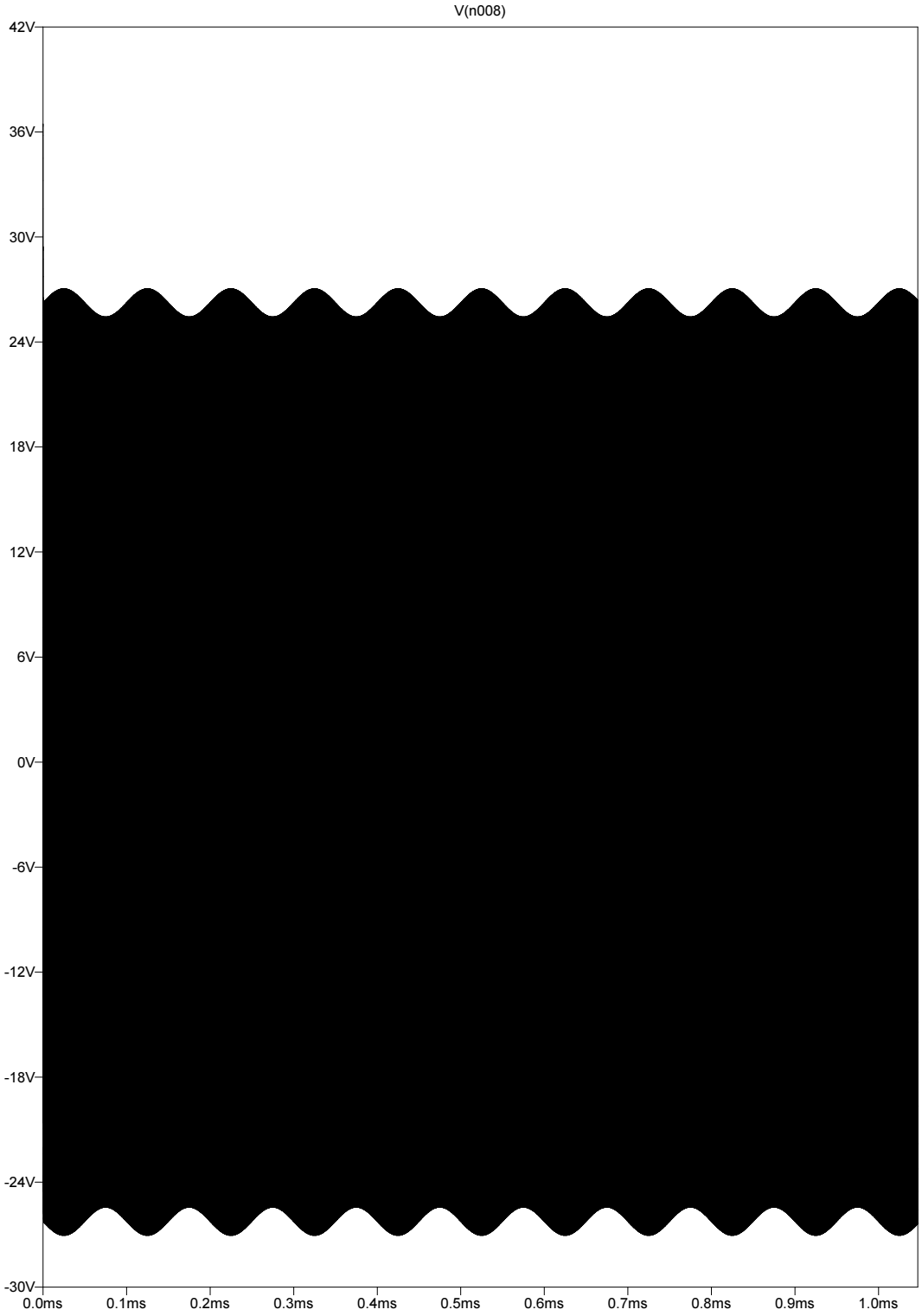

Figure 2.3: Example of transient simulation of HF condenser microphone

2.3 State of the art

There were two periods in history during which this kind of circuit made progress:

1. The 1920s when thermo-ionic tubes made rapid progress. These tubes had poor vacuum, and the conventional cathode follower suffered a noise and stability (grid leak) problem. These microphones have the form of a mere simple resonant circuit, the microphone playing the role of a capacitor, which was excited by a stable oscillator with quartz filter, and the resulting AM signal was envelope detected. This kind of circuit is referred to Reiger (Weynmann, 1944) and at the time belonged to the very low- noise microphones. Another circuit had the form of an untuned transformer bridge. It is not particurlarly interesting at this point to comment on these historical circuits, only should be mentioned that the microphone connected in the oscillator as part of a frequency modulated circuit was rejected at the time because of the notable 1/f part of the circuit noise.[1]

2. In the 1960s, when bipolar transistors became relatively common, and the sortiment of JFETs suitable for the input follower stage was limited. In this period two basic circuits were perfected and given to routine use: the transformer bridge (untuned and tuned) and ratio detector.

3. In the 1990s when end-user digital media set-up a new standard of dynamic range in the recording industry. The development of the HF microphone circuit paradoxicaly concentrated on low-cost circuits rather than on performance.

[1] It is paradoxical situation, that nearly all newer papers on parametric microphone describes this false idea: (Pedersen, et al., 1998), (Mueller, et al., 2004), (Soel et al., 2007)

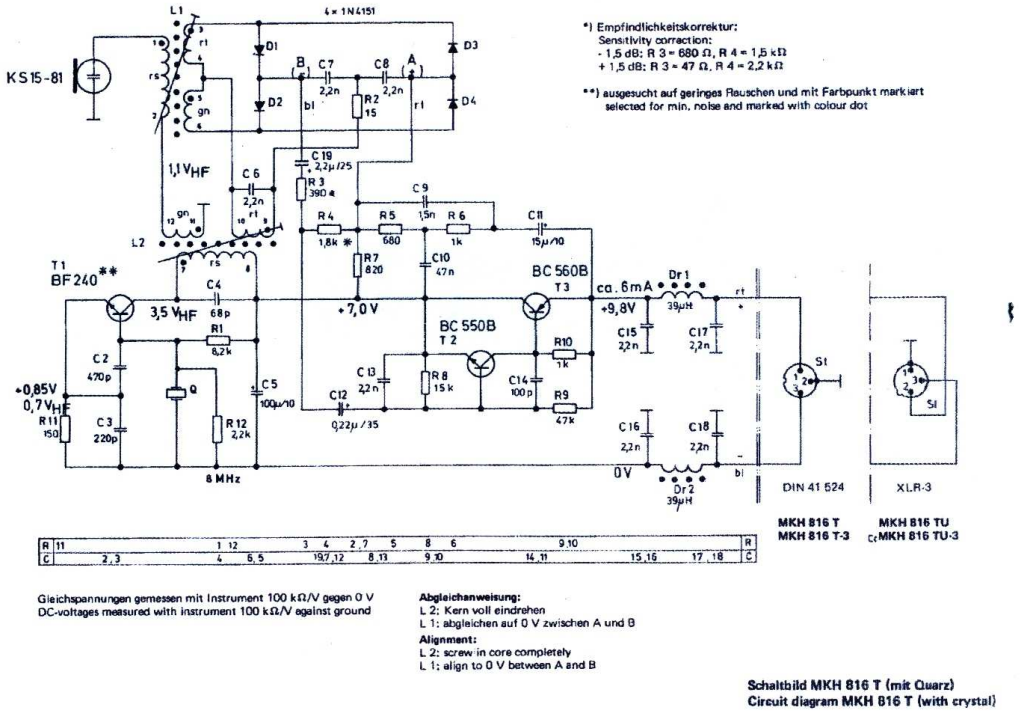

Figure 2.4: Ratio detector

As an example of the microphone without bridge (Zuckerwar et al., 1974), (Hansen, et al., 2004)[1] we will examine the scheme of the microphone based on the ratio detector (fig. 2.4) designed by Griese (1969). The topology of the circuit stems from the 1960s, only using slightly more modern components. Transistor T1 serves as a Gouriet (1950) oscillator with quartz. The oscillator has no external amplitude-limitation circuits which could degrade the in-system quartz Q-factor. The tuned transformer L2 in the collector of T1 has several functions:

1. It provides proper impedance output for the microphone tuned circuit (L1).
2. It provides DC decoupling for the collector of T1.
3. It provides demodulator circuit floating for the audio signal.

The main series resonant circuit (L1 - microphone) operates at the plateau of the resonance-curve. The resulting signal is then phase-modulated and is detected by the diode gate circuit which is symetrical and current-driven by R2. The system works only with one diode pair (D1-D2) or (D3-D4) which was used in other commercial constructions. Another interesting point is that the output amplifier works in so-called T-power, where the signal pins have both opposite signals and DC-power potential. This powering was relatively common in the 1970s because the firm NAGRA makes tape recorders with inputs for film location recordings.

[1] Both systems uses inappropriate (UHF and microwave) devices for demodulation in the baseband, and must have noticeable amount of 1/f noise in the acoustic band

AF amplifiers (T2,T3) have also built-in frequency corrections[1]. As an example of the microphone with bridge(Arends, 1963), (Baxandall, 1963), (Paerschke, 1965)) we shall examine a typical actual product of the firm Senheiser (fig. 2.5). The circuit is designed by Hibbing (1996). Solo-oscillator T1 is stabilised by T2 and drives a Blumlein (1928) bridge with a symmetrical microphone capsule. The output from the bridge is tuned by L3 and fed to transformer L2. L2 has the function of DC and audio decoupling of the detector part and functions as an HF-pad if needed. D1 and D2 work as a gate. The peak current is stabilised by the $(\mathrm{R6}+\mathrm{R7})\|\mathrm{C3}$ leak, and thus a series resistor is not needed. Also the situation of the gate is reversed when compared with the ratio detector, because the input wave propagates to the winding middle point instead of the switching wave. The microphone has a standard phantom power and the AF amplifier has a relatively uncommon series topology with respect to DC power.

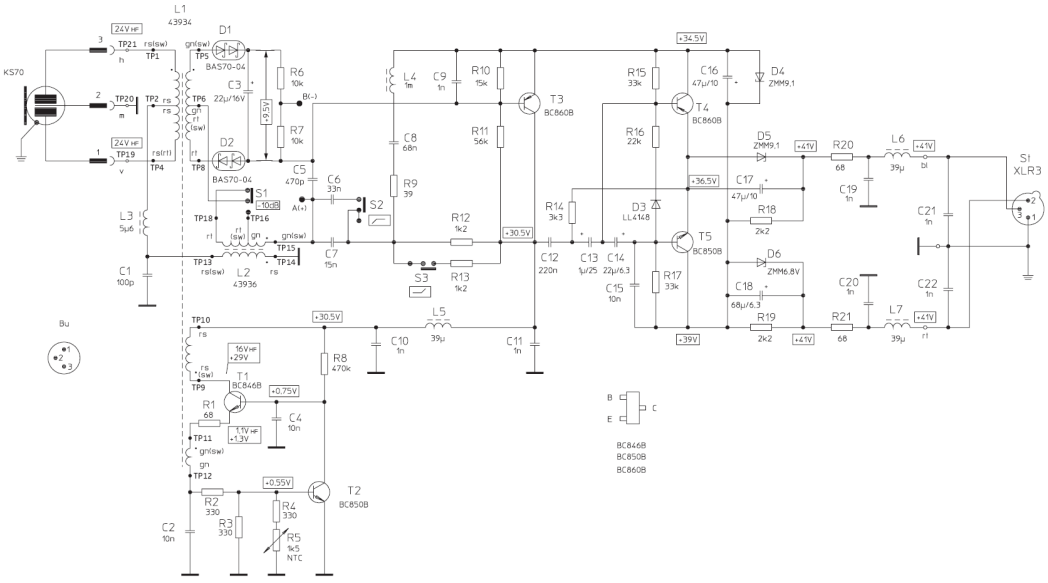

Figure 2.5: Tuned transformer bridge - solooscillator

2.4 New development

From this point of view, the modern HF microphone would have these properties:

- Source of pump frequency: high stable quartz oscillator.
- Circuit topology: resonant loaded transformer bridge with synthetical resistor loading.
- DSP signal processing at the idler frequency.
- Some form of peak elimination and restauration system (PERS) must be included.

Since only a part of the circuit was finished, we shall describe it.

[1] Critical damping of the diaphragm is needed for the flat frequency characteristics on an acoustic side. Damping is controlled by variing of the mechanical resistance of the air gap between the diaphragm and back electrode (by means of holes or slots in the backplate). This resistance (as all dissipative element) adds noise to the system. Common trade-off in the low-noise capsule manufacturing is to leave the capsule under-damped and to correct the frequency characteristics by an additional filter in the electronic circuit.

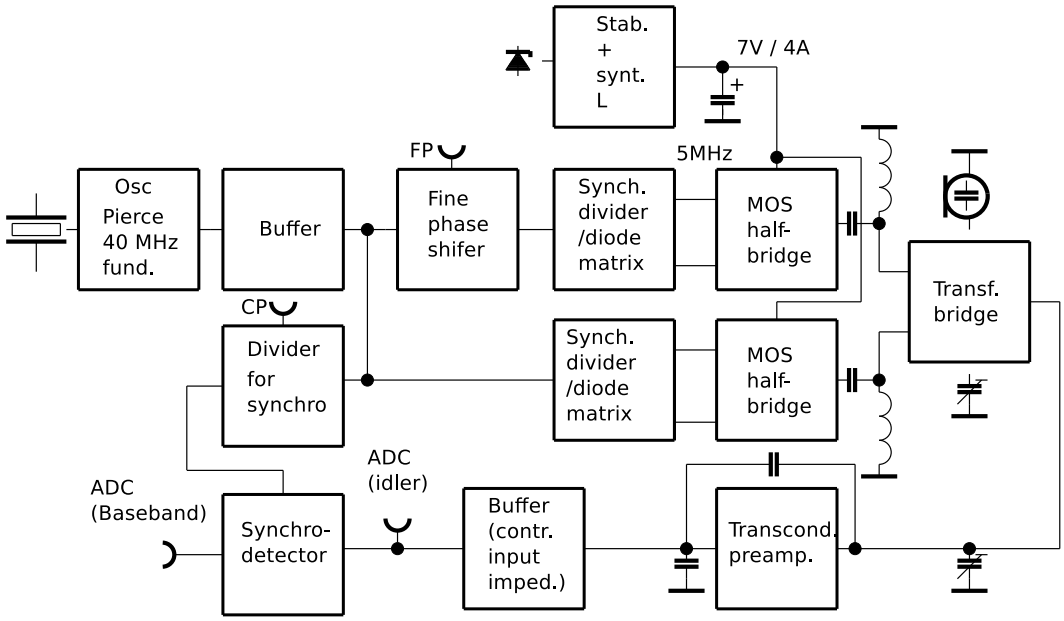

Figure 2.6: Block diagram of developed HF condenser microphone

A Pierce quartz oscillator of ordinary single-transistor construction oscillates at 40 MHz. After the decoupling stage, a synchronous ring counter is used as a generator of non-overlapping impulses for power MOSFETs. The speciality of the counter is a diode matrix with current output which uses the input part of S-TTL invertors as current-to-voltage converters.

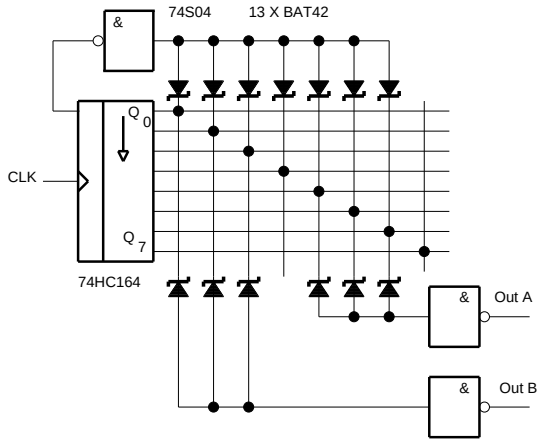

Figure 2.7: Synchronous divider - non-overlapping outputs

The drivers are of classical half bridge topology using Elantec circuits. The power stage (PA) is based on complementary MOSFET topology, which is relatively commonly used in class-D PA stages. The speciality of the power stage is dominant induction loading, which lowers the switching noise of the stage and allows the phase-to-amplitude conversion mode of the stage that is essential for PERS function. The power stage requires power consumption which is (although the system deals with pure reactances) fudamental for the low-noise switched regime at relatively high frequencies. This power is mainly composed of switching

losses and, using MOSFETs of a newer generation could reduce it. In experimental set-up 2 A 7 V consumption was noted. The power dissipation of 14 W per stage needs a proper heater. Simple passive heater will suffice. A double inductive balun is used for transforming the impedance of the PA and for balancing the output between the microphone and dummy load. An ordinary tube ceramic capacitor worked best as the dummy load.

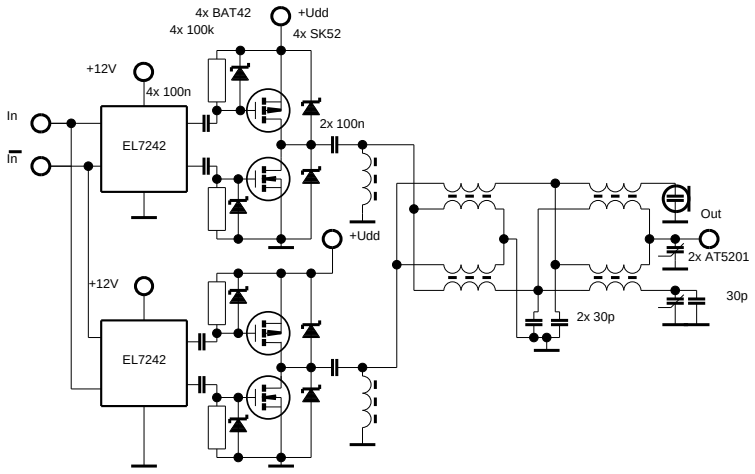

Figure 2.8: Microphone PA

The input amplifier (fig.2.9) is a folded cascode with FET in the first stage in CS and BJT in the CB at second stage. The second stage is loaded by a shunt capacitor 30 pF. 1 pF of the paralel feedback capacitor forms the synthetic resistor to terminate the bridge. The third and fourth stages form the decoupling stage needed for further processing. The CE-CE BJT cascade with 100% parallel voltage feedback is used instead of the CC stage because this type of circuit provides better stability for a strong signal. It is application of circuit with controlled input impedance to avoid parasitic oscillator structure (fig. 1.6).

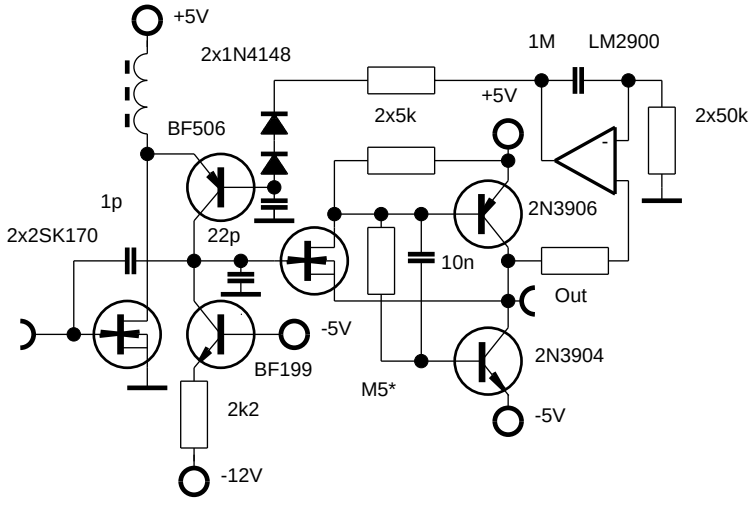

Figure 2.9: Microphone input amplifier

For experimental purposes, only a synchronous detector is used (fig.2.10). This type of detector provides supporting output suitable for experimenting with the circuit without

needing of high-resolution high-frequency A/D converter. The coherent digital signal needed for detection is given by an additional row of diodes in the divider diode matrix.

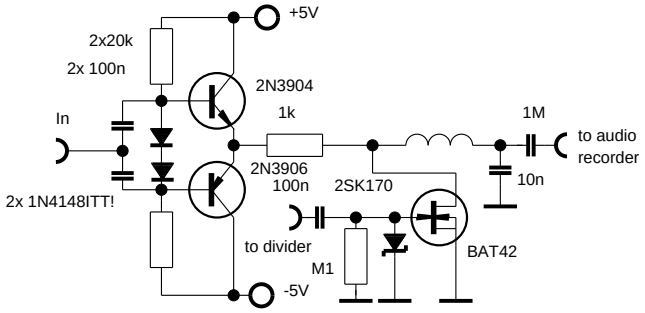

Figure 2.10: Synchrodetector for experiments

Since the dynamic range of modern condenser microphones for recording purposes can go up to 130 dB of the peak sound pressure level, microphone must have a peak elimination and restauration system (PERS). Since a high purity power source is used for the PA supply, the only way to achieve PERS is to use a phase-to-amplitude bridge (Chireix, 1935). The system consists of a synchronous shifter and comparator. The disadvantage of this system is the need for high frequency of the master oscillator. Cellular asynchronous logic can handle these requirements without a problem in modern FPGA RTL designs. An example of such a system is in fig. 2.11 .

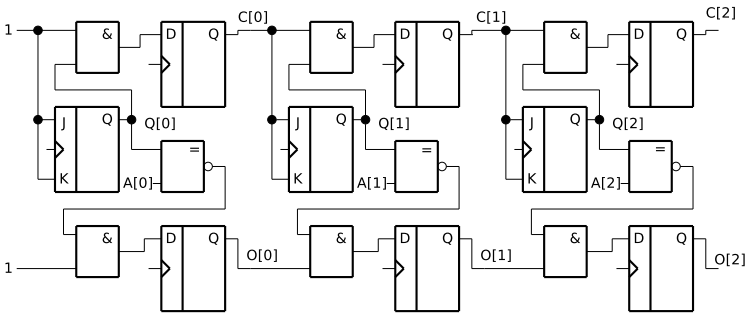

Figure 2.11: Divider

This system is a systolic synchronous divider with a comparator. The output of the section of the divider is delayed by the number of the sections, the output from the comparator is delayed by twice the number of the sections. The circuit consists of several cells connected in series, one cell serving as phase shifter of one bit. Consider a 200 MHz SAW oscillator, which FPGA divides by $200/2^5 = 6.25$ MHz. There is also the possibility of using a different modulus to obtain 5 MHz exactly as with a quartz oscillator, and using an analogue circuit without modification. A five-bit system yields a shift of 32 positions which yields a headroom of $6 \times 5 = 30$ dB The next part of the dynamics must be created by the decimation structure.
Another solution of the fine shift which does not depends on the frequency of the main oscillator is based on a Delay Lock Loop.

The DLL system (fig.2.12), originaly developped by Combes (1994) is commonly used as a frequency-multiplier in the modern digital devices i.e. microprocessors. It is based on the RC lumped delay-line with constant delay per step (thus it does not have equal components

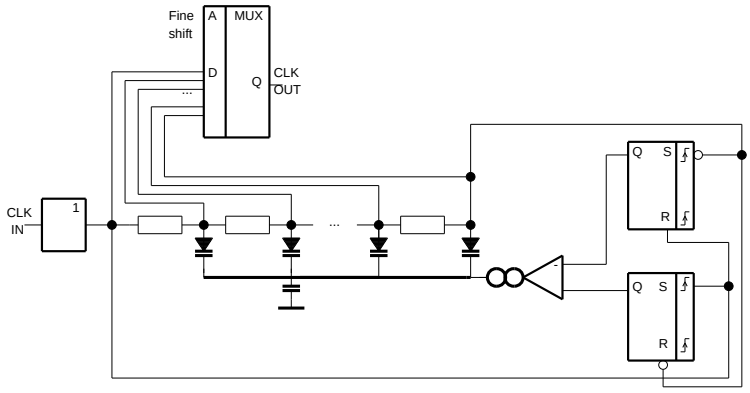

Figure 2.12: DLL fine shifter

values) and where C is realised by a varactor. Total delay of the line is stabilised by a phase sensitive detector which compares input and output and varies varactor bias to align the input and the output pulse. Main advantage of this solution is that jitter property of the output signal is dependent on the main oscillator and not on the VCO as in the case of PLL. When an additional noise source is added to the varactor bias, spread-spectrum of the output wave can be made what is useful to reduce EMI problems in the digital system[1]. Because no such systems was accesible for author in time of construction of the microphone circuit, simple shifter was developped using standard logic circuits. This system is on fig. 2.13. It is binary-weighted time shifter based on dissimilarity of the two RC integrators connected to the one input of the CMOS XOR. Full shift of the circuit is period of oscillator (25 ns). It is highly reccomended, that significant bits are weighted in unary (thermometer) code to obtain low jitter.

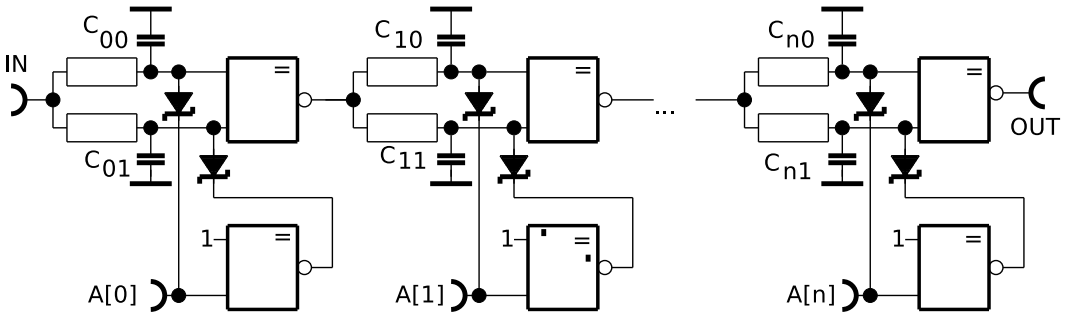

Figure 2.13: Phase shifter with standard logic

2.5 Realisation

Function of discussed circuit function was proved by breadboarding. The breadboarding itself gives the direction in the circuit modification to obtain best signal to noise ratio for given microphone AC HF voltage and defined capacitance change. This is figure of merit of

[1] Analogic system is known in the acoustics over 50 years in the form of vibrato unit of the famous Hammond (1946) organs.

the electronic circuit. Functionality was also tried with improvised capsule as can be seen at the pictures.

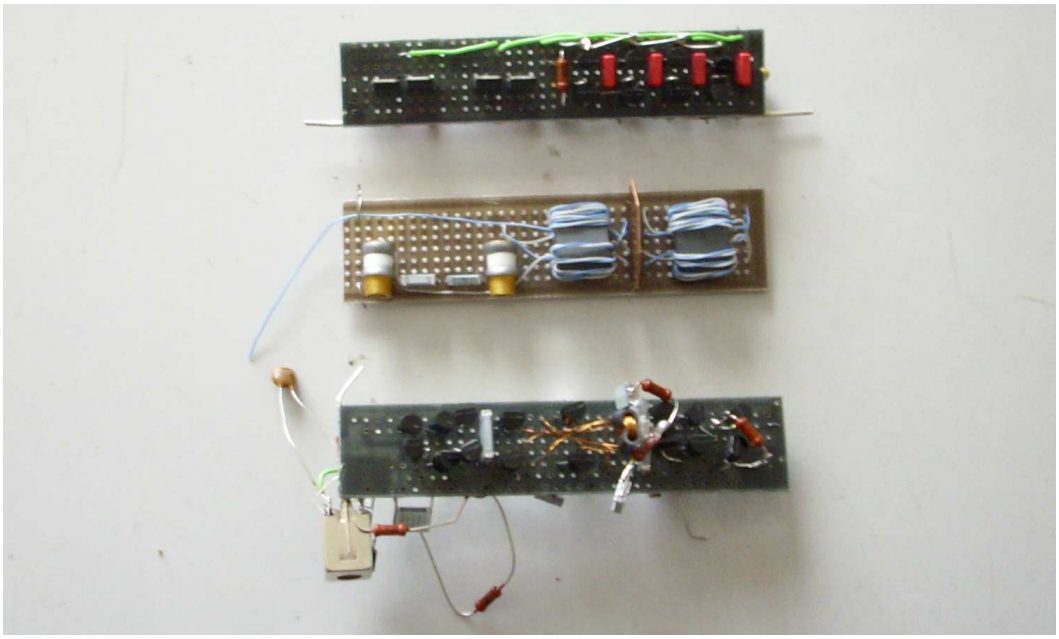

Figure 2.14: Microphone circuit blocks

On the fig. 2.14 is photograph of buiding blocks of the microphone. From bottom: PA with small discrete CMOS inverters (BS170 and BS250). Its performance was bad. In the middle are HF bridge constructed of two-hole core from ferite material N05 (EPCOS). In the left is air tunning capacitors for reference and preamplifier. Low noise preamplifier is on the opposite part of the breadboard PCB. In the top is PA form complementar power MOSFETS with discrete elements driver. It was replaced by integrated high-speed IC drivers from Elantec discussed in the work.

On the fig .2.15 is complete microphone set-up. On the left-low corner is improvised microphone. the first plate is preamplifier. in the middle is PA with discrete driver and in the right-lower corner is oscillator, divider and RC phase circuit simillar to that discussed on fig. 2.13. On the upper left-middle part is stabiliser with main filter capacitor The stabiliser is very similar to one used in 120V source of the fluxgate. On the upper-right part is synchronnous detector for testing. The blue coaxial cable (from preamplifier to detector) is decoupled for signal with the balun.

2.6 Conclusion

The noise property was estimated by dummy microphone (fig. 2.16). The dummy microphone was constructed as a T - circuit, the purpose of which is to create a capacity jump of 20 fF over and above the basic capacity of 30 pF. A mercury-wetted relay (Hermeyer St57) was used for this purpose.

The comparison of the recording of the step to noise at 1 kHz, reduced to the audio bandwidth of 20 kHz and the sensitivity of an ordinary 50 V DC polarised recording capsule yields 7 dB of unweighted self noise of the electronics over the audio band.
Although the project of the digital microphone has not been finished, The developed codes

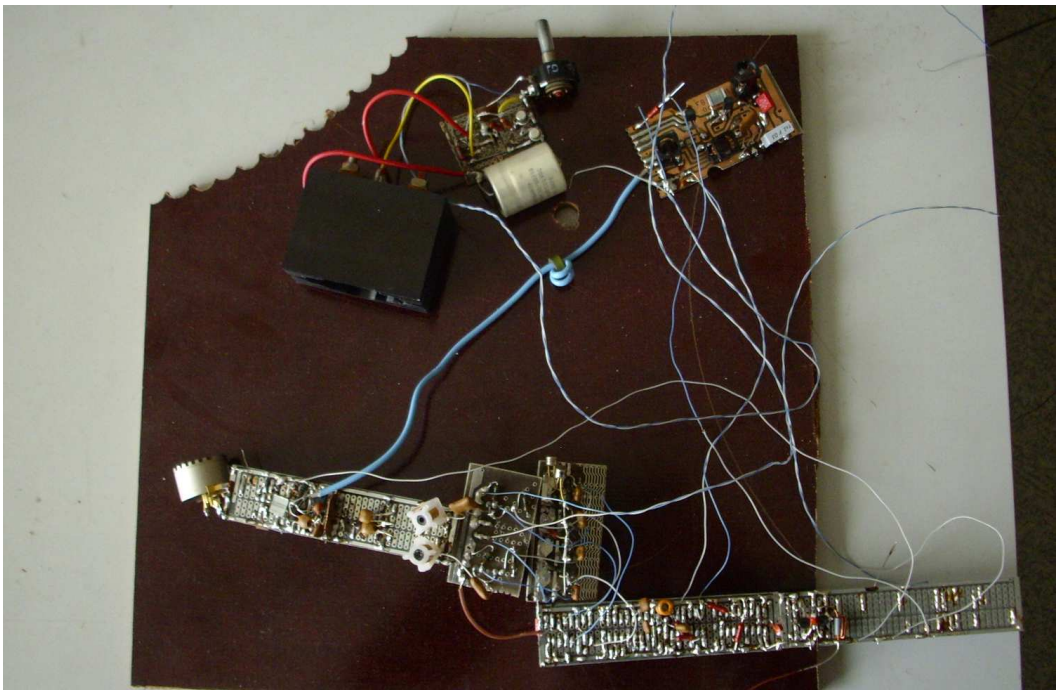

Figure 2.15: Microphone test setup

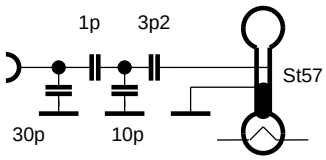

Figure 2.16: Dummy microphone

were used to create the background of the digital fluxgate described in the next section. The only difference of DSP between the microphone and the fluxgate is in fact, that the frequencies used in the digital microphone are two orders higher than frequencies used in the fluxgate. A pure software radio system, based on the ANSI-C code, is then used for processing the fluxgate data. RTL logics must be synthetised in FPGA to process the microphone data. Although the author has all the needed cods written at the RTL level in the VHDL and has simulated it in MODELSIM software, dedicated hardware must be made to make these codes run. The cost of developing the hardware in small quantity with BGA based parts was the main limiting factor. Because analogue part is finished and its main disadvantage - big switching losses of the pump PA with MOSFETs can be solved by today's power GaN HEMTs - it is possible, that the research will continue.

3 Second-harmonic fluxgate

3.1 Geomagnetic Survey instruments

Surveys of the geomagnetic field have great history. The oldest instrument the compass, has been known since old China. The compass is a primitive form of declinometer. It measures only the direction of the horizontal component of the magnetic induction vector. Typically the horizontal component in the Czech Republic is 20000 nT and the vertical component 44000 nT. A typical compass is a rod magnet suspended from a point axis (in this case the vertical force must be balanced by additional mass) or floating in a fluid. More modern instruments (known since Gauss) use wire suspension. The wire can be made of organic material like silk, or gold alloy, platinum - irridium alloy and fused silica. The later are the most stable and are still being used in survey instrument. A typical property of the geomagnetic field is that rapid phenomena (pulsations) are usually of small amplitude. Phenomena of high amplitude are the daily variation and magnetic storm. The ltter occurs only sporadically. A typical recording apparatus is the La Cour variometer (fig. 3.1). It is named after its inventor, the Danish physicist Dan La Cour (1876-1942), son of the co-inventor of telephone, Poul la Cour (1846-1908).

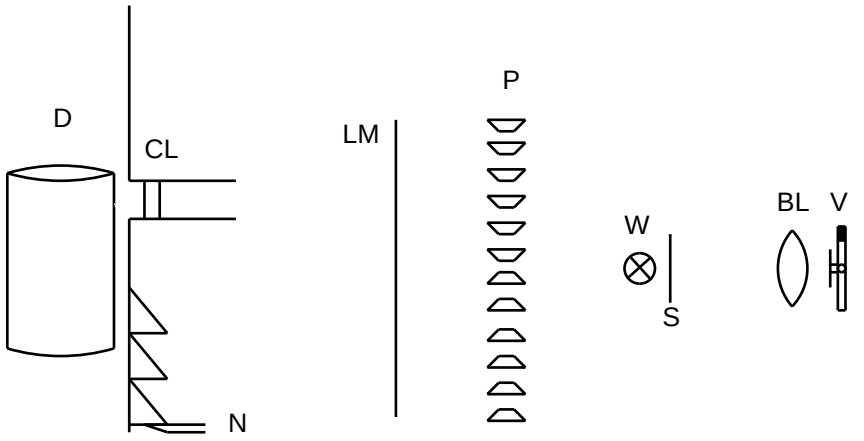

Figure 3.1: La Cour variometer

An incadescent lamp with straight wire $\mathbf{W}$ is shielded by $\mathbf{S}$ so that its light can pass only through prisms $\mathbf{P}$ where it is multiplied, to the line mirror $\mathbf{LM}$, and is then reflected to the variometer $\mathbf{V}$, consisting of a rod magnet with a mirror fixed on it and suspended on a fused silica wire. The variometer reflects lamp images through lens $\mathbf{BL}$ onto rotating drum $\mathbf{D}$ with photopaper, where only one image is selected by the collimator and focused by the cylindrical lens $\mathbf{CL}$. The position of the $\mathbf{CL}$ is changed in steps synchronised with the drum's rotation by mechanism $\mathbf{N}$.
The main purpose of this system is to perform "peak elimination and restauration" strategy optically. Since the sensitivity of the paper is limited, sensitivity of the system must be high (in terms of nT/mm). However on a 24-hour record made on generally available paper one

hour of record represents a few centimetres. The solution is to have the record composed of several lines which are equidistant, only one is being displayed on the paper at one moment. The actual La Cour system is somewhat more complicated: it has a total of 50 prisms and uses three variometers, line mirrors, collimators and cylindrical lenses. Quartz variometers were improved continually over several centuries and modern types of the Bobrov (1962) apparatus when aged have an annual stability of 3 nT, noise level of 10 $\mathrm{pT}/\sqrt{\mathrm{Hz}}$ and are used with a proper digitalisation unit as survey instruments comparable to the best fluxgates, in terms of $1/f$ noise and EMC even better. Quartz magnetometers are fragile and need a stable optical bench several metres long and are thus impractical for mobile and space research.

Space research in the 1960s accelerated the development of fluxgate magnetometers, because they are insensitive to vibrations. The noise of top instruments are now of the order of 1 $\mathrm{pT}/\sqrt{\mathrm{Hz}}$@1Hz. The peak-to-peak drift error is under 5 nT/year which is sufficient to meet international standards for the observatory run. /newline Better noise can be obtained theoretically with cryogenic magnetometers, SQUIDs, but they needs cryostat and therefore are not suitable for observatory operations where instruments are used over periods of several decades. SERF optically-pumped (Setzler et al., 2004) potassium vapour -gas masers could have better noise performance than fluxgates, but such instruments are still in development. Their noise level is in parts of 1 $\mathrm{fT}/\sqrt{\mathrm{Hz}}$ which can be degraded by eddy currents in conventional permalloy shielding. An inner ferrite shield layer is thus recommended. The SERF magnetometer also needs heating to approx. 200°C which need not be great problem in the observatory, but is a problem at distant stations where power for heating is limited. SERF magnetometers are based on laser-diode pumping, and the semiconductor industry may possibly produce cheaper laser diodes, thus bringing the price of the SERF magnetometer below that of the high-quality fluxgate magnetometer. Technological noise now dominates in the construction of vector SERF which decreases its performance to 10 $\mathrm{pT}/\sqrt{\mathrm{Hz}}$, comparable to or worse than the ordinary fluxgate. Also solid-state organic-quartz laser-cooled masers are being developed in laboratories (Oxborrow et al., 2012) and could be rivals of the SERFs in the future because they work at laboratory temperature without oven heating.

3.2 Ring core fluxgate

Basic contruction of ringcore probe consists of core with toroidal pump winding (pump) and solenoidal winding outside the core (fig. 3.2).

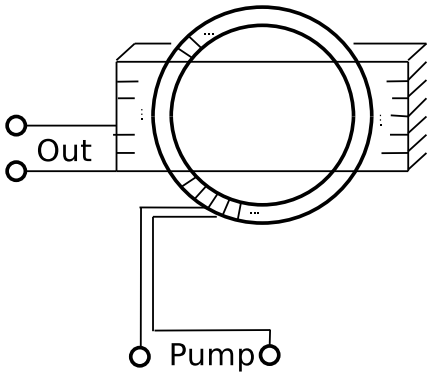

Figure 3.2: Fluxgate probe

Pump winding is usually driven by ferroresonant system, originally usued in power electrical engineering for decreasing mains electromagnetic pollution and for rough voltage stabilisation. It has been shown that ferroresonant principle have number of advantages in application to fluxgate pump circuit (Korepanov et al., 2013). One of them is fine stabilisation of the pump current, second one is a fact, that probe can not be damaged due to any failure in the electronic part of pump circuit. This fact is of great importance - price of good triaxial probe set is 30k USD and its manufacturing is not a simple task (Narod, 2014), (Gordon et al., 1968), (Sery, et al., 1968) For proper design of this circuit good model is helpful.
The most penetrating modelling system is SPICE. It is part of many CAD systems i.e. CADence ORCAD, and it is also distributed as freeware, as PSpice or LTSpice - SwitcherCAD. The design of the simulation circuit does not need to be straightforward, mainly if there are several phenomena in the analysed system and only the dominant one need to be modelled. The ferroresonant system is in its basic concept a resonant circuit with non-linear inductance. It is relatively hard to imagine non-linear inductance, because non-linearity is basically driven by current. It is much simpler to imagine a non-linear capacitor. But there is the gyrator which transforms capacity into inductance. Gyrator is in fact an anti-parallel connection of voltage controlled current sources. It is not difficult to draw a model of the non-linear inductor using the gyrator (fig. 3.3).

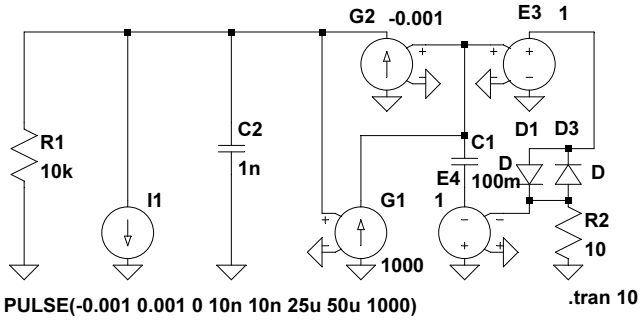

Figure 3.3: Nonlinear L model with gyrator

The result of the simulation for the stationary state is in fig. 3.4.

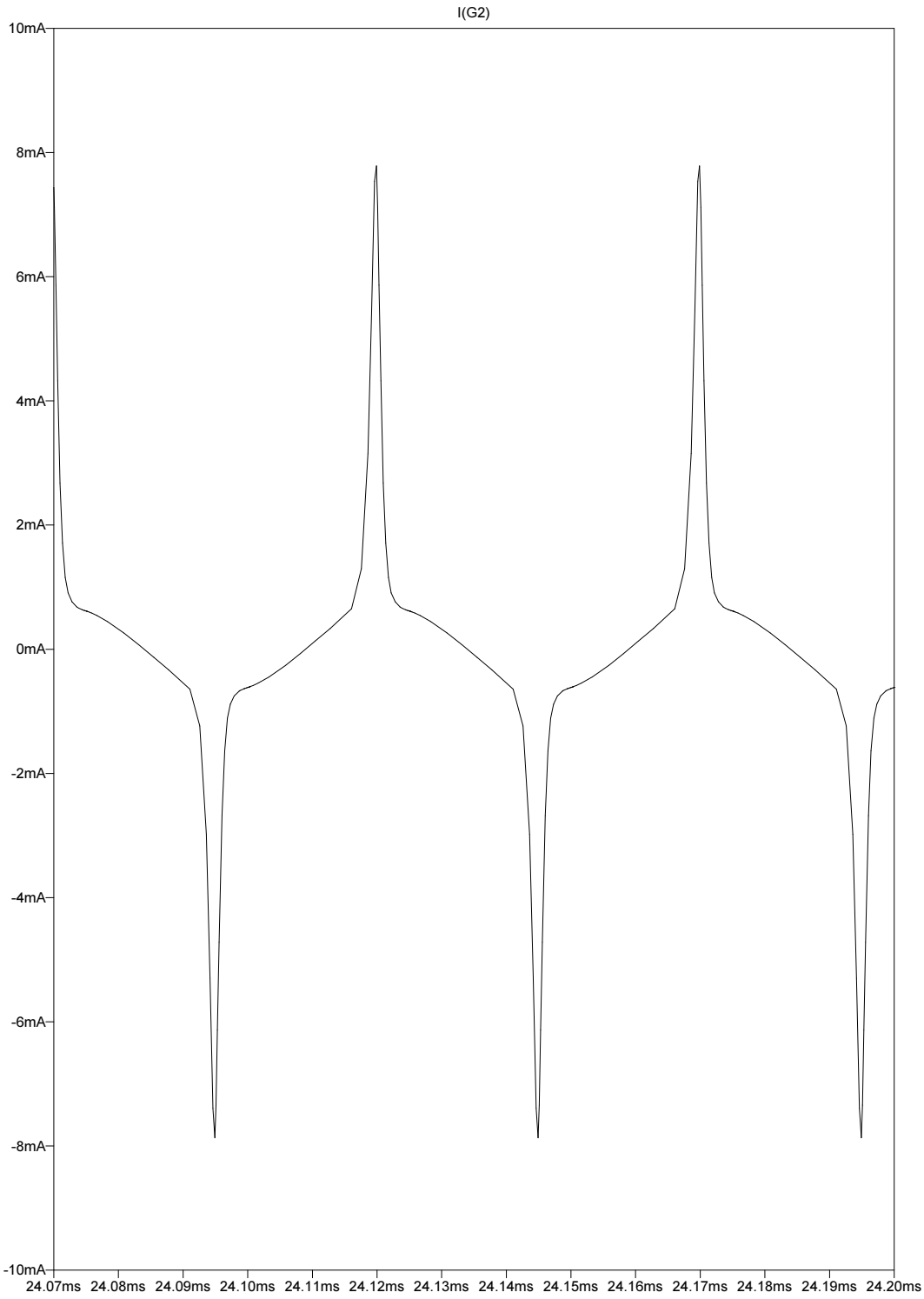

Figure 3.4: result of L model with gyrator

Note here, that all dissipative phenomena, like copper and iron losses, are included in R_1. Without this, simulation usually hardly converges.
The model with the gyrator includes a total of four controlled sources. It is thus relatively complicated. Let us redraw the non-linear part of the circuit using a unilateral voltage

follower (which is in fact gamma cascade of a series nullator and shunt norator (fig. 3.5)).

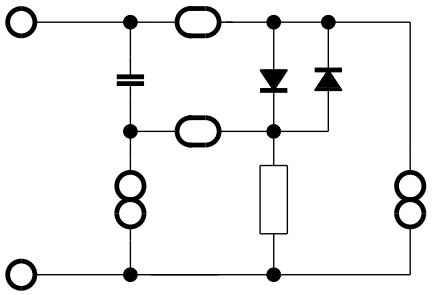

Figure 3.5: Nonlinear C model with nullors

This model describes the non-linear capacitor. The non-linear inductor can be modelled as a dual circuit from the model of the non-linear capacitor. The dual circuit can be produced from every planar circuit in the folowing:

1. The node of the dual graph is drawn in the centre of every area, into which the plane is divided by a circuit graph. (In analogy with the complex analysis, the exterior is also considered to be an area.)

2. Every pair of dual nodes in neighbouring areas is connected by one or more branches. The new branch always crosses the old branch between two nodes.

Dual pairs (Mitra, 1963) are inductance - capacitance, resistance - conductance. The nonlinear dual elements have the same characteristics as swapped I - U axes. The nullator and norator are their own duals[1] When the dual model has been constructed, it is rather complicated to make inverse characteristics of anti-parallel diodes. But because this part is used only as a nonlinear divider, it is possible to swap diodes and resistor in the divider to obtain the required dual characteristics (fig. 3.6).

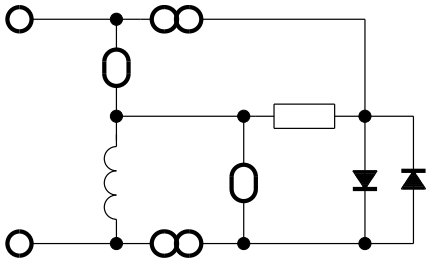

Figure 3.6: Non-linear L model with nullors

[1] Constructing dual circuit cannot be interchanged with constructing adjoint circuit. These circuit synthesis steps leaves operational transfer characteristics unchanged, but in the dual circuit topological graph of the circuit is changed, what can be done only for circuits with planar topology. In the adjoin circuit: (voltage driven) input is changed to (current) output, (voltage) output is changed to (current) input and each nullator is changed to norator and vice versa. Adjoint circuit can be used as part of network synthesis or computationally-efficient noise analysis - i.e. noise analysis in SPICE software is realised by this way. Spice noise analysis as part of frequency domain analysis can not work for circuits with principal nonlinearity - parametric amplifiers - and all noise computations must be computed using transfer parameters computed from the all noisy sources via time-domain analysis. For each (uncorrelated) noise source, one run of the analysis must be done and resulting output noise must be quadratically superposed via the energetic sum. In case of correlated noise, matrix of corellation is needed. It is recomended to avoid this case with equivallent circuits of noisy elements where uncorellated noises are used. It can be done simply using of singullar elements and noise factors.

After redrawing the unilateral voltage follower to a controlled voltage source, we get the final model of non-linear inductance (fig. 3.7).

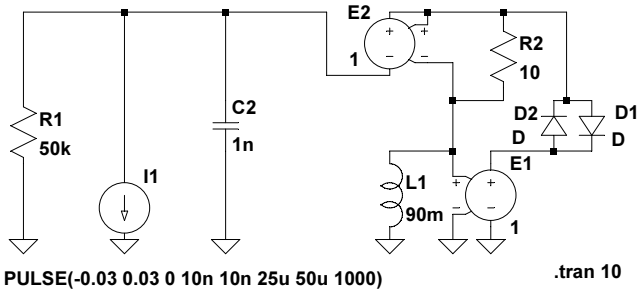

Figure 3.7: Nonlinear L model with controlled sources

The resulting model is simpler: it has only two controlled sources, but this is hard to understand at the first glance. The results are similar (fig. 3.8):

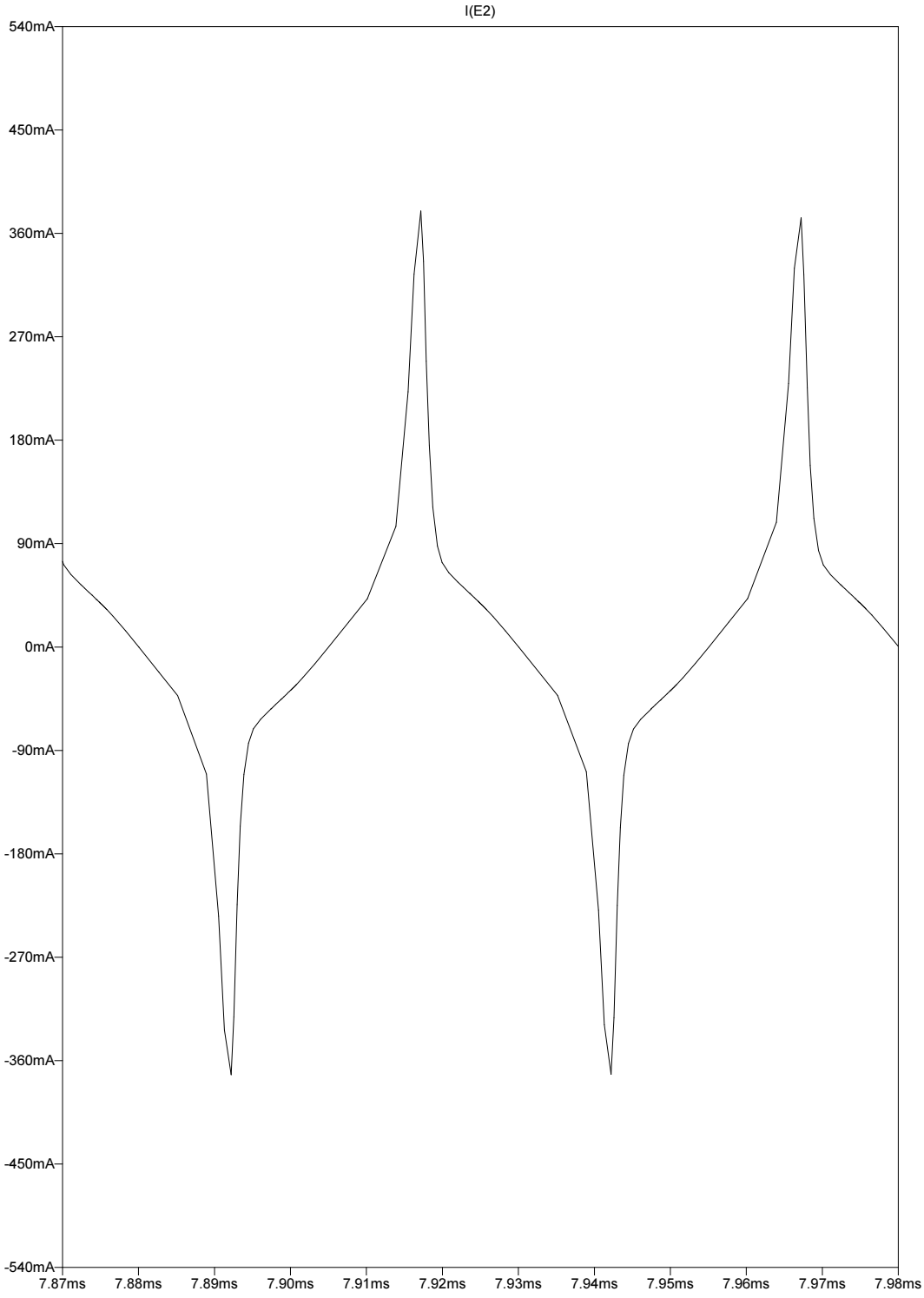

Figure 3.8: Result of L model without gyrator

The same circuit can be used for modelling of sense circuit. The only difference is application of antiparallel diode rings instead of simple diodes. The ring circuit is used in analogue operation of multipication is in fig. 3.9.

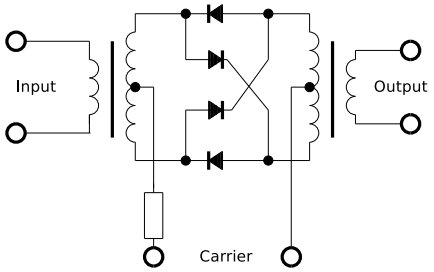

Figure 3.9: Diode ring modullator

One disadvantage of the circuit in fig. 3.9 is limitation of signal amplitude to twice of diode theshold voltage (Jagoš, 1989). Better circuit - switched modullator (fig. 3.10) was used in frequency-divided telephone chanell multiplexing units constructed by company Ericsson

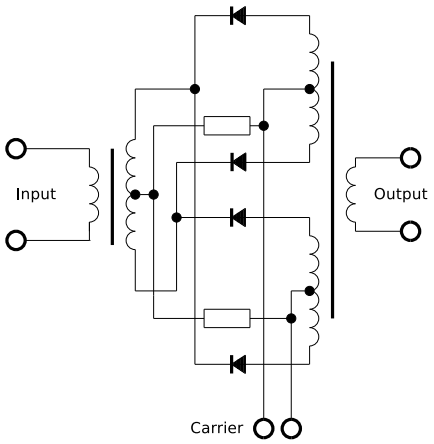

Figure 3.10: Diode ring modullator improved

Maximal signal amplitude was enlarged to level of carrier generator amplitude. Input transformer can be removed at the cost of added diodes (fig. 3.11).

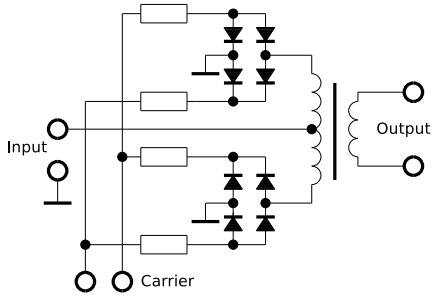

Figure 3.11: Switched diode modullator

Inherent dynamic limitation of the ring circuit can be an advantage in modelling of the tuned fluxgate sensing circuit.

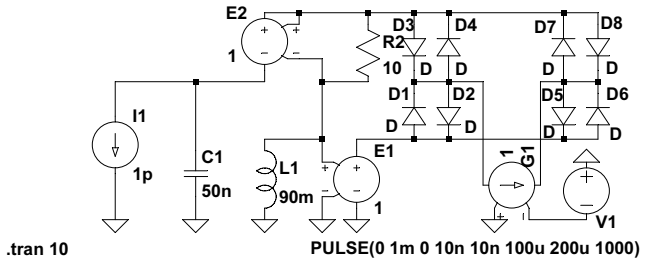

Figure 3.12: Fluxgate loaded by capacitor

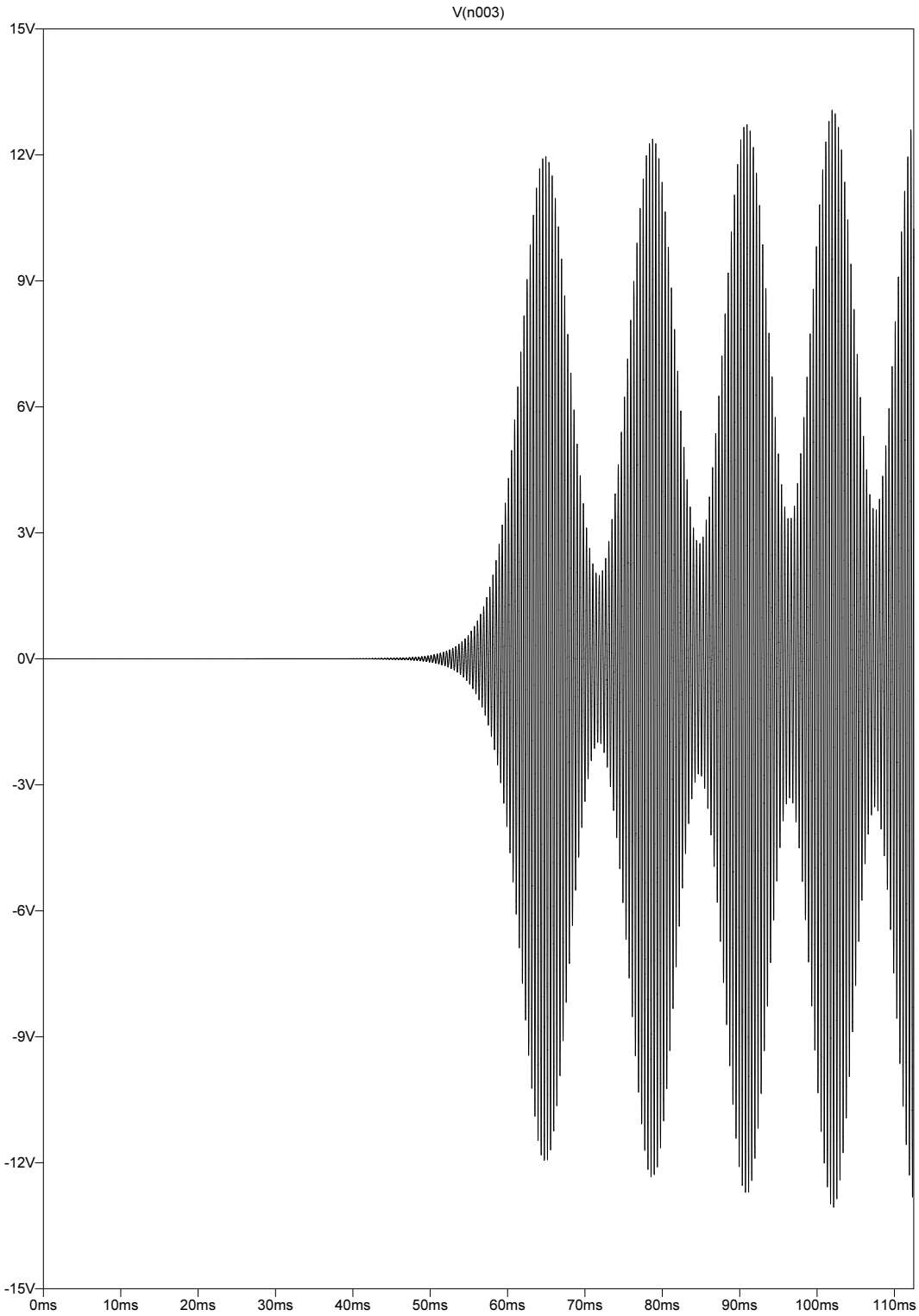

Figure 3.13: Output voltage of fluxgate loaded by capacitor

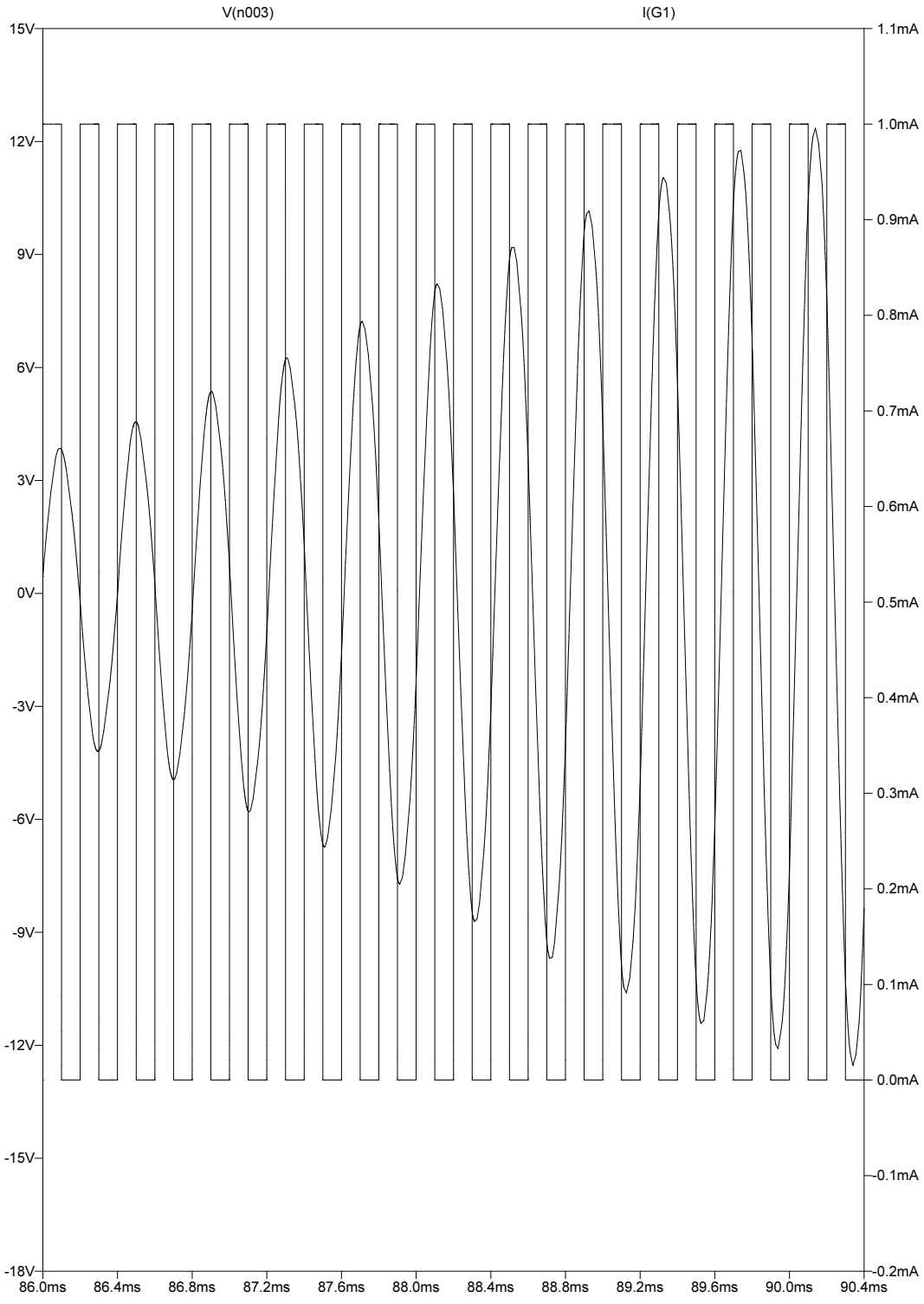

Figure 3.14: Output voltage of fluxgate loaded by capacitor: detail with +1 pA disturbing current

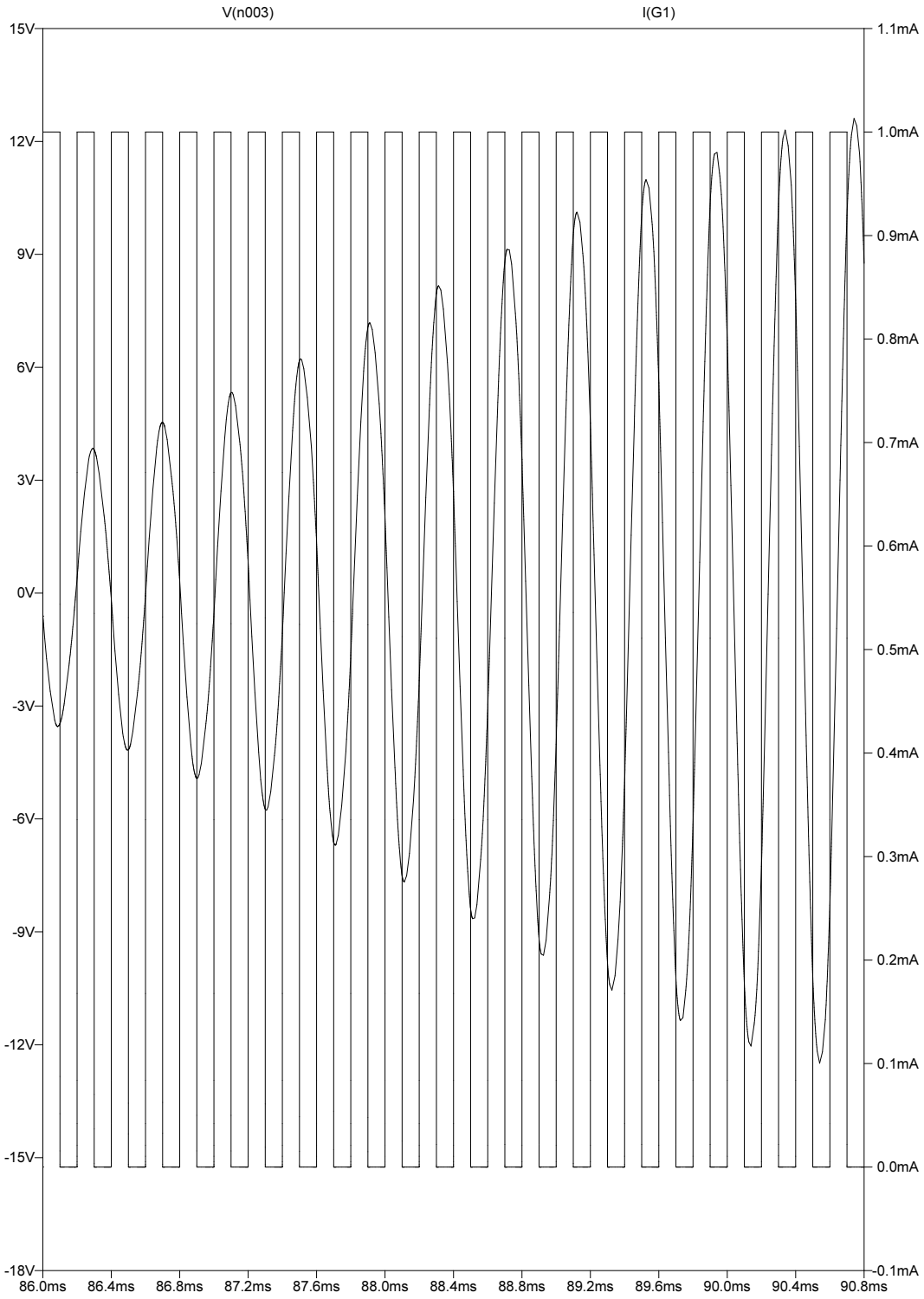

Figure 3.15: Output voltage of fluxgate loaded by capacitor: detail with -1 pA disturbing current

In fig. 3.12 is model of fluxgate based on previous model of the inductor and antiparalel ring-modulators pumped by rectangullar current[1]. Fluxgate is disturbed by signal 1 pA; pumped by an unipolar rectangular signal [2] and tuned by a Capacitor. Signal wave (voltage on C1) have amplitude independent on disturbing signal and is in fig. 3.13. Fluxgate works in parametric resonance regime and its amplitude is limited by ferroresonance which occurs in signal circuit.

On the detail (fig. 3.14) we can see phase relationship of output voltage and pump current. When the disturbing signal (I1) is inverted, output signal is also inverted(fig. 3.15).

This phenomenon is analogical to superregenerative receivers and can be used in simple, sensitive, non-continuously operated devices. Example of this system is Double pumped magnetometer constructed by Baltag (2013).

For maintaining amplitude of output signal depended to disturbing signal, we can partially damp the parametric resonance what is shown in fig. 3.16.

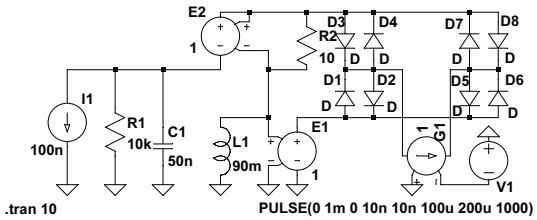

Figure 3.16: Fluxgate damped by resistor

Results of voltages on C1 for 100nA and 200nA are on fig. 3.18 and 3.19 respectively. Noiseless damping, discussed before, ane depicted on fig. 3.17 have the same effect as an simple resistor (fig. 3.20).

[1]Due to inherent symetry of the antiparalel ring circuits it is not important wether pump signal is unipolar or bipolar. Bipolar pump signal have advantages that ferroresonant circuit is simple LC passive circuit. For unipolar ferroresonant circuit some form of switched electronic circuit must be used as in Television Cathode Ray Tube flyback generator (Zworykin, 1954). Another advantage of bipolar pumping is, that pump frequency and signal frequency occupies different frequency bands (signal frequency is typicaly odd harmonic of the pump one), what simplifies construction of the instrument. The only advantage of unipolar pumping is that Barkhausen noise is typically weaker. Unipolary pumped fluxgates have also strong spurious signals (offsetts) which may be caused by unsuitable shape of known units (Sasada, 2002); simple long wire with cyllindrical magnetic layer, with one terminal return astatised by nonmagnetic wire - frame (as used in ribbon microphones) may give better results. Author's opinion is, that offset in case of ring-core fluxgate is caused by nonhomogenity of the core. Preliminary experiments showed, that tertial winding connected in series with the pump sources, when properly adjusted so that have zero coupling to sense coil, can cancell offsett in the unipolary pumped ring core fluxgate. This type of offsett is usally supressed by bipollar pumping (Musmann and Anfassiev, 2010) p.4 .

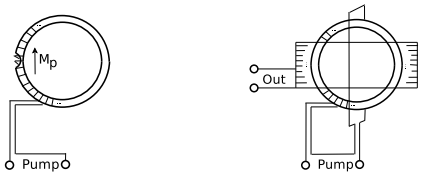

[2]Effect of rectangullar pump signal duty factor on fluxgate performance was discussed by simplified analysis of Mathieu equation by Russell el al. (1983) and Player (1988). These papers contradicts.

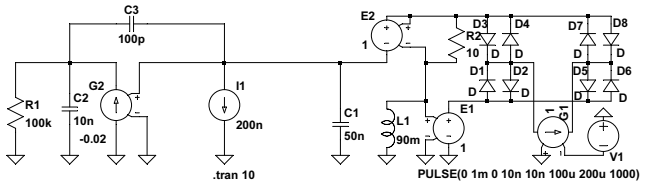

Figure 3.17: Fluxgate with noiseless damping

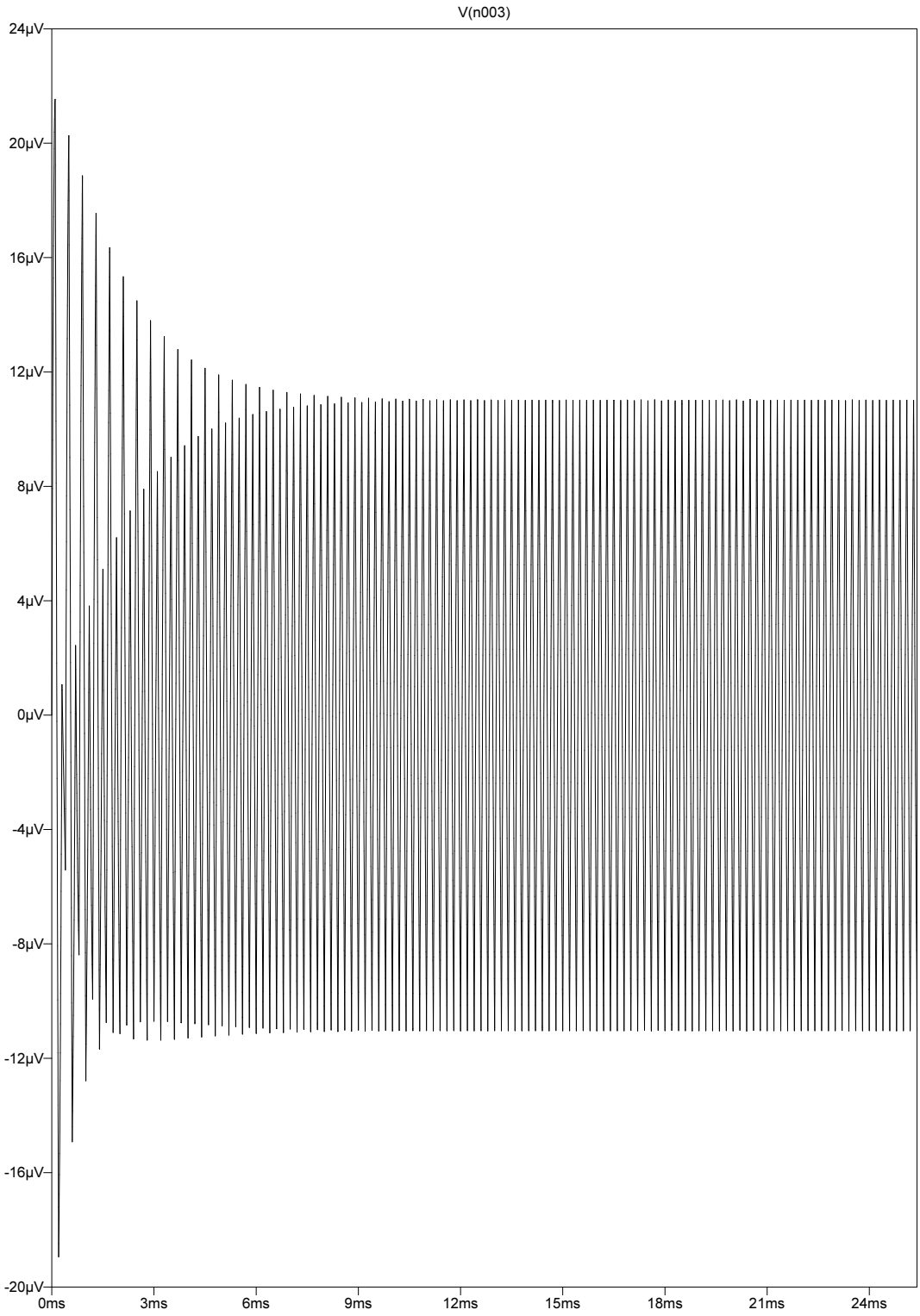

Figure 3.18: Output voltage of fluxgate damped by resistor and 100 nA disturbing current

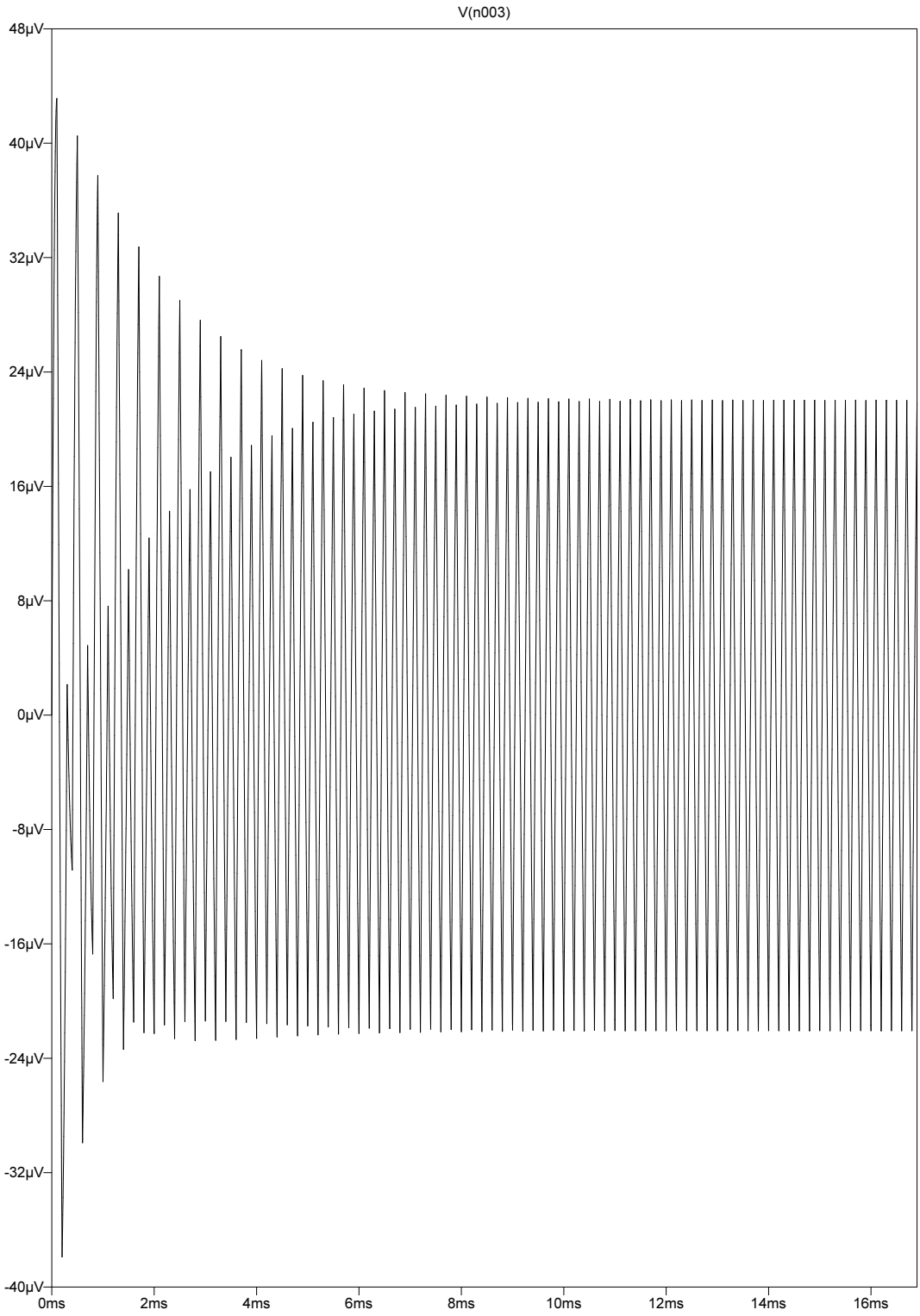

Figure 3.19: Output voltage of fluxgate damped by resistor and 200 nA disturbing current

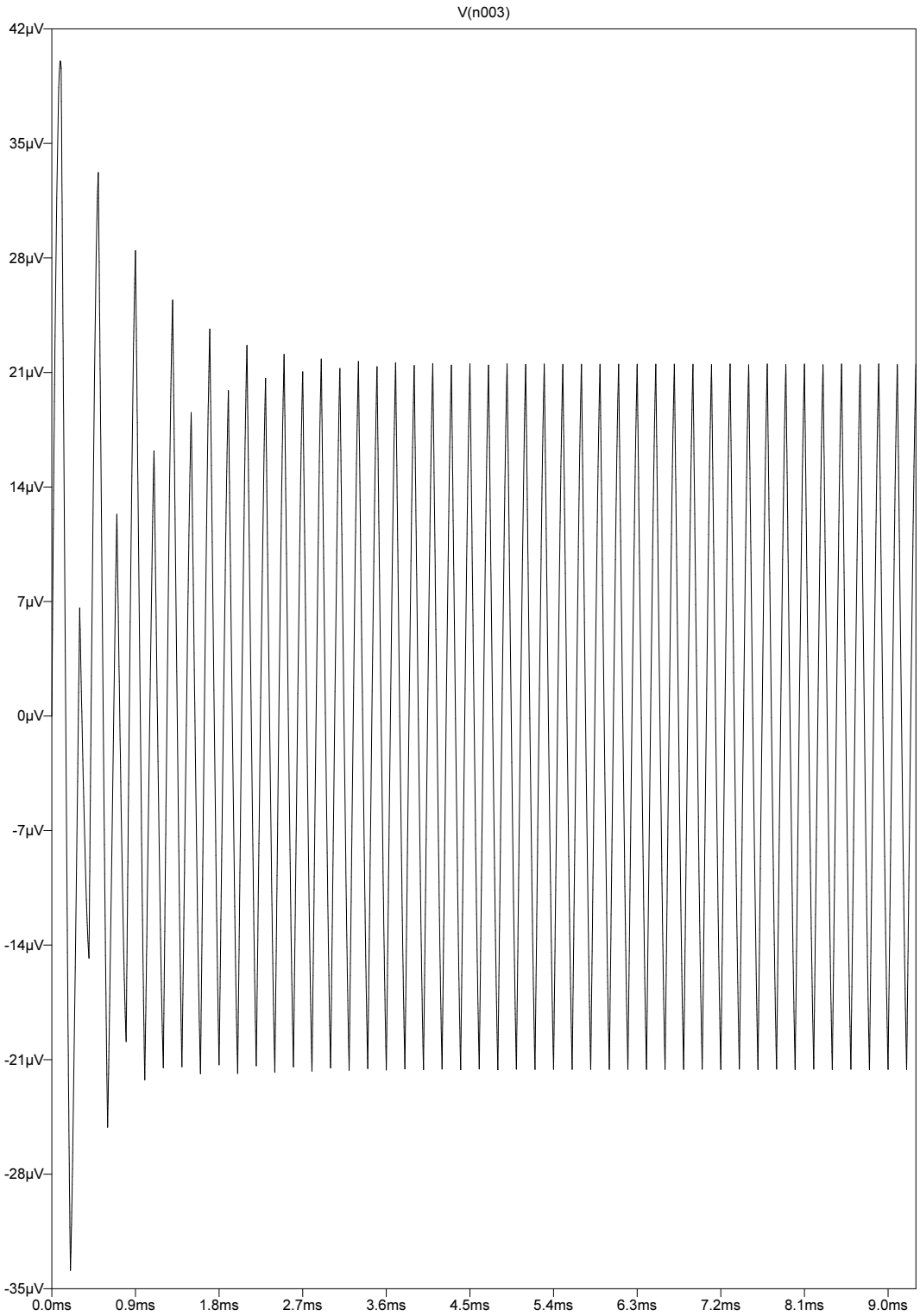

Figure 3.20: Output voltage of fluxgate with noiseless damping

3.3 Coupled systems approach

More straight deduction can be done from energy equation of inductor 6.36 described with generalised coordinate Φ and force I. Definition of magnetic flow $U = \frac{\partial \Phi}{\partial t}$ defines the mutator which transforms resistive element group to reactive element group[1]. Because fluxgate's core (like every magnetic amplifier) equivallent circuit have form of nonliear symmetrical lattice (Guillemin, 1953) and its realisation with diodes are antiparalel diode ring, this element with addded resistor gamma network on each side (to simulate magnetic leak) and bracketted by two nongyrating mutators gives model of complete magnetic amplifier (fig. 3.21). Note, that magnetostatic circuit (Heaviside, 1922) on the left side of the mutator has dual form (resistance corresponds to permeance P_m); This is standard meaning of magnetostatic analogy, because Hopkinson's law for a reluctance resembles inverse of the Ohm's law:

$$R_m = \frac{I_m}{\Phi} \qquad R = \frac{U}{I} \tag{3.1}$$

And for permeance holds analogy of Ohm's law directly:

$$P_m = \frac{1}{R_m} \qquad P_m = \frac{\Phi}{I_m} \tag{3.2}$$

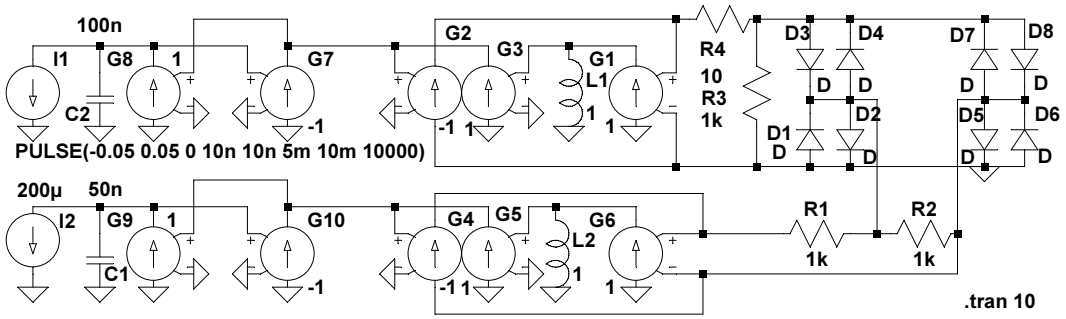

Figure 3.21: Magnetic amplifier: Coupled system model

Nongyrating mutators can be simutated as cascade of normal mutator (three VCCS) and gyrator (two VCCS). Hence total number of controlled surces needed for simulation is ten (instead of two used in fig. 3.12). These models can be useful for simulation of cross-coupling phenomena in the ferroresonant parametric transformers in power electronics (Hannemann, et al., 1977). Figure resembles model of the condenser microphone (fig. 2.2), with only one difference that both branches are in the electric domain. In the case of microphone model, one branch is in the acoustical domain and the next one is in the mechanical or acoustical domain. In semiconductor physics modelling there are also circuits where some branches believes to the electron / hole concentration in the semiconductor. These models were introduced by Linvill (1963). Another interesting fact is, that model is (excluding resistor) symmetric. This resembles, that pump and sense winding of the fluxgate sensor (fig. 3.2) can be interchanged. Because of different magnetic leak, this "reciprocal" fluxgate has big spurious signal and can be used as an sensitive indicator of quality of manufacturing of the sensor unit.

[1] Mutators in combination with nonlinear elements can be used for modelling of more exotic elements as the memristor (resistor with the charge memory) as described by Chua (1971)

3.4 State of the art

Fluxgate magnetometers are based on magnetic amplifiers. Magnetic amplifiers was used in power electrical engineering (Zell, 1899) [1] power radio electronics (Alexanderson, 1916) and telecommunications since the beginning of the 20-th century (Petterson, 1929). They use ferromagnetic material which changes its permeability inside a sensing coil and thus pumps up parametric resonance in the sensing coil - capacitor system. The construction of the pumping coil determines the type of magnetometer (Primdahl, 1970). The orthogonal fluxgate magnetises the material perpendicular to the measured field. Other types of magnetometer (Vacquier, Foertster, ring-core (Aschenbrenner et al., 1936), rat-race) magnetise the material in the direction of the measured field, hence the balancing of pumping coil(s) causes no coupling of the pump signal into the sensing coil. Ring-core, rat-race and orthogonal fluxgates works without an air-gap in the pump circuit and allow saturation of the core, which is analogous to power-cooling in varactor parametric amplifiers (Penfeld et al., 1962) and is fundamental for low-noise performance. The construction of fluxgate magnetometers has improved somewhat in time. Serson et al. (1957) used a tuned sensing coil. Acuna (1974) used ferroresonant pumping. Temperature stability was also solved by the thermistor (Primdahl, 1970) or by the temperature dependence of sense winding of the sensor using a Howard current source in the field-compensation mechanism (sometimes augmented with platinum wire thermometers) (Narod, 1987). A diagram of a typical thermally uncompensated fluxgate is shown in fig.3.22.

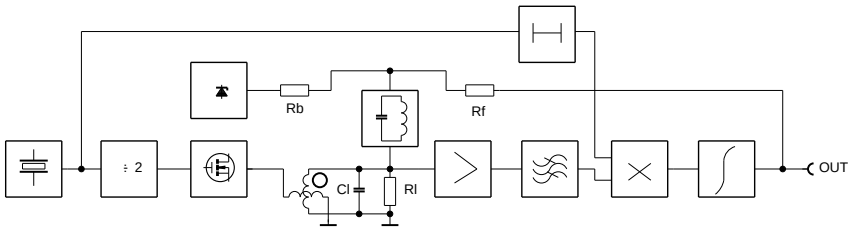

Figure 3.22: Fluxgate magnetometer typical schematics

Classical design of Acuna et al. (1978) is highly accepted till today (Connerney, 2012) as a very low-noise instrument and facsimile of his drawing are on figs. 3.23 and 3.24.

[1] It is interesting, that simplier apparatus - transductor - was patented lately by Lahmeyer (1902)

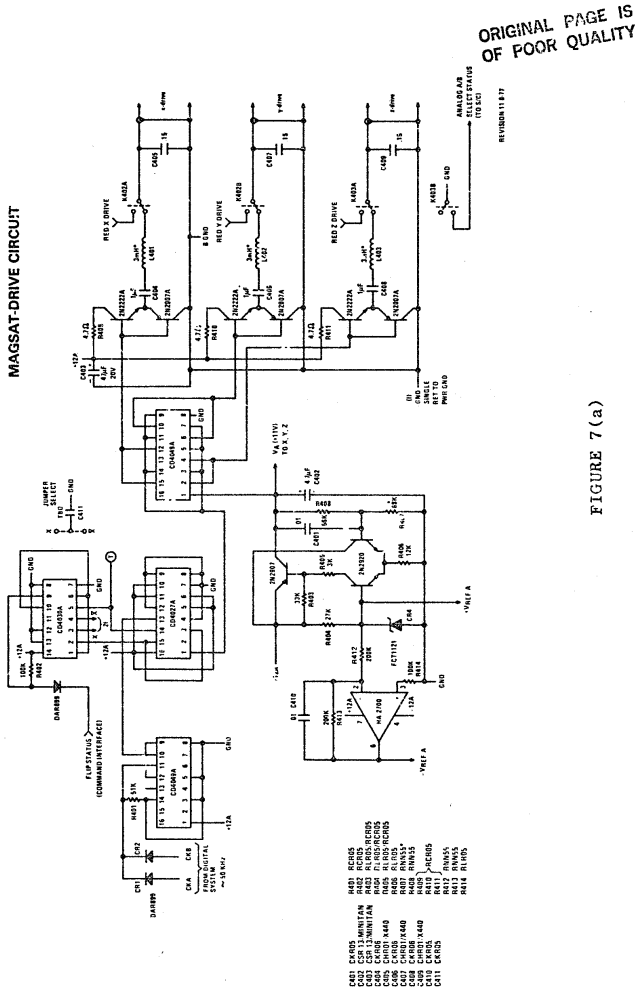

Figure 3.23: Acuna's magnetometer: pump unit

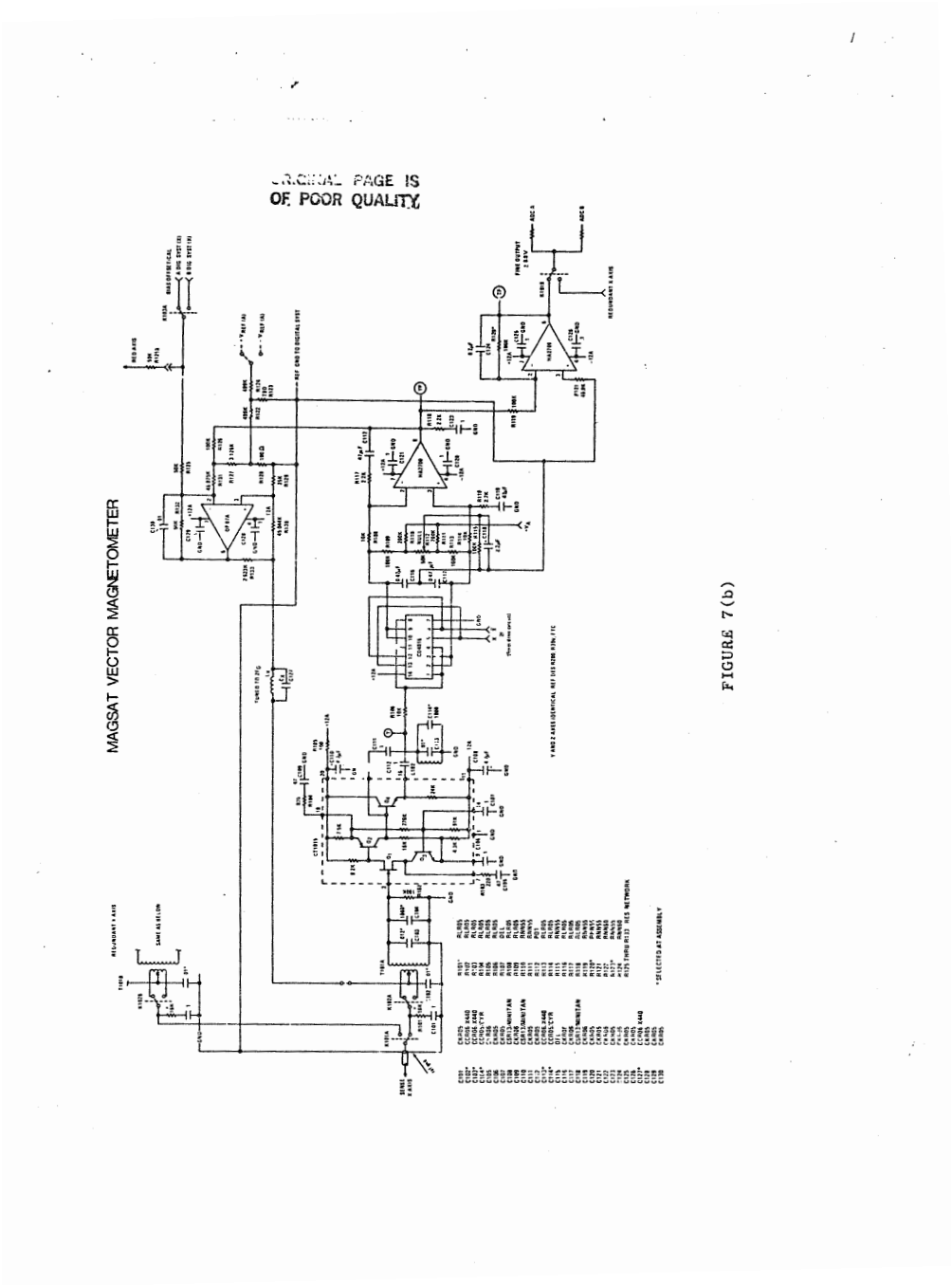

Figure 3.24: Acuna's magnetometer: preamplifiers

This type of magnetometer has several noisy elements which can be omitted or reduced:

- Pump oscillator and dividers must be low noise - (part of $1/f$ noise depends on it) - use low noise topology of Quartz oscillator and synchronous divider;
- Core driver must be low-noise (use switched MOS PA with external commutation);
- Load resistor R_l can be realised by reactance-feedback with low noise.
- Tuned notch can be removed by using different circuit topology;

- Bias resistor can be higher (with lower current noise) if reference voltage is higher;
- Phase detector is sensitive to phase shift - use envelope detector instead of phase sensitive detector[1];
- Resulting analogue signal is affected by $1/f$ noise of A/D converter - use DSP at sensing (idler) frequency instead of analogue processing at the baseband. [2]

3.5 New development

System diagram of the developped analogue electronic is on fig. 3.25 .

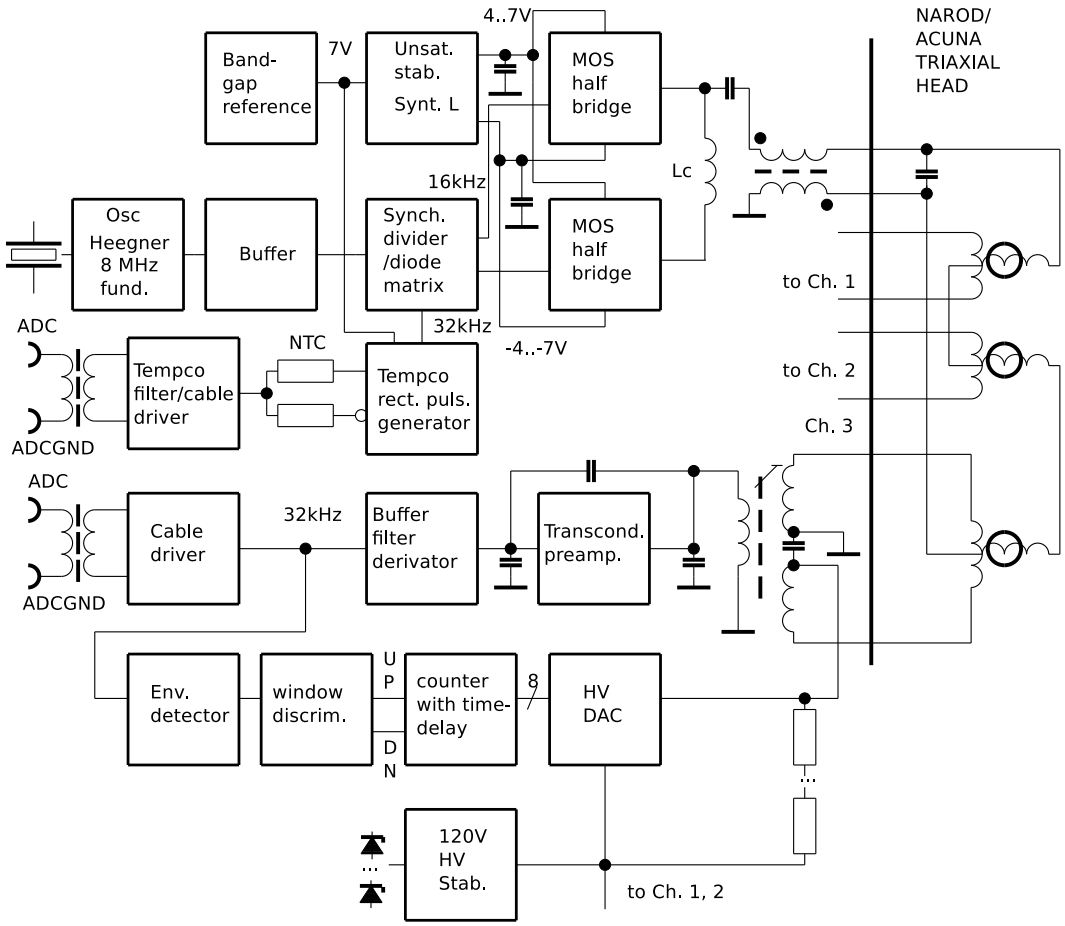

Figure 3.25: Fluxgate magnetometer schematics

First part of the pumping system is an oscillator. It is known, that significant fraction of the low-frequency noise of the parametric amplifier is caused by its phase instability. The

[1] Cerman, et al. (2008) showed, that parasitic phase shift of the DC feedback null type fluxgate with ferroresonant pumping and phase-sensitive detector is a dominant source of its temperature drift. He realised DPLL in FPGA for adjusting voltage pulses from ferroresonant pumping system to phase sensitive detector and this rather complicated circuit compensates the drift.

[2] Someone can have an conjencture, that modern auto-zero operational amplifiers's (i.e. OPA335) self $1/f$ noise can be neglected. The main problem lies in internal oscillator of these component which can not be locked on the frequency source of the magnetometer and thus can cause interferences in the instrument.

oscillator noise in the older magnetometer design was so drastic that they worked in the feedback mode, in which the noise of the oscillator is partially attenuated. Since feedback mode processing is hard to digitise, we decided to improve the parameters of the pump circuit to fall be below the noise of the sensor.

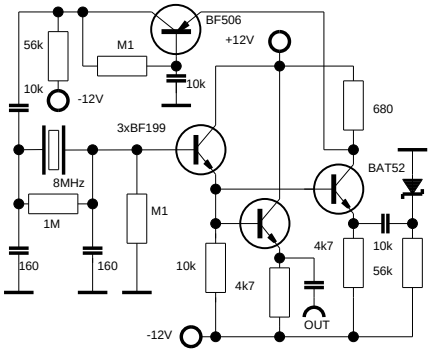

Figure 3.26: Heegner oscillator

The designed oscillator (fig. 3.26) uses 8.448 MHz fundamental mode (first-harmonic) quartz in rather uncommon Heegner topology. It is known that the in-system Q-factor of a pieso-electric resonator can be much lower than its physical Q-factor, which is of the order of millions for the best units. The main degradation is caused by the resistive part of "what is seen by quartz". To decouple the resistive part, it is best to load the unit with large capacitors. Also the resistive part can be artificially augmented by limitation of the oscillation at the stage near the quartz. The limitation of this amplitude is prevented in the second stage by amplitude dependent negative feedback. Clockmakers know that the oscillator (pendulum) must be affected by clock mechanism for as short a time as possible. This is the electrical realisation of this fact. The circuit starts oscillations as a normal A-class oscillator and, when the amplitude increases, it goes to class C. The next stage is the shaping circuit (fig. 3.27).

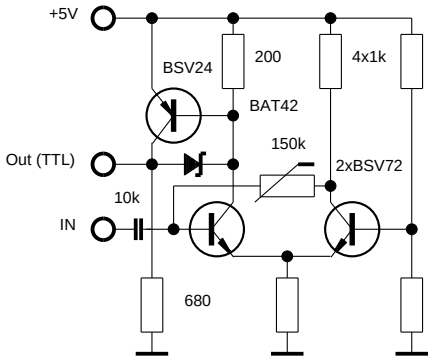

Figure 3.27: Shapper

The shaping circuit is a two-stage CE amplifier, the first stage being emitor coupled to CB helper transistor, which completes the positive feedback loop into the input stage and what helps to shape the output rectangullar wave. The second stage CE amplifier has a desaturation diode and couples the output signal to the Schottky logic buffer. After the buffer signal has been divided by the synchronous divider by 2^6 (cascaded two 74HC163) to obtain the frequency of 132 kHz, the next divider by 2^3 is shown in fig. 3.28:

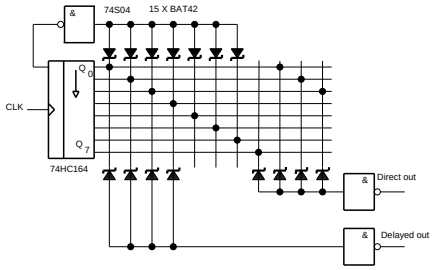

Figure 3.28: Divider with overlapping output

The divider generates two 16.5 kHz rectangular slightly shifted waves. The reason is that the ferroresonant circuit, where pumping is realised by rectangular voltage and a series reactor does not have the autocommutation property needed for low noise run of switched MOSFET PA (fig. 3.29). The external reactor between the amplifiers is used only for the commutation. This property was confirmed by before PA circuit design. The power amplifier respects the design of the very small VLF transmitter, in which the IC normally used as a power transistor driver is used as a power element.

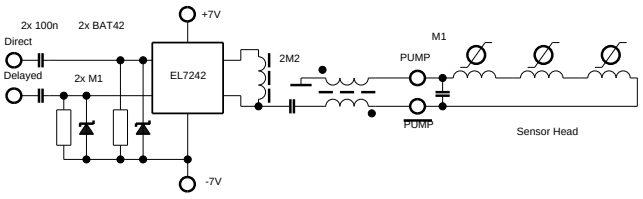

Figure 3.29: Power Amplifier

The ferroresonant circuit uses a transformer instead of choke which symmetrises somewhat the output signal. Since the pump signal must have low second-harmonic content, the symmetry of the rectangular wave is critical. To obtain the symmetry, the power supply to the switched PA is made of two complementary sections and is stabilised by a proprietary unsaturable stabiliser (fig.).

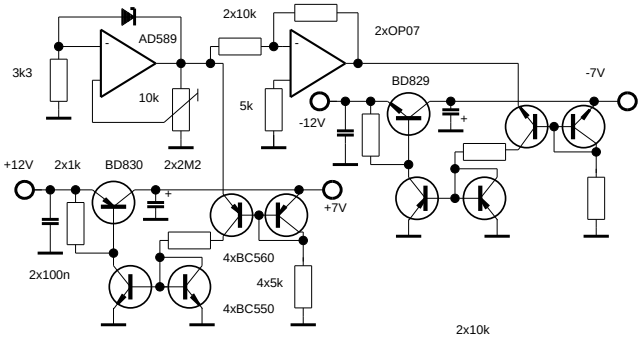

Figure 3.30: PA Stabiliser

There is only one pump section in the triaxial magnetometer. The signal sections are three. There is one complete system for each axis. The system is modular, which simplifies repair. It is easy to repair the module in the axis where the signal can be cancelled mechanically by

turning of the arretation knob of the Ascania stand for axis D,I. In the Axis-F, the working unit is a must for beginning the operation. The signal induced in the sensing coil is fed into an amplifier (fig. 3.31).

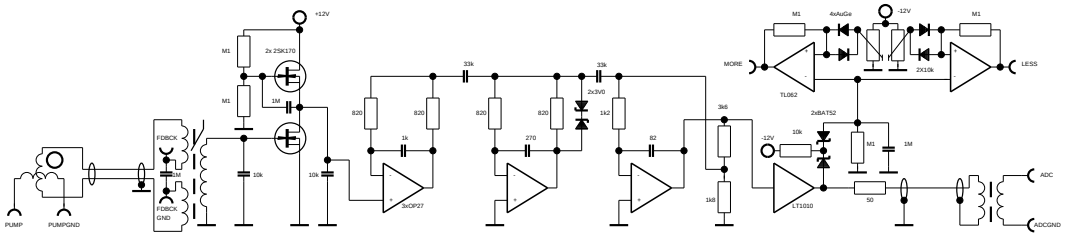

Figure 3.31: Input amplifier

The input transformer has a splitt primary winding for using symmetrical shielded input cables (this is called T-power in microphone technique). In the middle of the splitt primary winding there is a capacitor, which serves as an untuned decoupling element for the PERS System to be described below. The transformer is also constructed with an air gap, which allows some DC current to flow through it, and which is used for zeroing the geomagnetic field component in the case of the F axis. The secondary winding of the input transformer is loaded with a highly stable polystyrol capacitor. The shunt resistor is replaced by a special construction of input amplifier: inverting integrator bridged by a capacitor. The bridge capacitor is realised by the Miller capacity of the input transistor. The input impedance of this system behaves like resistor cooled to low temperature and it was described in the introduction of this thesis. Since the first stage works as an integrator, the remaining circuit must work as an derivator in the frequency band of interest to obtain flat frequency transfer. The filter-derivator was synthetised with leaky synthetic L building blocks with somewhat non-standard input and output. For the purpose of design, the whole input amplifier was simulated to determine its sensitivity to component variation. The simulated circuit is shown in fig. 3.32.

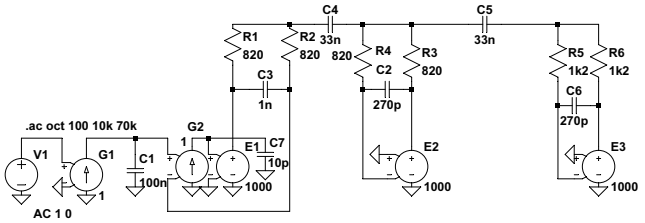

Figure 3.32: Model of input amplifier

Sensitivity of the derivator was checked-up by simulation using SPICE in the frequency domain. The deformation of the frequency transfer curve due to the dominant pole of the first operational amplifier is in fig. 3.33:

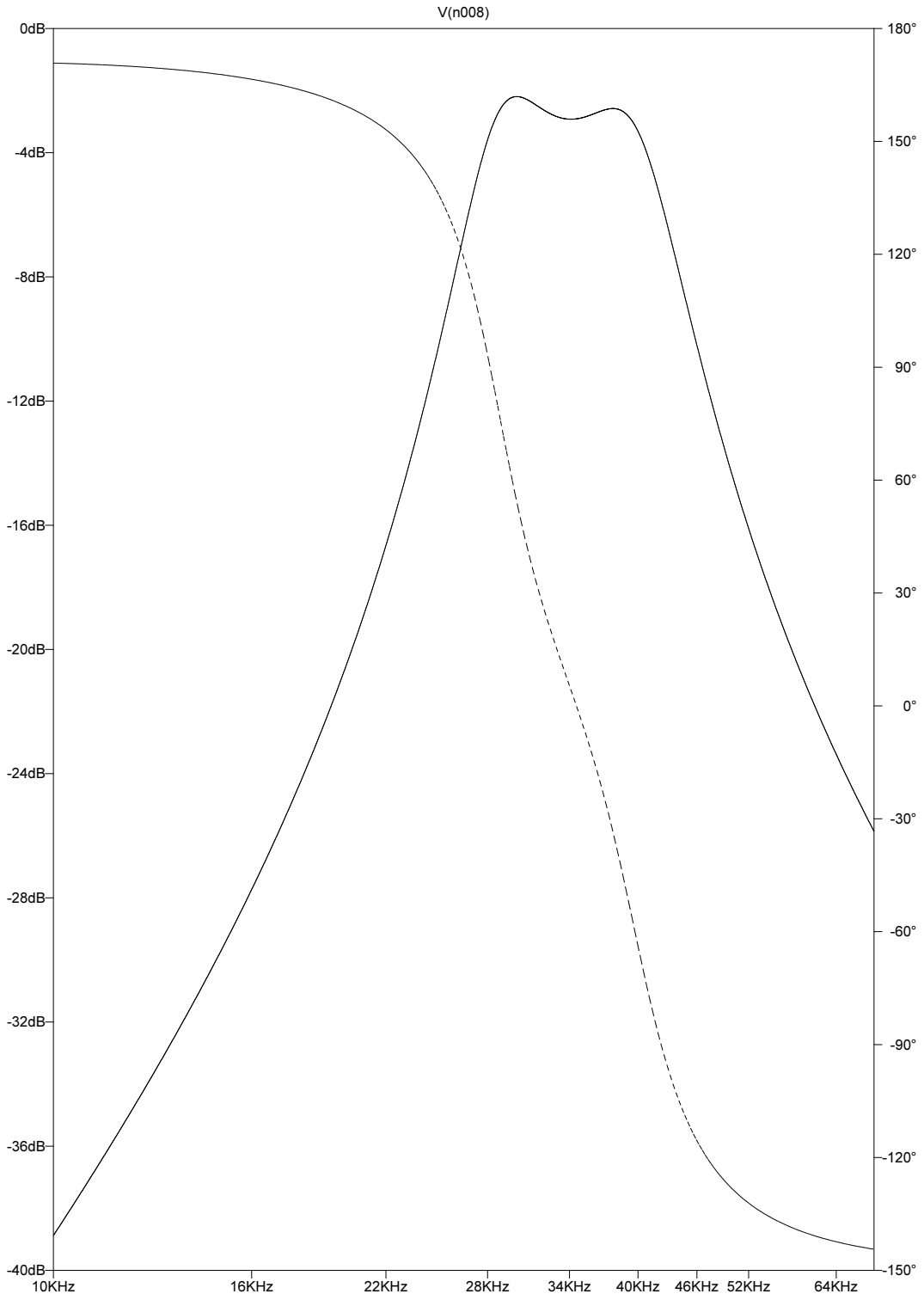

Figure 3.33: Transfer characteristics of the model

The input circuit also consists of a line-buffer and helper envelope detector and comparators which yield signals for PERS, realised independently of DSP. An interesting point of the scheme are the Zenners antiseries inside the middle synthetic L, which works as a snubber for parasitic instability occuring when the system is overloaded. This situation may begin

when the system is started and the PERS has not yet choosen the crude range - and working as a counter.

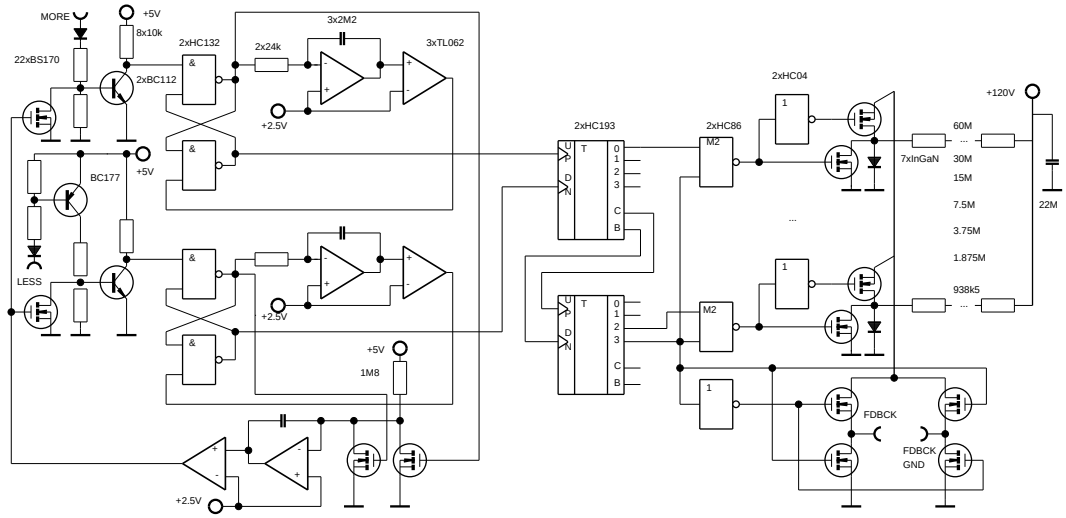

Figure 3.34: PERS

The peak elimination circuit was inspired by the La Cour recorder described above. This approach allowed us to use separate DSP for difference signal and analogue processing for PERS. The PERS circuit logics consists of the envelope detector, comparators, asynchronous counter, set of weighted resistor chains and MOS switches in current mode. The design idea remains the same as in the AMOS stand-alone controller, but asynchronous hardwired logics is used instead of a microprocessor (for minimisation of interferences), and discreete semi-conductor switches with resistor chains in wired assembly is used instead of D/A converters because of high voltage. High voltage was chosen because some reports ranked the noise of Narod (1987) system worse that of the original instrument of Acuna (1974) (which was in fact a low-field space magnetometer). The only difference between the two systems was the maximal measured field strength and, then, the value of the feedback resistor. If we want to use a bias resistor of the similar value like as Acuna's (in the order of 100 kOhms) for a high-field instrument, we must use high voltage. To achieve low $1/f$ noise of the resistor, chains are used instead of simple devices for lowering the device terminal DC voltage. A deeper analysis is in Appendix E. The PERS for D,I has a current-mode MOSFET commutator, The PERS for F has a bias resistor chain.

The PERS units use a 120 V precision source. It use a Zener diode chain - thermistor bridge in the feedback instead of the classical topology (reference - feedback divider comparison). The advantage of this topology is that we can use a chain of low-voltage Zener diodes in series which can decrease the noise (by 3 dB per doubled components). Also the properties of the Zener diode, instead of the avalanche diode, may be interesting if noise induced by cosmic radiation is the issue. It is today's trend it electronics to omit avalanche devices in electronic and opto-electronic systems. In fibre-optical networks, avalanche photodiodes were replaced by cascade EDFA - PIN photodiods for better noise performance. In reference sources, avalanche diodes are replaced by Widlar band-gap reference although the noise performance is limited by a current mirror.

Temperature sensing unit uses 32 kHz output from diode matrix of the synchronnous divider.Switched MOS circuit is used to generate rectangullar pulses to fed symetric line buffer connected as an invertor. First harmonic from the termistor half-bridge is filtered by resonator.

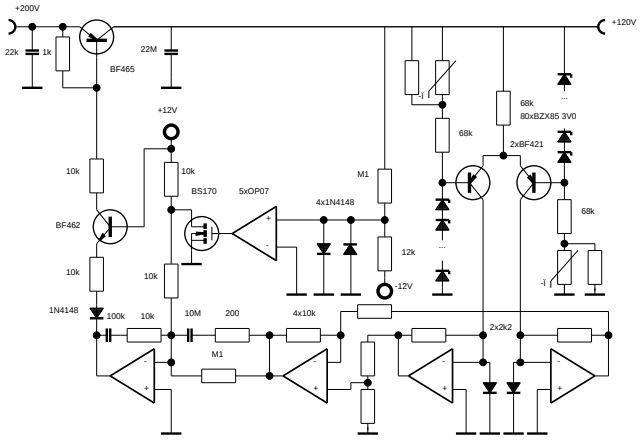

Figure 3.35: HV source

Signal is then fed via normal AC power cable to the acquisition house (with the distance of 60 m from the sensor) and processed by the same way as the fluxgate signal.

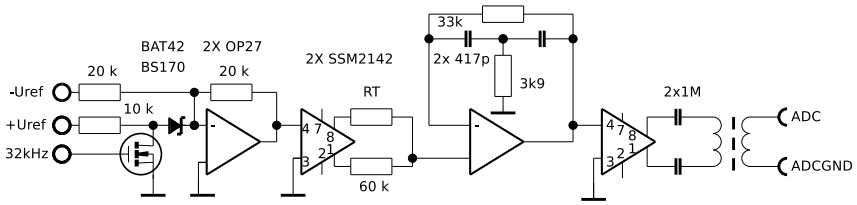

Figure 3.36: Temperature sensor

3.6 Solid state power amplifiers in switched mode

Circuit diagram in fig. 3.29 is small solid-state ultra low wave transmitter. Solid-state transmitters have several construction problems which must be properly handled to make construction reliable. Semiconductor devices are usually used outside the manufacturer-guaranteed regime, and good knowledge of technological device limitations is necessary. There also exist classical solutions, which are reliable and display well-known behaviour, but have difficulties in system design. Let us illustrate the situation on a simple half-bridge configuration.

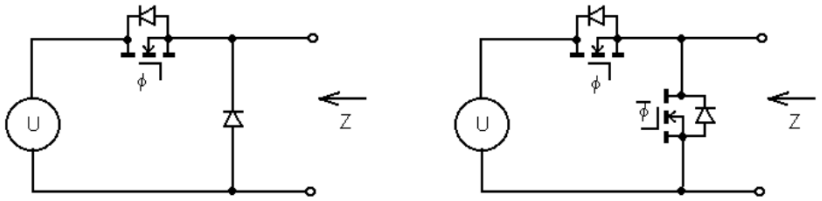

Figure 3.37: Two forms of half- bridge

Let us examine the circuit on the left-hand side of fig. 3.37. If the load is pure - resistive,

the duty cycle of ϕ has direct impact on the output power. But when the load is lossless filter-loaded resistance, behaviour of the output power depends also on the property of the filter. The impedance, which loads the filter at its input side, depends, on the polarity of the input current when ϕ is in the closed state. The circuit in the right-hand part (half-bridge) has no such difficulty at first glance, but when the switching frequency increases and the transistors do not have equal times of switch-on and switch-off, driving impulses ϕ and $\overline{\phi}$ must then have a dead time betwen them to prevent short-circuit of the power supply.

During the dead-time, the impedance at the input of the filter is also indefinite. Another problem is that the substrate diodes of the transistor have relatively slow recovery times and it is paramount to filter circuit to make conductive the diode of the transistor, which will become conductive after the dead-time ends. This property is called external commutation. If this property is maintained, the transistor switches to the zero voltage regime which decreases its switching losses and noise. It also makes the reliability higher, because the situation, in which lower diode is conducting and the upper transistor switches on, does not occur. Some circuits have the autocommutation property: i.e. Class D audio power amplifier half-bridges usually feeds the output series L shunt C gamma filter. Since the transition frequency of that ‘filter’ is far below the switching spectrum, autocommutation occurs. Other circuits are PWM modulators made for different reasons.
The typical construction of a general solid-state transmitter is in fig. 3.38.

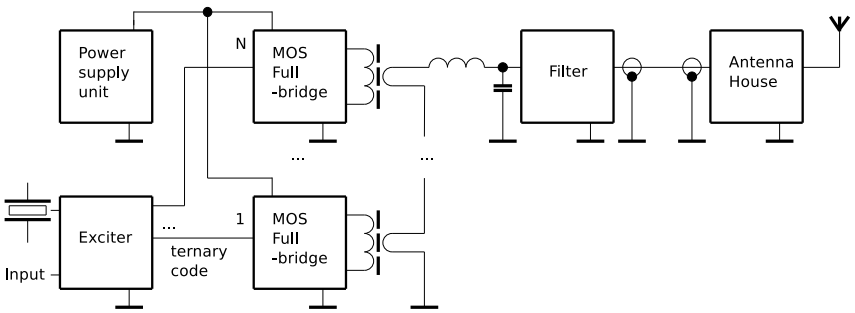

Figure 3.38: Solid-state transmitter

Amplitude modulation is effected by switching on the units. When better signal properties are required, part of the units in the transmitter are realised in binary-weighted scale of amplitude, normally up to 9 bits of resolution.

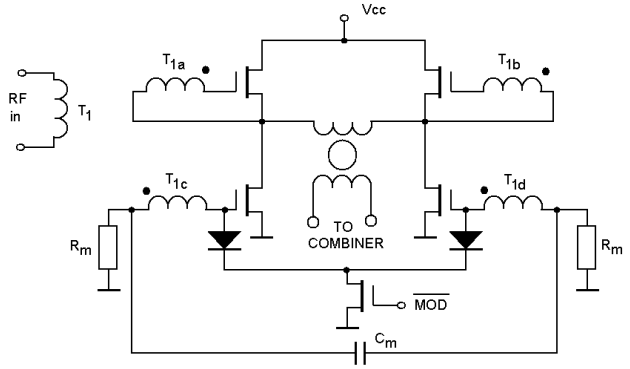

Figure 3.39: Swanson unit PA

Commutation is done by tuning of the output circuit, which is a series-L shunt-C gamma impedance transformer followed by a Zobel-type constant-impedance low-pass filter. The construction of the output circuits affects both transmitter reliability (commutation) and distortion of modulation (impedance properties of the unit in the off-state). The output circuits and their tuning procedure is then the know-how of the manufacturer. Evidently, that for the carrier frequency, the unit corresponds with the left-hand part of fig. 3.37 for DC.
A problem occurs when the commutation conditions of the external circuit cannot be fulfilled. Example of this situation is the narrow aerial in the ULW transmitter. Such that transmitters are used typically for military purposes as hot-swap for GPS/GLONASS/IRRIDIUM systems, because these systems can have drop-outs due to atmospheric and ionospheric disturbances. For optimal output-pulse forming of a typical LORAN transmitter, several ‘negative’ units are required in the combiner chain (fig. 3.40).

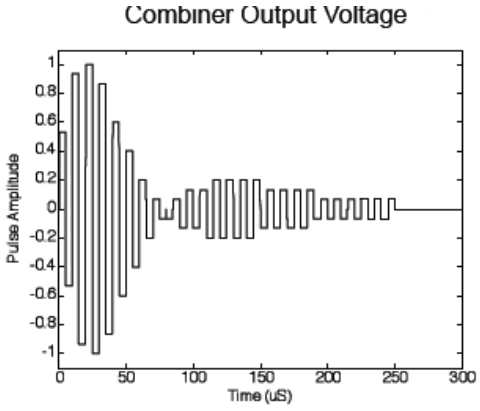

Figure 3.40: Loran - pulse modulation sequence (Hardy, 2008)

This can be done by adding additional units with an antiphased combinational transformer. But this solution will not work with Swanson units, because other units which are switched-off will behave as diodes in the opposite direction and decouple these negative units from the antenna. There is only one solution: to change the switching strategy of the elements in the H-bridge (fig. 3.41).

This principle does not only work correctly from its output impedance view, but it also allows outphasing modulation. This is so, because the commutation circuits are designed independently for each half-bridge, thus commutation is nearly independent of the load and thus also of the outphasing of the halves of the H-bridge. One disadvantage of this solution of the VLW transmitter is that the required commutation inductance is impractically bulky. Also the commutation inductance depends on the output frequency which may be a disadvantage when the transmitter must be retuned fast. It is better to create higher commutation frequencies by time-shift between two half-bridges which makes another half-bridge that forms the final H-bridge (fig. 3.42). This solution is rather fractal and it is possible that it will dominate in the future when the price of the transistors will be lower than the price of the capacitors.

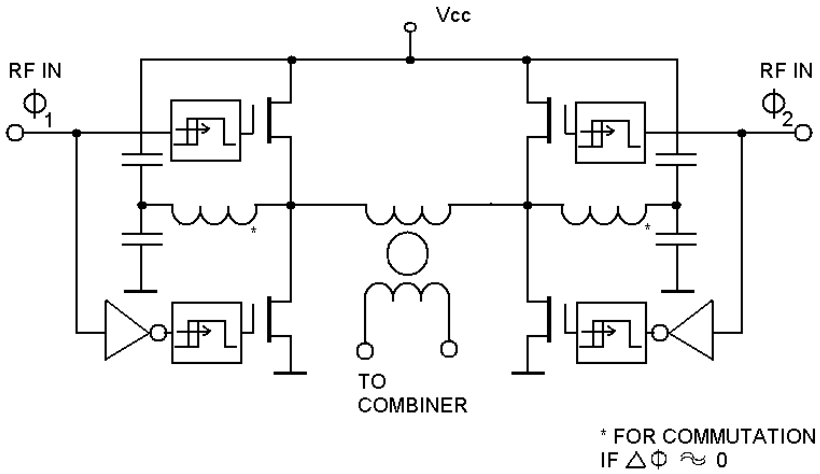

Figure 3.41: Westberg unit PA

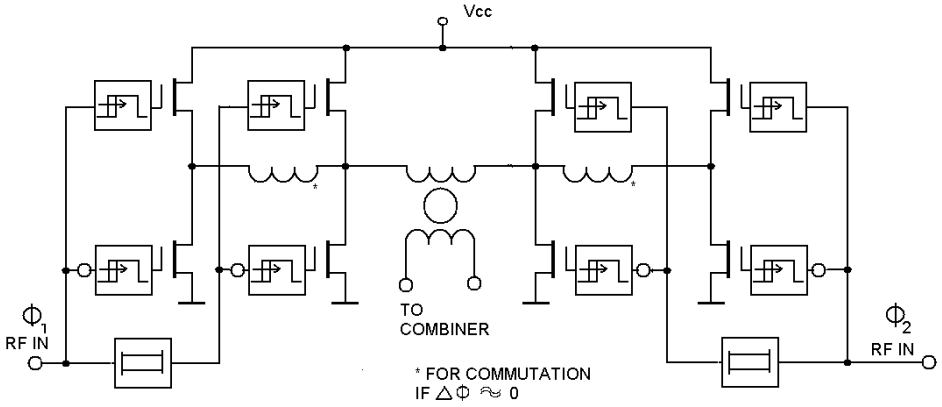

Figure 3.42: Variation on Westberg unit PA

3.7 Digital signal processing

Further processing of the signal is purely digital. The signal is digitised by an ordinary HD audio soundcard (Creative SB0570) at a sampling frequency of 96 kHz and bit depth of 16 bits. This soundcard has buggy UNIX drivers (both OSS and ALSA). When the card is used under UNIX at 96 kHz, its A/D converter operates at 48 kHz samplerate and the soundcard interpolates the signal to 96 kHz, which was established by measurement. When the MS windows driver was used, the card behaved correctly. The solution was to write software for UNIX with a platform independent library (portaudio.h) and to cross-compile the code with a MINGW32 cross-compiler to windows. The code is relatively compact and it is given in Appendix C. The code presented on the acquisition computers (there are two because there is no possibility to run two soundcards in a windows computer without device conflict and three channels are needed for the triaxial fluxgate instrument). Its output is a 187.5 Hz raw data binary hourly file. The acquisition computer is also connected to the local NTP (stratum 3) server via a dedicated LAN.

The sampled signal is band-pass filtered by a 200 Hz filter centered at 33 kHz. The reason for this is removing the power-line and A/D converter noise. The signal is then fed through a

first-order allpass filter whose quadrature is at 33 kHz.

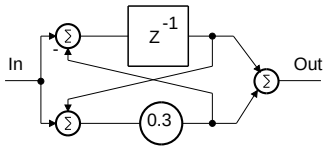

Figure 3.43: Allpass filter

The result approximates the Hilbert transform for the signal with a narrow spectrum. Since the Hilbert transform of the harmonic signal has this property:

$$\mathscr{H}\{\sin(t)\} = -\cos(t) \tag{3.3}$$

And the required information is presented in the envelope:

$$A\sin(t) \tag{3.4}$$

The addition of the squares of the quadrature signal will be:

$$(A\sin(t))^2 + (-A\cos(t))^2 = A^2(\sin^2(t) + \cos^2(t)) = A^2 \tag{3.5}$$

By square-rooting the resulting signal, we get the envelope. Note, that this simple thing, linear envelope detector, is hardly realisable in the analogue domain. As a result we have a signal which corresponds to the residual magnetic field (which is not compensated by the PERS). This residual magnetic field can never reach zero, because at this point the noise can dominate over the signal and this noise, after envelope detection, has a finite DC component. This is the dis advantage of the envelope detector as compared with the coherent detector. But the coherent detector is sensitive to the parasitic phase shift between the signal and reference wave, which can enlarge offset in a tuned-output tuned-pump fluxgate. The result must be decimated to obtain the required sampling frequency. A cascade of IIR filters is used:

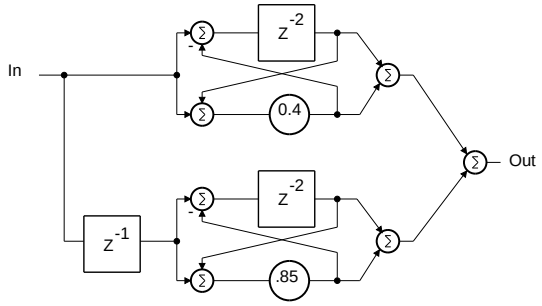

Figure 3.44: Decimation filter

This filter is used rather regularly in today's sigmadelta A/D chips. Nine such units are included in the cascade to obtain a 187.5 Hz sample rate signal. The crude data are saved in the file in an i ntel-float binary format. After the one-hour block is finished, The precise time when the last used sample was picked up is recorded at the end of the file also as a floating number. This is needed in the post-processing routine, which can remove part of the jitter induced in the NTP chain.

The postprocessing code is given in Appendix D. It is run as post-processing routine and its output is the IAGA2002 second data file. Firstly, the last data file of the preceding, whole processed day and the first data file of the next day are loaded into the memory. The time marks and data amounts for each instrument are then unwrapped, and a straight line is fitted to the points using the RMS algorithm. The parameters of the line define plesiochronous resampling. It is needed because each axis has its own time-scale driven by a free-running quartz oscillator in the soundcard. All data are firstly resampled by 2^4 by the same decimating chain as used in the acquisition system. The data from each equipment are then resampled plesiochronously (Strnad, 2013) according to the computed straigh line parameters. The resulting data are on a time scale given by the NTP server at a rate of 13 Hz.

3.8 Plesiochronous interpolation

Complex electronic systems are commonly divided into small autonomous parts - blocks. This improves construction and reliability. If each block has its own clock, there need be no central clock distribution - construction is simpler. Also a quality free-running clock with quartz resonator performs better from the jitter-point of view than a voltage controlled quartz oscillator, mainly because the varicap, which is needed to retune the quartz resonator, significantly reduces the in- system resonator quality factor. Also resonator aging can complicate the VCXO design, because the required in-system Q factor limits the tuning range. But when the quartz ages, the central frequency shifts and the useful range decreases. This is a problem of high-quality OVCXO units used in atomic standards, and the result is, that the designed lifetime of these units is 10 years. When part of the system is realised in the software, some kind of buffering is used for maintaining the stability of the code in a given operating system. From this point of view, fast response of the buffered system is impossible, and the plesiochronous system is a rule.
Let us study the general parametric system:

$$y(t) = \int_{-\infty}^{\infty} H(t,q)x(q)\,\mathrm{d}q \tag{3.6}$$

This transforms signal x to signal y. The function of two variables $H(t,q)$ is called the ‘kernel’ of the transformation.

The simple kernel is the identity:

$$H(t,q) = \delta(t-q) \tag{3.7}$$

Another kernel is the linear time-invarian system (filter):

$$H(t,q) = h(t-q) \tag{3.8}$$

where the function of one variable $h(t)$ is called the ‘impulse response’.
A special case of the filter is time shift:

$$\delta(t-q+d) \tag{3.9}$$

A system similar to identity (Eq.: 3.7) is the time stretch:

$$\delta(kt-q) \tag{3.10}$$

This system is parametric: if the input is a periodic signal, the period of the output signal differs by k.

If the time-discrete signal is processed numerically, some kind of time discretisation must be performed. The most simplified discretisation procedure is equidistant sampling. It can be modelled as multiplication of the signal by a pulse train:

$$y(t) = x(t) \sum_{n=-\infty}^{\infty} \delta(t - nT_s) \tag{3.11}$$

Since the pulse train is invariant for the Fourier transformation, its image in the frequency domain will be another pulse train with distances:

$$\Omega = \frac{2\pi}{T_s} \tag{3.12}$$

Since multiplication in the time-domain is transformed into convolution, the frequency range the signal $x(t)$ must be limited to $\Omega/2$ to prevent bands not overlapping.

There is a class of time-discrete filters which have a continuous prototype. These filters must have the same limitation to frequency contents as signals - their power spectrum must be sufficiently low at frequencies higher than $\Omega/2$ before they are sampled.

When we have a continuous prototype of filter with impulse response

$$y(t) = \mathrm{FIR}(t) \tag{3.13}$$

We can then set up an interpollator kernel

$$y(t) = \sum_{n=-\infty}^{\infty} \mathrm{FIR}(kT_s t - nT_s q)x(q) \tag{3.14}$$

Suitable low-pass filters can be made by multiplying function:

$$\sin(\frac{\alpha\pi n}{T_s})/\frac{\alpha\pi n}{T_s} \tag{3.15}$$

and window:

$$1.0 - (0.35875 - 0.48829\cos(Q) + 0.14128\cos(2.0Q) - 0.01168\cos(3.0Q)) \tag{3.16}$$

where α is smaller than 1 and represents the transient bandwidth of the filter (can be made narrower wether filter have more coefficients). Used Blackmann-Harris window gives yelds good results and is noticeably simple (Q lies in the interval $0..2\pi$). One practical implementation of such interpolator is routine in the appendix C.

The last decimation step must be linear-phase, because data are classified visually. An intermagnet-approved (5 sec to 1 min) Gaussian FIR filter is chosen. Since the range of the signal processing system is about 120 nT (range of peak elimination circuit is $3.8\ \mu$T), the resulting magnetograms resemble La Cour records if the day is not quiet.

3.9 Realisation

The Narod-Acuna triaxial set was modifiet without dismounting (all platinum thermal sensing resistors were shorted by a tin drop) and attached to Ascania stand for possibility of arretation in two angles (declination and inclination)(Fig. 3.45).

All described circuits were made on universal PCB breadboard plate and mounted into aluminium-alloy Schroff rack modified to be non-magnetic (fig.). From the left: Pump unit,

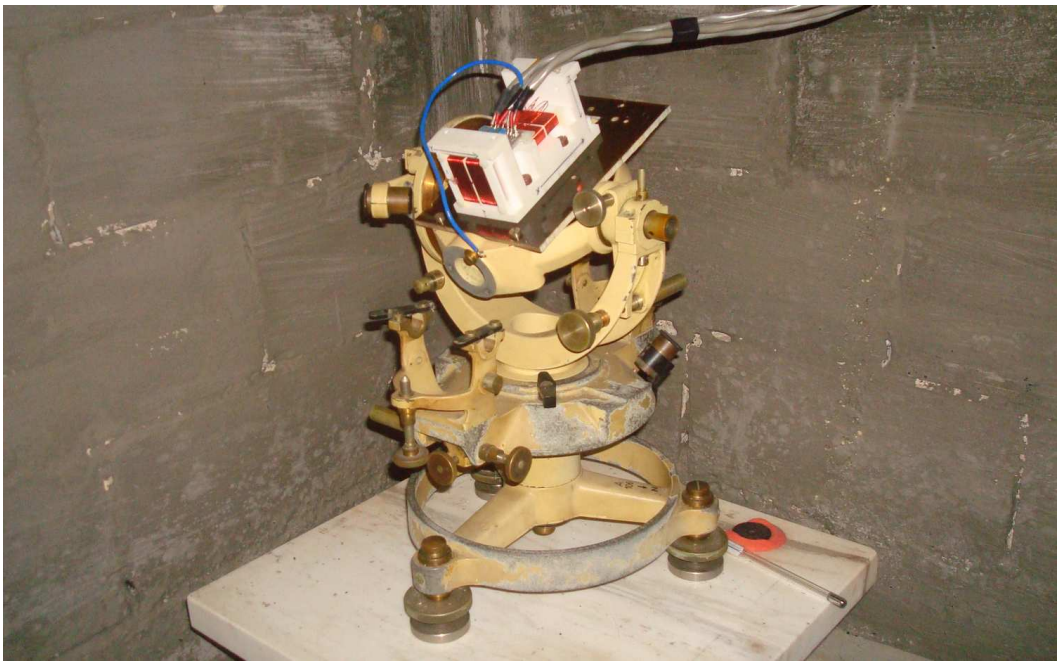

Figure 3.45: Ascania stand

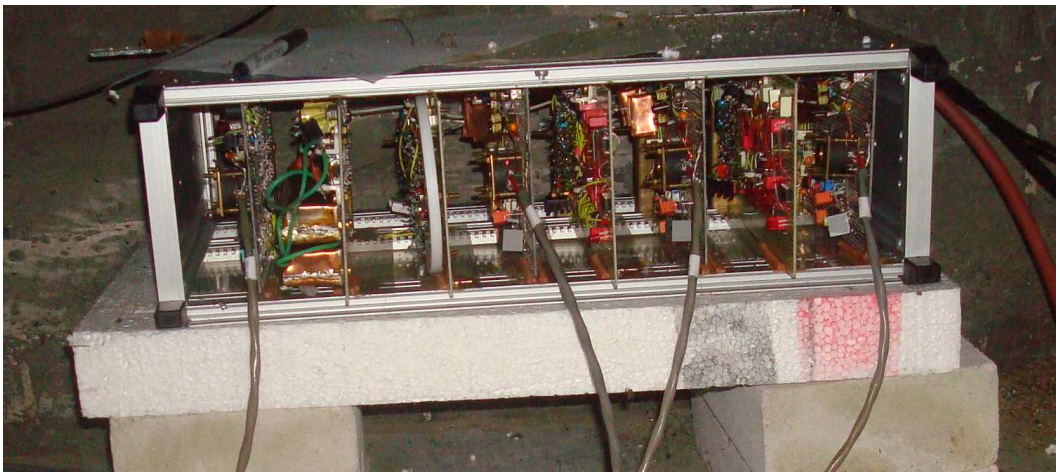

Figure 3.46: Schroff rack

HV stabiliser, F PERS unit with bias resistor on the teflon ring, F preamp, I PERS, I preamp, D PERS and D preamp.

On fig. 3.47 is preamplifier. In upper-right part of the plate is precision polystyrol capacitor what makes parametric resonance with the tuned input transformer/fluxgate system. The only element to tune is input transformer.

On fig. 3.47 is 120 V precision zener chain voltage source. Porcelain members were used where necessary. Teflon insulation CuAg wires were used for wiring. Reference diodes were sealed into wax.

On fig. 3.49 is PERS. In the left part is delayed counter, in the right part is HV resistor chains with MOS switches what is in fact current - mode high-voltage D/A converter

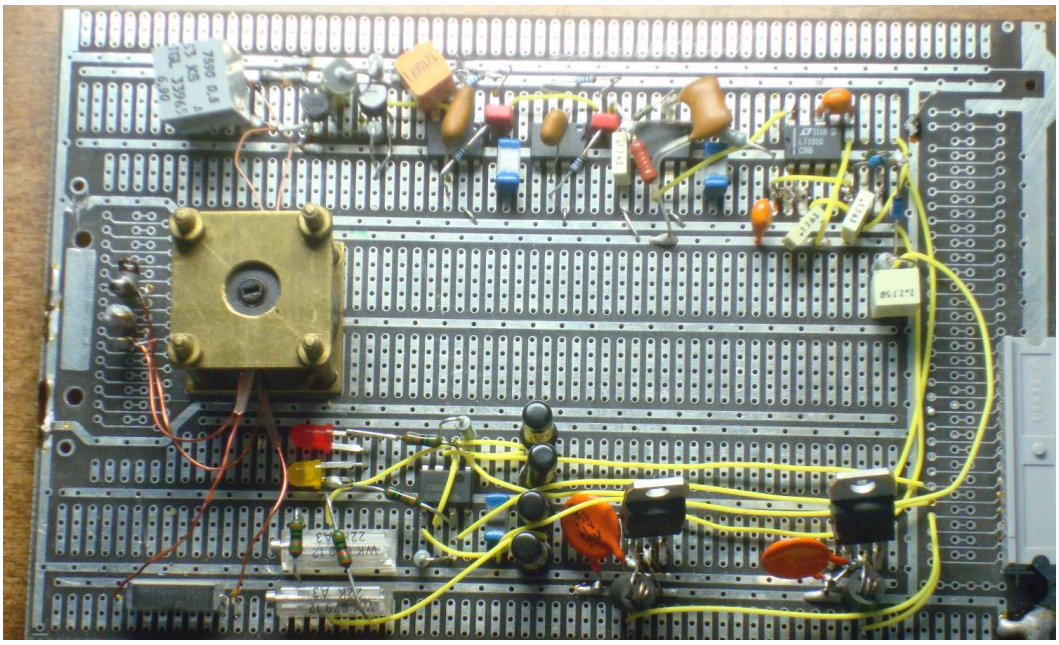

Figure 3.47: Preamp breadboard

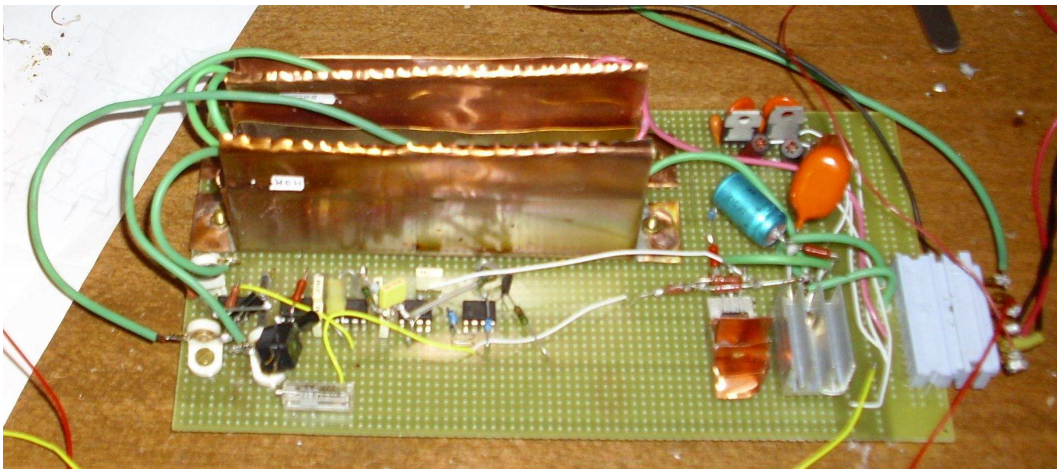

Figure 3.48: HV stabiliser

3.10 Measured values

Analogue part of the system was finished in the november of the year 2012. Since this time, nearly continual data series is logged. Digital data processing (1 sec datas to IAGA2002 files) was developped in the may of the year 2013. During lighting - caused failure in the may 2014 thermal sense system was developped, which allow us to compensate instability in the F axis. Since 14.5.2014, thermally compensated data are logged on. Thermal compensation is achieved by adding of next gauss - filter and time-delay implemented digitally on the one-second temperature data to the F axis data. Instrument have name AMOS (Advanced Magnetic Observatory System). Intercomparsion of F channell is done with two instruments: high sampling - rate Overhauser proton precession magnetometer (GSM90F1) with resolution

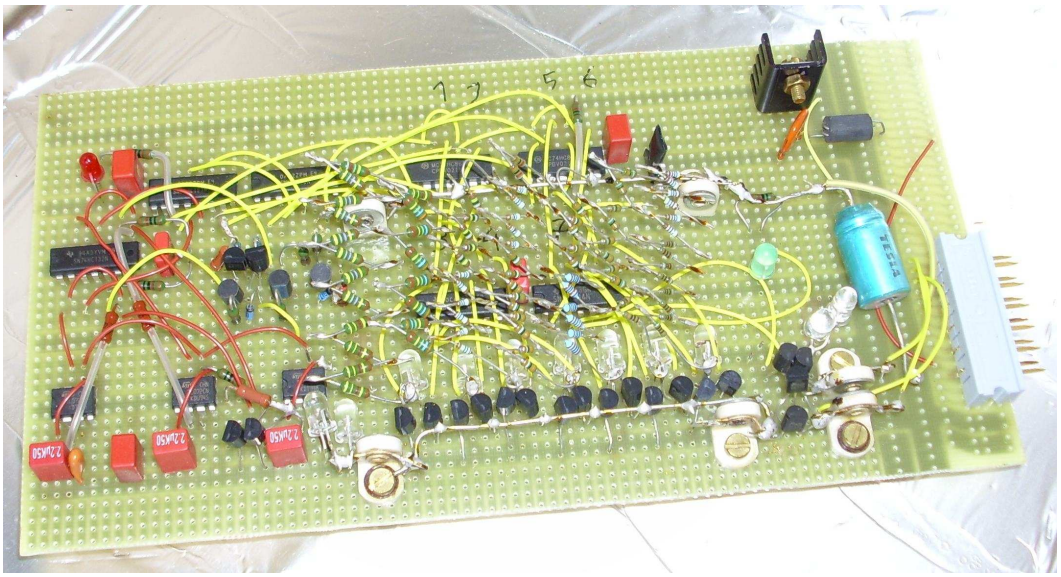

Figure 3.49: PERS

of 10 pT and sampling rate of 1 Hz. This instrument is registering since 1.4.2014 and is placed in the underground variometric room with themperature control. Next instrument is DMI suspended orthogonal ferite - core triaxial fluxgate variometer with custom PSU for low-noise 1 Hz data. Its configuration was unchanged since june 2011 and it is part od main acquisition unit GDAS (developped in BGS Edinburgh on ARM processor platform) The GDAS unit is battery powered for highest data reliability. Sensor of this instrument is oriented in HDZ direction, then data was recomputed to DIF direction to make intercomparsion. Firstly, the true horizontal intensity was determined by the vector sum:

$$H* = \sqrt{H^2 + D*^2} \tag{3.17}$$

Where H is prebased value of DMI horisontal intensity, D* is value of DMI declination (E) without prebasing and H* is true horisontal intensity. Total intensity was determined by the vector sum:

$$F = \sqrt{H^2 + D*^2 + Z^2} = \sqrt{H*^2 + Z^2} \tag{3.18}$$

Where F is total intensity and Z is prebased value of vertical intensity. Intercomparsion of total intensity of all observatory instruments is on fig. 3.50 (baseline values of AMOS and DMI was artificialy enlarged for clarity)

Intercomparsion of declination (E) is simple, because this axis is common to both instruments. It is (with base enlarged for AMOS) on fig. 3.51 .

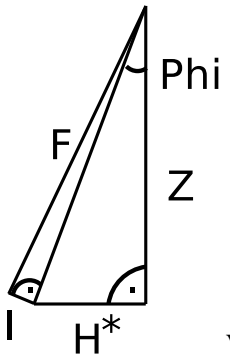

Value of inclination (V) is computed according figure in the left.

$$V = F \sin\left(\arctan \sqrt{H^2 + D^2}/Z - \Phi\right) \tag{3.19}$$

Baseline of AMOS is enlarged for clarity. Intercomparsion is on fig. 3.52. On the next figure (fig. 3.53) is hour detail of the intercomparsion V.

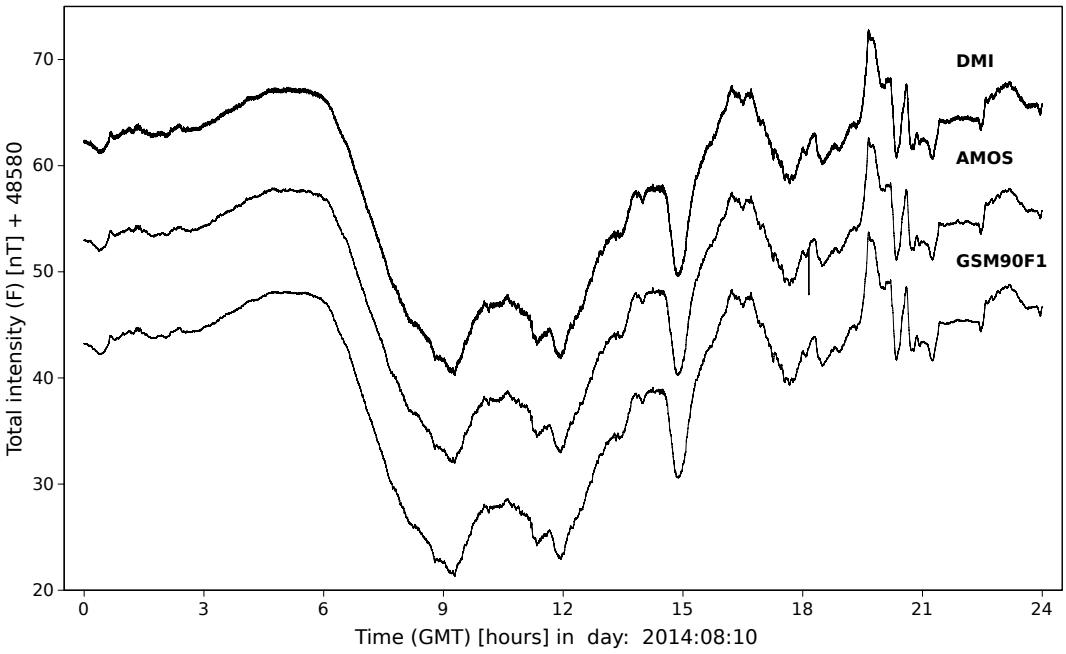

Figure 3.50: Total intensity (F) intercomparsion

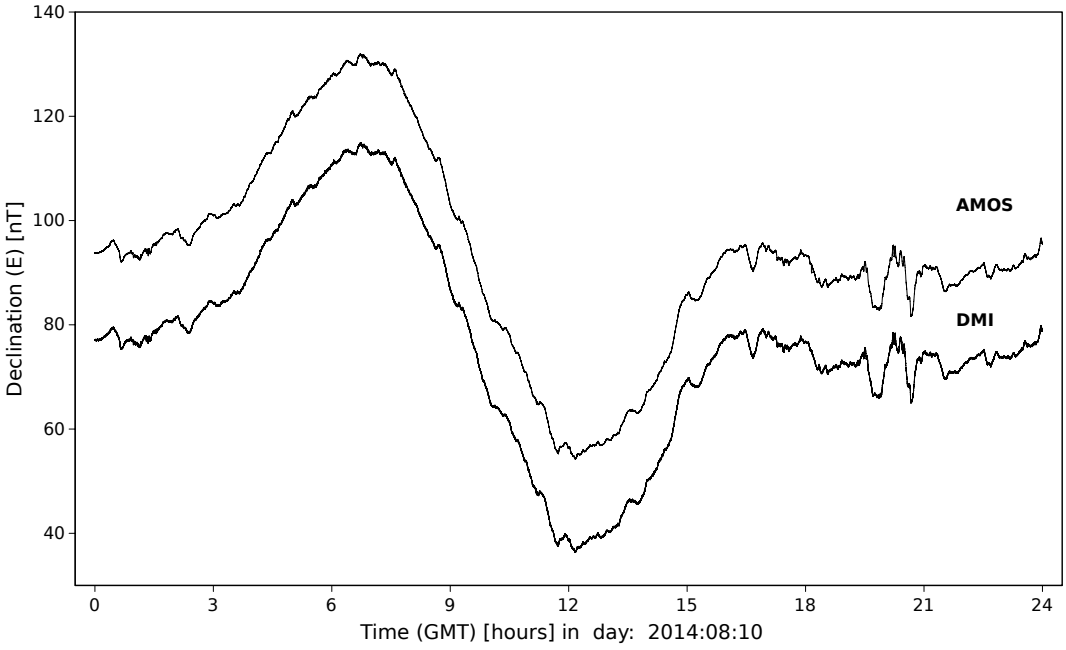

Figure 3.51: Declination (E) intercomparsion

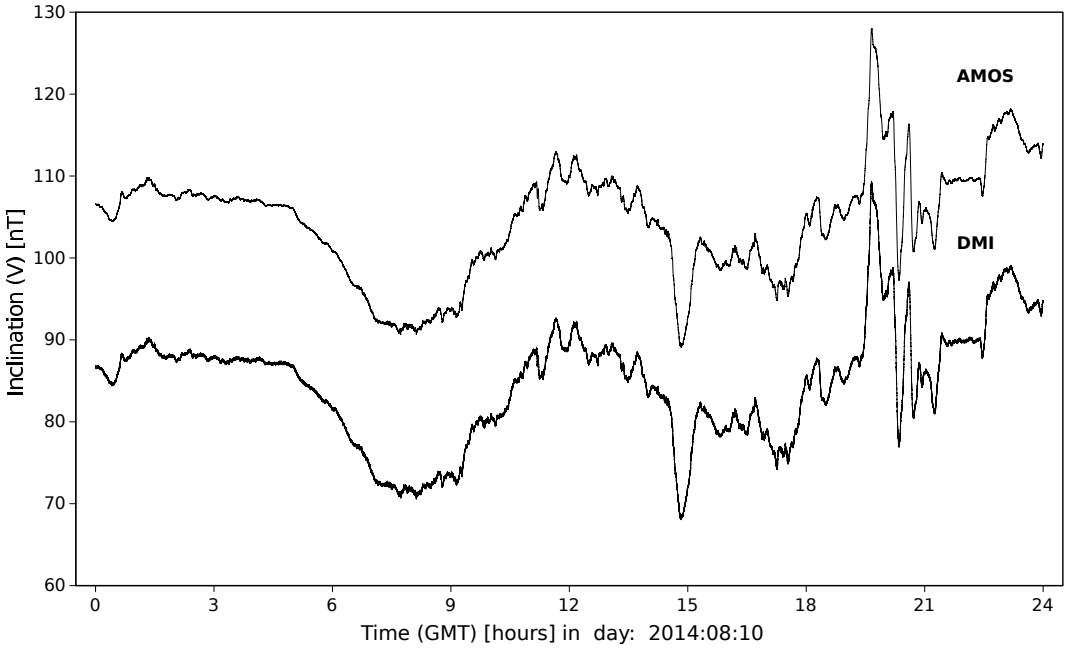

Figure 3.52: Inclination (V) intercomparsion

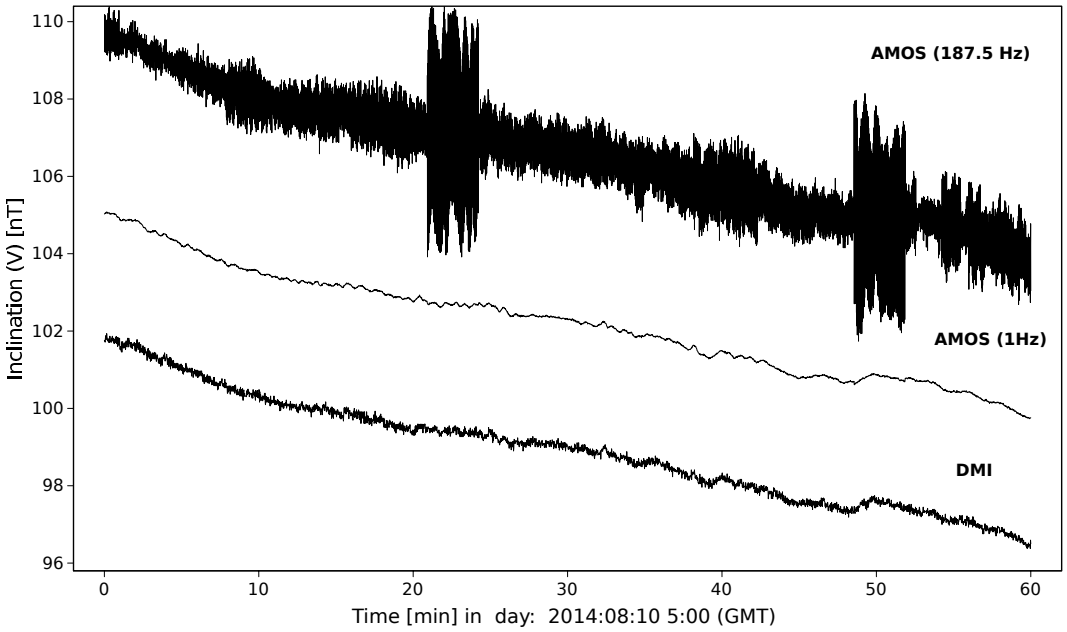

Figure 3.53: Inclination (V) intercomparsion: detail

3.11 Frequency-domain processing

Because high-frequency record is highly contaminated by power electricity (230/400V $\sim$ 50 Hz), what is variable due to temperature regullation in the variometric hut, it is better to perform spectral analysis. The analysis was done for one hour datas of the instrument "AMOS" (fig. 3.53) and are on fig. 3.54

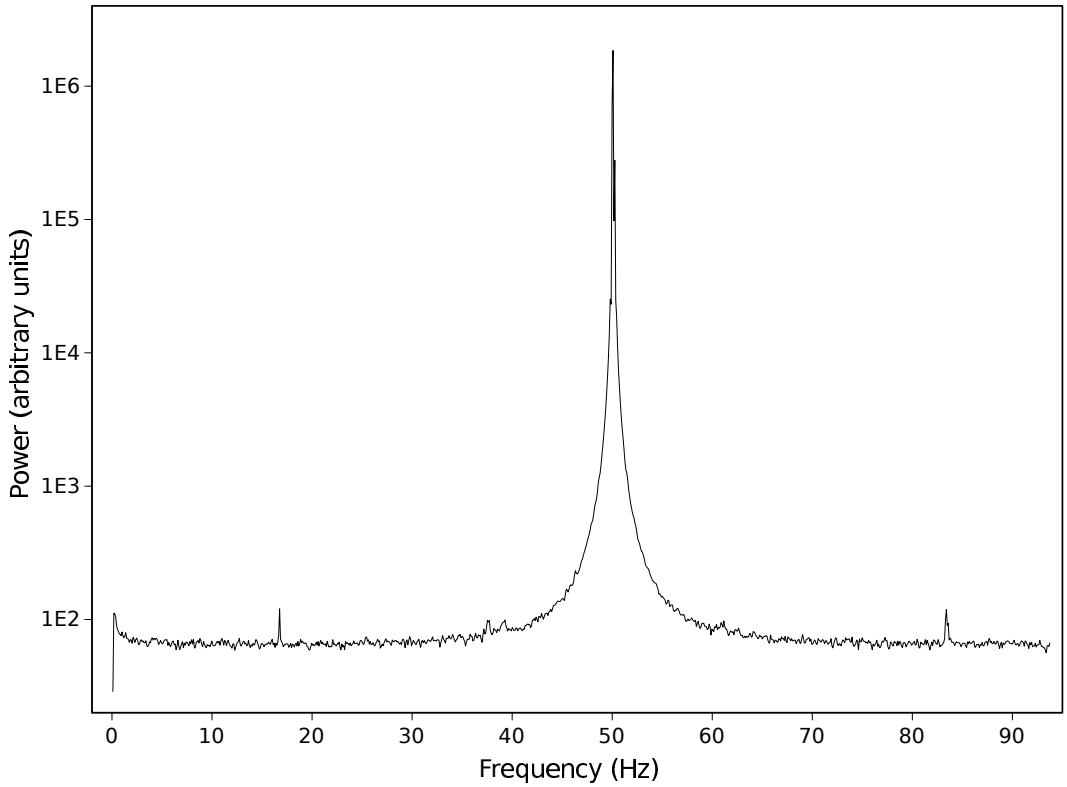

Figure 3.54: Inclination (V): energy spectrum

Spectral analysis was done with 2048 samples blocks, Blackmann-Harris window and 1000 samples step from the one-hour 187.5 Hz inclination data. DC level and slope of each block are deprecated by RMS method. Result is on fig. 3.54. The big peak is contamination by 50 Hz power electricity network, the small peak left from the 80 Hz mark is alias of the second harmonic of the 50 Hz. Interesting is the peak left from the 20 Hz mark, what is possibly frequency of austrian and german railways traction what is 16.7 Hz. Observatory have no other instrument to make intercomparsion in the ELF band.
It is possible to estimate energetic spectra of noise of the instrument in the case of having three instruments which measures the same quantity. The menthod is analogical to the method of reciprocity calibration of microphones (Ballantine, 1929). Let us have three instruments measuring the same quantity (fig. 3.55).

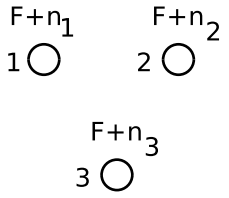

Figure 3.55: Three noisy instruments

The instruments have uncorellated noise and there is no coupling between them. Measured values (F) are contaminated by noise:

$$\begin{aligned} F_1 &= F + n_1 \\ F_2 &= F + n_2 \\ F_3 &= F + n_3 \end{aligned} \tag{3.20}$$

Then for the diferences of the output signals holds:

$$\begin{aligned} F_1 - F_2 &= F + n_1 - (F + n_2) = n_1 \boxplus n_2 \\ F_1 - F_3 &= F + n_1 - (F + n_3) = n_1 \boxplus n_3 \\ F_2 - F_3 &= F + n_1 - (F + n_2) = n_2 \boxplus n_3 \end{aligned} \tag{3.21}$$

Where $A \boxplus B = \sqrt{A^2 + B^2}$ is quadratic superposition. Squaring eqs. 3.21 gives set of linear equations, which can be solved to give noise parameters of all three instruments:

$$\begin{aligned} (F_1 - F_2)^2 &= n_1^2 + n_2^2 \\ (F_1 - F_3)^2 &= n_1^2 + n_3^2 \\ (F_2 - F_3)^2 &= n_2^2 + n_3^2 \end{aligned} \tag{3.22}$$

First step of data processing is determination of equivallent noise bandwidth of used spectral analyser (it depends on used window and overlap ratio). the simple way is to use MLS sequence with unity RMS value, generated by this code[1]:

```
for(m=1;;)
{
int b=0b11010001111010101; // MLS 17
m=(m>>1)^((m&1)*b);
out=(((m&1)*(-2)+1));
}
```

Due to Plancherel et al. (1910) theorem and knowledge, that MLS have flat energetic spectrum (Schroeder, 2009), we can calibrate the analyser in terms of $\mathrm{pT}/\sqrt{\mathrm{Hz}}$ Result of processing of datas from fig. 3.50 is on fig. 3.56 The analyser is the same as in the case of fig. 3.54, only the input sample rate is 1 Hz

[1] Author uses MLS sequence also for time-varied coeficients of digital filters. It can overcame problems with coeficient quantisation in fixed length arithmetics

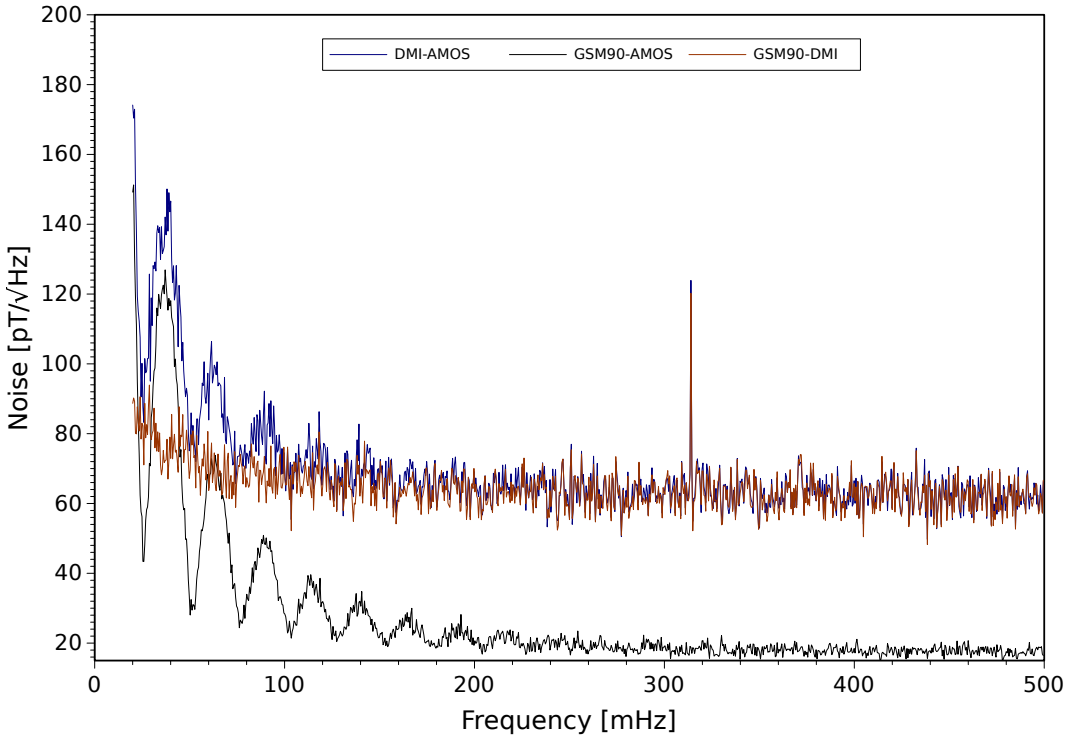

Figure 3.56: Noise of three noisy instruments

The frequency range 350 to 450 mHz is free from artefacts (the waves on the left are residues of discontinuous thermal regulation of AMOS instrument (which is thermally unshielded), peak near 310 mHz from DMI is unknown) and was used for estimation of noise of instruments in the F axis. Constructed instrument (AMOS) has noise 13.8 $\mathrm{pT}/\sqrt{\mathrm{Hz}}$. Noise of standard observatory equipments was also estimated: Overhauser PPM GSM90F1: 11.4 $\mathrm{pT}/\sqrt{\mathrm{Hz}}$ and DMI fluxgate: 61.3 $\mathrm{pT}/\sqrt{\mathrm{Hz}}$. This method of noise intercomparsion is used instead of usually used direct measurement. Because constructed instrument uses envelope detection, does not work in the zero field and can not be tested in the magnetic shield.

4 Conclusions

In this thesis, methods of singular elements, developed for filter synthesis in the 1970s, were used to solve an acoustical problem (non-linear electrostatic transducer) and the problem of the magnetostatic circuit (fluxgate magnetometer). Both problems are so simillar that the author believes that they both can be considered electro-acoustical problems. The first problem - parametric microphone - was solved only partially. Only the analogue part was designed and breadboarded. For future development, some form of the digital system must be constructed. Problems with electromagnetic compatibility of the NAROD magnetometer (based closely on the Acuna design) led the author to develop electronics for the magnetometer, whose desighwas simillar to the previously constructed microphone. Since the magnetometer for observatory use is basically a very low-frequency instrument, some additional parts were needed, including a highly stable thermally compensated reference voltage source and precision temperature measurement unit. The digital part was based on DSP codes of plesiochronnous signal processing developed originally for the digital exciter of a MW transmitter in TESLA Hloubětín. It was shown that magnetometer electronics, constructed with specially designed input amplifiers, have a better SNR (fig. 3.53) achieved by the good EMI properties of the designed systems and lower physical noise sources. This was compared with clasicall equipment constructed with low-noise operational amplifiers and switched-circuit analogue processing (DMI Fluxgate). The author believes that DSP routines, used in constructing the digital magnetometer, can be used as a basis for constructing studio or measurement system based on the discussed parametric microphones, where no analogue audio signal in the baseband and no global synchronisation circuit will be present in the recording chain, and with some parameters (EMC, dynamic range) exceeding today's best analogue technology.
The author's original work:

- Model of nonlinear electrostatic transduction based on mutator and nonlinear VCCSs (fig. 2.2), published in (Vlk, 7-2008)
- Model of magnetostatic circuits based on singular elements graph manipulation, (fig.3.8), published in (Vlk, 2014).
- DSP technique of plesiochronous interpolation based on sampled continuous prototype filter (Eg. 3.14) , published in (Vlk, 2005).
- Circuit of folded cascode with reactor powering used as low-noise input amplifier for parametric microphone (fig. 2.9), published in (Vlk, 2010).
- Commutation of VLF H-bridge trasmitter based on additional phase delayed H-bridge and used in fluxgate low-noise pump circuit.

5 References

5.1 Cited documents

Aschenbrenner, H.; Goubau, G.: Eine Anordnung zur Registrierung rascher magnetischer Stoerungen *Hochfrequenz-technik und Electroakustik* Vol. *47 (1936)* No. pp. 177-181

Acuna, M.: Fluxgate magnetometers for outer planets exploration; *IEEE Trans. Mag.* Vol. *10 (1974)* No. *3* pp. 519-523

Acuna, M. H; Scearce, C. S.; Seek, J. B.; Scheifele, J. : *The MAGSAT vector magnetometer - a precision fluxgate magnetometer for the measurement of the geomagnetic field NASA Technical memorandum* No. *79656* Greenbelt, Maryland 1978

Arends, G.F.J.: De codensatormocrofoon met halfgleiders; *Polytechnisch Tijdschrift, Uitgave E*, Vol. *18(1963)* No. *7* pp. 241-247

Alexanderson, E.F.W.; Nixdorf, S.P.: A Magnetic Amplifier for Radio Telephony *Proc. IRE* Vol. *4 (1916)* No. 2 pp. 101-120

Ballantine, Stuart: Reciprocity in electromagnetic, mechanical, acoustical, and interconnected systems; *Proc. IRE* Vol. *17 (1929)* No. *6 (June)* pp. 929-951

Baltag, O.: Double Pumping Fluxgate Magnetometer *Sensor Letters* Vol. *11 (2013)* No. 1 pp. 149-152

Baxandall, P.J.: New Low-noise Transistor Circuit for Electrostatic Microphone *Wireless World (1963)* No. 11-12, pp. 538-542;593-597

Blumlein, Alan Dower: Alternating Current Bridge Circuits; British pat. 323037 filled: *13.9.1928*

Bobrov, V.N.: Serija kvarcevych magnitnych variometrov *Geomagnetizm i aeronomija 2 (1962)* No. 2 p.348

Braun, Jaromír: *Kombinatorické metody v analýze a modelování elektronických soustav*; Prague: Academia *1990*

Braun, K. : Elektroakustische Vierpole; *TFT* Bd. *33 (1944)*, H. *5* pp. 84-95

Castigliano, A.: *Intorno ai sistemi elastici* Turin *1873* dissertation

Cerman, A.; Merayo, J.M.G.; Brauer, P.; Primdahl, F.: Self-Compensating Excitation of Fluxgate Sensors for Space Magnetometers *I2MTC - IEEE International Instrumentation and Measurement Technology Conference* Victoria, Vancouver Island *12.-15.5.2008*

Charkevič, Aleksandr Aleksandrovič: *Teorija elektroakustičeskych preobrazovatelej; Volnovyje processy*; Moscow: Nauka *1973*

Chireix, H.: High Power Outphasing Modulation *Proc. IRE* Vol. *23 (1935)* No. *11* pp. 1370-1392

Chua, L. O.: Memristor-the missing circuit element, *IEEE Transaction on Circuit and System* Vol. *18 (1971)* No. *5* pp. 507-519

Combes, Michel: *Un générateur paramétrable de multiplieur de fréquence utilisant des techniques numeriques* Paris: Université de Paris 06 *1994* - Doctoral thesis

Connerney Jack, et al.: *Mars Atmosphere and Volatile Mission (MAVEN) - Magnetometer Invesatigation (MAG)* University of Colorado: Community meeting, 2.12.2012

Dement'jev, Jevgenij Petrovič: *Elementy obščej teorii i rasčeta šumjaščich linejnych cepej*; Moscow: Gosenergoizdat *1963*

Fakhfakh, Mourad -ed.: *Design of Analog Circuits through Symbolic Analysis*; Bentham e-books *2012*

Feussner, W.: Zur Berechnung der Stromstarke in netzformigen Leitern *Annalen der Physik* Vol. *15 (1904)* No. *12* pp. 385-394

Frederiksen, Erling: A method and a coupling for reducing the harmonic distortion of a capacitive transducer World patent WO 94/23547 published *13.10.1994*

Gabler, Miloš; Haškovec, Jiří; Tománek, Evžen: *Magnetické zesilovače* Prague: SNTL *1950*

Gayford, M.L.: *Acoustical Techniques and Transducetrs* London: STC *1961*

Gordon, D.I. ; Sery, R.S.: Effects of charged particles and neutrons on magnetic materials *IEEE Trans. Comm. Electr.* Vol. *83 (1964)* No. *73* pp. 357-361

Gordon, D.I. ; Sery, R.S.: Irradiation of Iron and 5-79 Mo Permalloy with 2-MeV Electrons *Journal of Applied Physics* Vol. *35 (1964)* No. *3* pp. 879-880

Gordon, D.I. ; Sery, R.S. : Uniaxial anisotropy by "radiomagnetic" treatment; controlling factors in a new process *IEEE Trans. Magn.* Vol. *1 (1965)* No. *4* pp. 277-280

Gordon, D.I. ; Sery, R.S. : Uniaxial Anisotropy Induced by a Low-Temperature Magnetic Anneal Following Electron Irradiation *Journal of Applied Physics* Vol. *37 (1966)* No. *3* pp. 1219-1217

Gordon, D. I.; Lundsten, R. H.; Chiarodo, R. A.; Helms, H. H. Jr.: A fluxgate sensor of high stability for low field magnetometry *IEEE Trans. Mag.* vol. *MAG-4(1968)* No. *3*, pp.397-401

Gouriet, G. G.: High-Stability Oscillator *Wireless Engineer (Apr. 1950)*

Griese, Hans Joachim: US. Pat. 3422225 pub. *1969* (compare with firm literature to add capacitor to complete Clapp circuit)

Guillemin, Ernst Adolph: *Theorie der Frequenzvervielfachung durch Eisenkernkoppelung* Muenchen: Sc.D. Thesis *1926*

Guillemin, Ernst Adolph: *Introductory Circuit Theory* New York: J. Willey *1953*

Gyimesi, M.; Avdeev, I.; Ostergaard, D.: Finiteelement simulation of micro-electromechanical systems (MEMS) by strongly coupled electromechanical transducers *IEEE Transactions on Magnetics* vol. *40(2004)* no. *2 (march)* pp. 557-560

Hammond, Laurens; Hanert, John M. : *Vibrato apparatus* US Patent: 2560568 (1946)

Hannemann, Dennis M; Huang, Kwang, Ta ; Shiroma, M.: *Parametric energy coupled unitnterruptible power supply* US Patent: 4115704 (filled: 19.9.1977)

Hansen, S.T.; Ergun, A.S.; Liou, W.; Alud, B.A.; Khuri-Jakub, B.T.: Wideband micromachined capacitive microphones with radio frequency detection *JASA* Vol. *116 (2004)*, No. *2 (August)* pp.828-842

Hardy, Tim: *Next Generation LF Transmitter Technology for (e) Loran Systems* Unpublished report Nautel *2008*

Harris, Frederic J.: On the Use of Windows fo Harmonic Analysis with the Discrete Fourier Transform *Proc. IEEE* Vol.*66 (1978)* No. 1 pp. 172-205

Heaviside, Oliver: *Electromagnetic Theory, vol. 1-3* London: Benn Brothers *1922*

Hibbing, Manfred: Deutsche patent 4300379 publ.*1996* (Compare with firm literature to complete gamma LC with series inductor to tune the bridge.)

Hunt, Frederick V.: *Electroacoustics: The Analysis of transduction, and its historical background*; Cambridge: Harvard University Press *1954*

Husník, L.: Influence of Transfer Functions of Transducers Constituting the Loudspeaker with the Direct D/A Conversion on the Performance of the System, *115-th convention of AES*, New York, *2003* Paper No.: *6519*

Jagoš, M.: Zmiešavač v spínacom režime *Súbor prednńšok z celoslovenského seminára rádioamatérov zväzarmu Vysoké Tatry 1989*

Korepanov, V.; Marusenkov, A.: Flux-Gate Magnetometers Design Peculiarities *Surveys in Geophysics* Vol.*33 (2012)* No. *5* pp. 1059-1079

Kovář, D.: Typy elektrod pro mikrofony s přrímou A/D přeměnou, *Proceedings of the ATP*, Brno, *2004*

Kvasil, Josef: *Mikroelektronické transformační bloky*; Prague: SNTL *1981*

Lahmeyer, W: Transformator mit Sekundaerwickelungen auf verschiedenen Schenkeln German Pat. DE149761 (26.8.1902)

Lamb, H.: *Higher Mechanics*; London: Cambridge at the University Press *1920*

Lenk, Arno: *Elektromechanische Systeme Bd. 1: Systeme mit konzentrieren parametern* Berlin: VEB Verlag Technik *1973*

Lenk, Arno: *Elektromechanische Systeme Bd. 2: Systeme mit verteilten parametern* Berlin: VEB Verlag Technik *1974*

Lenk, Arno: *Elektromechanische Systeme Bd. 3: Systeme mit hilfenergie* Berlin: VEB Verlag Technik *1975*

Linvill, John G.: *Models of transistors and diodes* New York: McGraw-Hill *1963*

Macoun, Zbyněk; Nádvorník, Bohumil: *Liniový vlakový zabezpečovač LS H, LS III, LS IV* Prague: NADAS *1971*

Manley, J.M.; Rowe, H.E.: Some general properties of nonlinear elements- part 1. General energy relations *Proc. IRE 44 (1956)* pp. 904-913

Marie, G.: Amplificateurs paramétriques basses fréquences à commande magnétique orthogonale; *Acta Electronica*, Vol.*8 (1964)*, No. *1* pp 7-81.

Mason, W.P.: *Electromechanical transducers and wave filters* New York: D. Van Nostrand Comp.*1942*

Mathieu E.: Mémoire sur Le Mouvement Vibratoire d'une Membrane de forme Elliptique; *Journal de Mathématiques Pures et Appliquées* pp 137-203

Miller, G.: *Stylus-Groove Relations in Phonograph Records* Cambridge: Harvard University *1950* - Doctoral thesis

Mitra, S.K.: *Analysis and Synthesis of Linear Active Networks*, New York: J.Wiley *1963*

Motchenbacher,C.D; Fitchen, F.C.: *Low-noise electronic design* New York: J.Wiley *1973*

Moos, Petr: *Nulorové modely kvazilineárních a nelineárních elektronických prvků*; Prague: Academia *1983*

Musmann, G.; Anfassiev, Y.: Fluxgate Magnetometers for Space Research Norderstedt: Books on Demand *2010*

Motl, K.: Elektroakustický vysílač s přímou D/A přeměnou, *Proceedings of the ATP* Prague, *2005*

Mueller, R.; Holstein, P.: About a Digital RF-Condenser microphone; Convention Paper 6130 *116-th Convention AES* Berlin: *May 8-11 2004*

Narod, B; Russell, R.D.: Steady-State Characteristics of the Capacitively Loaded Flux Gate Sensor; *IEEE Trans. Mag.* Vol. *20 (1984)* No. *4* pp 592-597.

Narod, B. *NGL S-100 service manual*; Vancouver: Narod Geophysics Ltd. *1987*

Narod, B.: The origin of noise and magnetic hysteresis in crystalline permalloy ring-core fluxgate sensors *Geosci. Instrum. Method. Data Syst. Discuss. (2014)* No. *4* pp. 319-352

Otala, Matti: Circuit Design Modifications for Minimizing Transient Intermodulation Distortion in Audio Amplifiers *JAES 20 (1972)* No. 5 (June) pp. 396-399

Ott,H.W.: *Noise reduction techniques in electronic systems* New York: Wiley-Bell Tel. lab. *1976*

Oxborrow, Mark; Breeze, Jonathan D.; Alford, Neil M.: Room-temperature solid-state maser *Nature 488 (2012)* pp. 353-356

Paerschke, R.: Ein Hf- Kondensatormikrofon mit Transistoren *Funkschau 1965* No. *2* pp. 113-114

Parten, Michael E.: *Linear network analysis by Nullator-Norator residual networks* Lubbock: Texas Tech University(1972) - Doctoral thesis

Pastille, Holger: Ueber die Nichtlinearitaeten am Kondensatormikrofon unter besonderen Beruecksichtigung der Membran; Berlin, III. Fakultaet, 2011 - Doctoral thesis

Pedersen, M.; Olthuis, W.; Bergveld, P.: An integrated silicon capacitive microphone with frequency-modulated digital output *Sensors and Actuators* vol. A69 (1998) pp. 267-275

Penfield, Paul; Rafuse, Robert P.:*Varactor Applications* Cambridge: The MIT Press *1962*

Petterson, E.: *Magnetic wave amplifiing repeater* US PAT. 1884844 *1929*

Pimonow, Léonid: *Les Infra-sons* Paris: CNRS *1976*

Player, P.A.: Parametric amplification in fluxgate sensors *Journal of Physics D:* Vol. *21 (1988)* No. pp. 1473-1480

Plancherel, Michel; Mittag-Leffler: Contribution à l'étude de la représentation d'une fonction arbitraire par les intégrales définies *Rendiconti del Circolo Matematico di Palermo* Vol. *30 (1910)* No. *1* pp. 289-335

Primdahl, Fritz: Temperature compensation of fluxgate magnetometers *IEEE Trans. Mag. 6 (1970)* No. 4 pp. 819-822

Radeka, V.: Signal, Noise and Resolution in Position-Sensitive Detectors; *IEEE Trans. Nucl. Sci.*, Vol. *21 (1974)*, No. *1* pp 51-64.

Rieger, F. : *Lineární Obvody*; Prague: SNTL *1967*

Ripka, Pavel : *Magnetometry s feromagnetickou sondou*; Prague: CVUT (Doctoral Thesis) *1988*

Russell, R.D.; Narod, B.B; Kollar, F.: Characteristics of the Capacitively Loaded Flux Gate Sensor *IEEE Trans. Mag.*, Vol. *MAG-19 (1983)*, No. *2* pp. 126-130

Sasada, I.: Symmetric response obtained with an orthogonal fluxgate operating in fundamental mode *IEEE Trans. Mag.*, Vol. *MAG-38 (2002)*, No. *5* pp. 3377-3379

Sattinger, D. H: *Lie Groups and Algebras with Applications to Physics,Geometry and Mechanics* New York : Springer *1986*

Schroeder, Manfred R.:*Number Theory in Science and Communication* New York: Springer *2009*

Serson, P. H.; Mack, S.Z.; Whitham, K.: *Publ. Dom. Obs. Ottawa*, *19 (1957)* pp. 15 - 97

Sery, R.S. ; Gordon, D.I.: Irradiation of Magnetic Materials with 1.5- and 4-MeV Protons *Journal of Applied Physics* Vol. *34 (1963)* No. *4* pp. 1311-1312

Sery, R.S. ; Gordon, D.I. : Activation Energy and Annealing Kinetics of Remanence Growth Caused by Low-Temperature Magnetic Anneal of Electron-Irradiated Nickel-Iron *Journal of Applied Physics* Vol. *39 (1968)* No. *2* pp. 991-992

Seltzer, S. J.; Romalis, M. V. : Unshielded three-axis vector operation of a spin-exchange-relaxation-free atomic magnetometer *Appl. Phys. Lett. 85 (2004)* p. 4804

Soell, S.; Porr, B.: An Undersampling Digital Microphone Utilising Second Order Noise Shaping, *14-th. International conference MIXDES2007* Ciechocinek, Poland *21.-23. June 2007*

Sommerfield, A.: *Vorlesungen ueber theoretische physik, band III-Elektrodynamik*; Leipzig: Geest and Portig *1949* p.11

St-Louis, Benôit, ed.: *Intermagnet Technical Reference Manual*; Edinburgh: BGS *2011*

Strnad, Ladislav: *Synchronizace sítí*; Prague: ČVUT publishing house *2013*

Sucksdorff, C.; Pirjola, R.; Häkkinen, L.: Computer production of K-indices based on linear elimination. *Geophys. Trans.* Vol. *36* pp. 333âĂŞ345

Suesse, R.; Civelek, C.: Analysis of engineering systems by means of Lagrange and Hamilton formalisms depending on contravariant, covariant tensorial variables; *Forschung im Ingenieurwesen* Bd. *68 (2003)* pp. 66 - 74

Swanson, Hilmer Irvin: *Amplitude modulator*, European Patent: 0083727 *1983*

Sýkora, Bohumil; Dudek, Pavel: Předzesilovače pro přenosku s pohyblivým magnetem *Amatérské radio A 68 (1990)* No. 1 - 2 pp. 65-70,105-108

Tomlinson, G.H. ; Galvin, P.: Analysis of skewing in amplitude distributions of filtered m sequences *Proc. of the IEE* Vol. *121 (1974)* No. *12* pp. 1475-1479

Vackář, Jiří: *Vysílače. 1., Teoretické základy* Prague: SNTL *1960*

Vágó, István: *Graph Theory : Application to the calculation electrical networks*; Budapest: Akadémiai Kiadó *1985*

Van der Pol, B.; Van der Mark, J.: Frequency demultiplication *Nature*, *120 (1927)*, pp.363-364

Vorperian, Vatché: *Fast Analytical Techniques for Electrical and Electronic Circuits*; London: Cambridge University Press *2002*

Westberg, Jerry: *Phase to amplitude H-bridge switching circuit*, US Patent: 7092269 *2006*

Weynmann, G.: Di Messung kleinster Schalldruecke mit dem kondensatormikrophon *Elektrische Nachrichtentechnik* Vol. *20 (1944)* No. *6*, p. 149-158

Whittaker, Edmund Taylor; Robinson, George: *The Calculus of Observations: A Treatise on Numerical Mathematics* London: Blackie and Son Limited *1937*

Yoshida, Kōsaku : *Operational Calculus: A Theory of Hyperfunctions* Berlin: Springer-Verlag *1984*

Zell, Clemens: Einrichtung zur Umwandlung von ein- oder mehrphasigen Wechselstrom in Gleichstrom und umgekehrt mit Hilfe von Selbstinduktionsspulen mit polarisirtem Eisenkern German patent DE113992 (25.4.1899)

Van der Ziel, A.: *Noise* Prentice-Hall *1954*

Zuckerwar, A.;S hope, W.W.: A Solid-State Converter for Measurement of Aircraft Noise and Sonic Boom *IEEE Trans. Instrum. and Meas.* Vol. *IM-23 (1974)* No.*1* p. 23-27

Zworykin, V.K.: Television; the electronics of image transmission in color and monochrome New York: J. Wiley *1954*

5.2 Author's document

Vlk, Michal: Blumleinův můstek Czech patent *CZ 302207* granted: *5. 11. 2010*

Vlk, Michal: *Šumové vlastnosti páskového rychlostního mikrofonu* Master thesis, Prague: ČVUT-FEL *2005*

Vlk, Michal: Plesiochronní převodník vzorkovací frekvence *Proceedings of the regional AES meeting ˋATPˊ* Prague *2005*

Vlk, Michal: A Novel Analogy for Time-Domain Simulation of the Nonlinear Electrostatic Transducer *Procedings of the conference Poster* Prague *15.5. 2008*

Vlk, Michal: Condenser microphone as parametric electroacoustic system and its time-domain modelling via equivallent electrical circuit in SPICE software *Proceedings of the conference Acoustics 08* Paris *29.6-4.7. 2008*

Vlk, Michal: Kondenzátorový mikrofon jinak *Proceedings of the 77-th Acoustic seminary of the Czech Acoustical Society* Zlenice *7.-9.10. 2008*

Vlk, Michal: Koncové stupně digitálních vysílačů *Proceedings of the conference Radiokomunikace* Pardubice *4.-6.11. 2009*

Vlk, Michal: Modernisation of the Narod fluxgate electronics at Budkov Geomagnetic observatory *Poster presented at EGU General Assembly* Wien *7.-12.4. 2013*

Hejda,P.; J. Horáček, J.; Vlk, M.; Bayer, T.: ON THE THUNDERSTORM OF 10 JULY 2011 AT MAGNETIC OBSERVATORY BUDKOV *Boletin ROA San Fernando* No.*3 2013*;

Vlk, Michal: Obvodové modely indukčnostního teslametru *Proceedings of the 89-th Acoustic seminary of the Czech Acoustical Society* Šlovice *7.-9.10. 2014*

6 Appendix A: Electromechanical transduction as an energy-conservative system

Assume the system to have n degrees of freedom and $q_1, ...q_n$ are generalized co-ordinates (Lamb, 1920). The partial derivatives of the generalized co-ordinates with respect to time are generalized velocities $\dot{q}_i = \frac{\partial q_i}{\partial t}$. Assume the energy of th system to be a function of co-ordinates only:

$$V = V(q_1, ...q_n) \tag{6.1}$$

This energy is called the potential energy and its partial derivative with respect to the i-th co-ordinate is called the generalized force:

$$F_i = \partial V(q_1, ...q_n)/\partial q_i \tag{6.2}$$

Assume the kinetic energy of system to be a function of only generalized velocity:

$$T = T(\dot{q}_1, ...\dot{q}_n) \tag{6.3}$$

Its partial derivative with respect to the i-th generalized velocity is then the generalized momentum:

$$p_i = -\partial T(\dot{q}_1, ...\dot{q}_n)/\partial \dot{q}_i \tag{6.4}$$

Equations 6.2 and 6.4 are dual. The minus sign must be in one of them. It is the author's decision to include it in the equation 6.4. Sometimes it may be useful to differentiate 6.4 with respect to time. We the get:

$$F_i = -\frac{d}{dt}(\partial T(\dot{q}_1, ...\dot{q}_n)/\partial \dot{q}_i) \tag{6.5}$$

We can add energetic functions freely, i.e. as Lagrange functions of the system:

$$L = T - V \tag{6.6}$$

Or to construct equations with them:

$$\frac{d}{dt}\frac{\partial L}{\partial \dot{q}^j} - \frac{\partial L}{\partial q^j} = 0 \tag{6.7}$$

The equation is merely a transcription of the commutativity properties of some differential operators:

$$\frac{d}{dt}\frac{\partial A}{\partial(\frac{dq}{dt})} = \frac{d}{dt}\frac{\partial A}{\frac{d}{dt}\partial q} = \frac{\partial A}{\partial q} \tag{6.8}$$

The reader can find further generalization in the Lie groups theory (Sattinger, 1986). We can also use alternative Hamilton equations for some problems or add the Helmholtz function in case of dissipative systems, but problems solved here are too simple to do that. Here we shall need only eq. 6.2 from classical mechanics. But electro-acoustics is rather more

electrodynamic than mechanics alone and thus we need to use mechanical and electrodynamic variables together. The natural way of combining them is to use energetic functions: The mathematical description of the energy conservation law. There are pairs of variables in the general electrodynamics called - `energetic influentia' (Sommerfield, 1949). Electrodynamic ones are: $1/2(HB)$, $1/2(DE)$, jE, $[EH]$ and mechanic ones are: $1/2(Fx)$ and $1/2(\sigma\epsilon)$ We can partially differentiate the energetic function by one variable from the pair to get another variable, i.e.: if we differentiate the energy function partially by F or x, we get x or F, respectively (In mechanics, it is used in solving elasticity problem as the Castigliano (1873) method). We can generalize this for mechanical and electrodynamic variables, but under the condition that the processes are reversible. For irreversible processes, we must take into account the entropy concept, and the interested reader in that can find information in every textbook of physical chemistry.
The potential energy of an electrostatic system is described by equation (Charkevic, 1973):

$$V = \frac{1}{2}\frac{q^2}{C} \tag{6.9}$$

where C is capacity and q is charge. If the transducer is simple (capacitor with infinite equidistant plates), the capacity is:

$$C = \frac{\epsilon A}{x} \tag{6.10}$$

Here A is the plate area , x is the distance between plates, and ϵ is the dielectric constant of air. for the potential energy of a simple transducer the following holds:

$$V = \frac{xq^2}{2\epsilon A} \tag{6.11}$$

Eq. 6.11 indicates, that the generalized co-ordinates are x and q. The corresponding generalized forces are then F and U:

$$F = \frac{\partial}{\partial x}V = \frac{q^2}{2\epsilon A} \tag{6.12}$$

$$U = \frac{\partial}{\partial q}V = \frac{xq}{\epsilon A} \tag{6.13}$$

Equations 6.12 and 6.13 are fundamental nonlinear equations of condenser transducer. They can be used for simulation in Spice-like software as discussed by the author in the thessis. It also holds:

$$I = \frac{\partial q}{\partial t} \tag{6.14}$$

The behaviuor of every non-linear function can be expanded via the Taylor series. The first two terms are constant and linear term. The process to assuming all higher terms to be zero is called linearization. Let us do this it for the generalized co-ordinates:

$$q = q_0 + \partial q \tag{6.15}$$

$$x = x_0 + \partial x \tag{6.16}$$

Substitution 6.15 and 6.16 into 6.12 and 6.13 gives two linear equations:

$$\partial F = \frac{q_0}{\epsilon A}\partial q \tag{6.17}$$

$$\partial U = \frac{x_0}{\epsilon A}\partial q + \frac{q_0}{\epsilon A}\partial x \tag{6.18}$$

Consider two linear equations. The equations have the same form for all linear transducers with two constants. The first constant is quasistatic electrical elastance (reciprocal value to quasistatic transducer electrical capacity):

$$S_0 = \frac{1}{C_0} = \frac{x_0}{\epsilon A} \tag{6.19}$$

The second constant is the transducer constant (corresponds to Mason's constant in piezoelectric transducer)

$$k = \frac{q_0}{\epsilon A} = \frac{U_0}{x_0} \tag{6.20}$$

Where U_0 is the polarization voltage of the transducer and x_0 is static the distance between the electrodes. If the electrostatic transducer is loaded to short at the electrical side (This may occur in an electrostatic speaker or a parametric microphone), equation 6.18 transforms to:

$$\frac{x_0}{\epsilon A}\partial q = -\frac{q_0}{\epsilon A}\partial x \tag{6.21}$$

After substitution of 6.17 into 6.21, we get:

$$\partial F = -\left(\frac{U_0}{x_0}\right)^2 C_0 \partial x = -k^2 C_0 \partial x \tag{6.22}$$

which describes negative compliance on the mechanical side in the form of transformed self-capacity. Let us write the equations of electrostatic conversion in the form of a matrix Rieger (1967) (we shall write the variables as lower-case letters, because they are small quantities in the linear model):

$$\begin{bmatrix} f \\ u \end{bmatrix} = \begin{bmatrix} q & x \end{bmatrix} \begin{bmatrix} \frac{q_0}{\epsilon A} & 0 \\ \frac{x_0}{\epsilon A} & \frac{q_0}{\epsilon A} \end{bmatrix} \tag{6.23}$$

Since the low signal value has zero initial condition (all transients are assumed to be finished), we can put:

$$i = \frac{\partial q}{\partial t} \cong i = pq \tag{6.24}$$

$$v = \frac{\partial x}{\partial t} \cong v = px \tag{6.25}$$

Where p is the operator of the time derivative. After substituting of 6.24 and 6.25 into 6.23, we get linear equations of electromechanical conversion in the form of a mixed matrix (mechanical and electrical variables are on one side). This form is known in piezo-electricity from the book of Mason (1942).

$$\begin{bmatrix} f \\ u \end{bmatrix} = \begin{bmatrix} i & v \end{bmatrix} \begin{bmatrix} \frac{q_0}{\epsilon A p} & 0 \\ \frac{x_0}{\epsilon A p} & \frac{q_0}{\epsilon A p} \end{bmatrix} \tag{6.26}$$

We cannot describe the type of matrix in the classical circuit theory without appending mechanical values to electrical in advance. In electrical circuit theory, there are only two

variables: current and voltage. Nevertheless, there are many forms of two-branch matrices (Z,Y,H,K,A,B), but only two basic operations are performed to convert between them. One operation (so-called matrix inversion) is commonly used everywhere, where general solving of the linear equation system is needed. Let us introduce an example of matrix inversion in recomputing of Z (impedance) and Y (admittance) matrices.

$$Z = Y^{-1} = \begin{bmatrix} \frac{y_{22}}{|Y|} & -\frac{y_{21}}{|Y|} \\ -\frac{y_{12}}{|Y|} & \frac{y_{11}}{|Y|} \end{bmatrix} \tag{6.27}$$

The reciprocal problem (Y and Z) is dual:

$$Y = Z^{-1} = \begin{bmatrix} \frac{z_{22}}{|Z|} & -\frac{z_{21}}{|Z|} \\ -\frac{z_{12}}{|Z|} & \frac{z_{11}}{|Z|} \end{bmatrix} \tag{6.28}$$

'Partial inversion' exists between the Z and H matrices. It probably has no counterpart in the general matrix theory. Let us illustrate this on an example of recomputing Z and H matrix:

$$Z = H^{-1(22)} = \begin{bmatrix} \frac{|H|}{h_{22}} & \frac{h_{12}}{h_{22}} \\ -\frac{h_{21}}{h_{22}} & \frac{1}{h_{22}} \end{bmatrix} \tag{6.29}$$

The reciprocal problem (H and Z) is dual:

$$H = Z^{-1(22)} = \begin{bmatrix} \frac{|Z|}{z_{22}} & \frac{z_{12}}{z_{22}} \\ -\frac{z_{21}}{z_{22}} & \frac{1}{z_{22}} \end{bmatrix} \tag{6.30}$$

We could do only partly invert matrix 6.26 over term (22). After doing so, we get the matrix in more convenient form, known from the book of Charkevic (1973):

$$\begin{bmatrix} f \\ v \end{bmatrix} = \begin{bmatrix} i & u \end{bmatrix} \begin{bmatrix} \frac{q_0}{\epsilon A p} & 0 \\ -\frac{x_0}{q_0} & \frac{\epsilon A p}{q_0} \end{bmatrix} \tag{6.31}$$

The next step is to mirror the matrix over the $u|i$ axis and add the sign at u (This is because of the conventions in the classical electro-acoustic analogy):

$$\begin{bmatrix} f \\ v \end{bmatrix} = \begin{bmatrix} -u & i \end{bmatrix} \begin{bmatrix} 0 & \frac{q_0}{\epsilon A p} \\ -\frac{\epsilon A p}{q_0} & -\frac{x_0}{q_0} \end{bmatrix} \tag{6.32}$$

Let us decompose matrix on the right-hand side of eq. 6.32 into two matrices:

$$\begin{bmatrix} 0 & \frac{q_0}{\epsilon A p} \\ -\frac{\epsilon A p}{q_0} & -\frac{x_0}{q_0} \end{bmatrix} = \begin{bmatrix} 0 & \frac{q_0}{\epsilon A p} \\ -\frac{\epsilon A p}{q_0} & 0 \end{bmatrix} \begin{bmatrix} 1 & \frac{x_0}{\epsilon A p} \\ 0 & 1 \end{bmatrix} = \begin{bmatrix} 0 & \left(\frac{x_0 p}{U_0}\right)^{-1} \\ -\frac{x_0 p}{U_0} & 0 \end{bmatrix} \begin{bmatrix} 1 & \frac{1}{pC_0} \\ 0 & 1 \end{bmatrix} \tag{6.33}$$

The first term of the product is the matrix of the reactance invertor (Kvasil, 1981) and the second one is the series self-capacitance on the electrical side. This equivalent circuit appears seldom in the literature (Hunt, 1954), The transformed variant with an ideal transformer is more common. There are methods to transform the PI or T two-branch into an ideal transformer with series/parallel elemens. These methods are called ‘The norton transformations’:

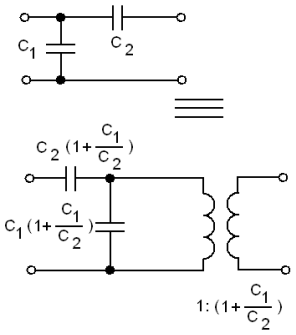

Figure 6.1: Norton transformations

A slightly modified method is applied to the gamma-type capacitor twobranch. Hint: Joint two series capacitors on the left, apply Norton transformation to the result with the shunt capacitor. Then transform the series capacitor from the right-hand side and join it with the series cap resulting from the previous step.

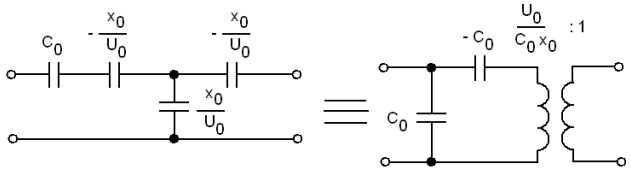

Figure 6.2: Linearised models of condenser transducer

The schematic representation of the reactance invertor has two equivalent forms. The first one has positive series capacitors and a negative shunt capacitor. and the second one has negative series capacitor and a positive shunt capacitor. Note here, that the transducer matrix remains the same. Insertion of ideal transformer is only the realization part of transducer model and this model is valid only with all the components.
The general form of the two-branch equation is the so-called affine approach. It uses two square matrices to form two homogenous linear equations where all two-branch variables are included. There is only one condition for the two-branch: to be autonomous (does not include independent sources).

$$\begin{bmatrix} 0 \\ 0 \end{bmatrix} = \begin{bmatrix} U_1 & U_2 & I_1 & I_2 \end{bmatrix} \begin{bmatrix} M & N \end{bmatrix} \tag{6.34}$$

Matrices can be manipulated, i.e. via the Gauss elimination method. We can get classical circuit matrices as elements in some places, where other places have prescribed values:

$$\begin{bmatrix} M & N \end{bmatrix} \approx \begin{bmatrix} y_{11} & y_{12} & -1 & 0 \\ y_{21} & y_{22} & 0 & -1 \end{bmatrix} \approx \begin{bmatrix} -1 & 0 & z_{11} & z_{12} \\ 0 & -1 & z_{21} & z_{22} \end{bmatrix} \approx \begin{bmatrix} -1 & h_{12} & h_{11} & 0 \\ 0 & h_{22} & h_{21} & -1 \end{bmatrix} \approx$$

$$\approx \begin{bmatrix} k_{11} & 0 & -1 & k_{11} \\ h_{21} & -1 & 0 & k_{22} \end{bmatrix} \approx \begin{bmatrix} -1 & a_{11} & 0 & @a_{12} \\ 0 & a_{21} & -1 & @a_{22} \end{bmatrix} \approx \begin{bmatrix} b_{11} & -1 & @b_{12} & 0 \\ a_{12} & 0 & @b_{22} & -1 \end{bmatrix} \tag{6.35}$$

Note, that symbol @ represents a sign for circuit matrices defined by the IEC convention, but notrespecting this leads in this case to simpler systematism. Using the sign makes transformation of the matrices complicated if the type of matrix is not nown a-priori (as in electroacoustics). This is the reason for putting signs in equation 6.32

There are other phenomena used for electromechanical transduction. They will be listed briefly. Consider a moving armature transducer where one turn of wire without resistance is present. Different number of turns can be expressed by an ideal transformer in cascade with the electrical part of the transducer. The potential energy of magnetostatic system reads:

$$V = \frac{1}{2} R_m \Phi^2 \tag{6.36}$$

Where R_m is the reluctance. For a simple form of transducer (magnetic gap) the reluctance reads:

$$R_m = \frac{x}{\mu A} \tag{6.37}$$

where x is the gap width, A is the armature cross-section and μ is air permeability. The simple form of the transducer formula for potential energy is:

$$V = \frac{x\Phi^2}{2\mu A} \tag{6.38}$$

Here, the generalised coordinates are x and Φ. The generalised forces will be F and I.

$$F = \frac{\partial V}{\partial x} = \frac{x\Phi^2}{2\mu A} \tag{6.39}$$

$$I = \frac{\partial V}{\partial \Phi} = \frac{x\Phi}{\mu A} \tag{6.40}$$

These are the fundamental equations of moving-reluctance transduction. It also holds:

$$U = \frac{\partial \Phi}{\partial t} \tag{6.41}$$

A secial kind of transducer is a transducer with linear energy transfer. Consider a general system with two degrees of freedom (i.e. one mechanical and one electrical), which is linear:

$$L(aA + bB) = aL(A) + bL(B) \tag{6.42}$$

The energy function of this system is:

$$V(y_1, y_2) = \frac{1}{2}(c_{11} y_1^2 + c_{22} y_2^2) + c_{12} y_1 y_2 \tag{6.43}$$

For some kinds of conversion principles, some coefficients may be equal to zero, but the coupling coefficient have one value. Here we can see the reciprocity and, from this point on, we conjencture, that reciprocity is the function of degrees of freedom of the transduction phenomenon.

The energy for piezo-electrical transduction reads:

$$V(D,\xi) = \frac{1}{2}\left(\frac{1}{\epsilon}D^2 + E_m\xi^2\right) + fD\xi \tag{6.44}$$

where D is electrical induction, ξ is the relative enlargement and f is Mason's constant. The partial derivatives with respect to variables D and ξ yields the piezo-electrical equations:

$$E = \frac{\partial T}{\partial D} = \frac{1}{\epsilon}D + f\xi \tag{6.45}$$

$$\sigma = \frac{\partial T}{\partial \xi} = fD + E_m\xi \tag{6.46}$$

Consider an ideal moving conductor transducer. Its kinetic co-energy (electrodynamic energy) is:

$$T = BlIv \tag{6.47}$$

Where Bl is the gyration factor (product of induction in the gap with perpendicular projection of the wire length onto induction). I is the electric current flowing through the wire and v is the velocity of the wire. Generalised velocities are v and I,the generalised momenta F and U. Note, that equation 6.47 is in bilinear form: it predicts that the fundamental transducer equations will be linear:

$$F = -\frac{\partial T}{\partial v} = @BlI \tag{6.48}$$

$$U = -\frac{\partial T}{\partial I} = @Blv \tag{6.49}$$

Where @ indicates that the signs are negative. In a particular example of the transducer the signum convention should conform to the Ampère right-hand rule.

7 Appendix B: Circuit determinant computation code

```
/*********************************************************
*               Determinant Computation
*               via Extended Sparse Tableau
*               Mapped as binary tree
*               core finished 14.1.2009
*               Memory allocated via garbage-collector
* translate with: gcc -Wl,--stack=500000000 sparse.c
*   (C) Michal Vlk vlk@ig.cas.cz
*********************************************************/

#include <math.h>
#include <stdio.h>
#include <stdarg.h>
#include <stdlib.h>
#include <string.h>

typedef struct spm_{
    struct spm_* left;
    struct spm_* right;
    int row;
    int col;
    int indx;  // 0 = not_used, terminating,
//1 = -1, 2 = +1 (vars), 3... (string var)
} spm;

// global memory
int gcol = 0;   //  garbage collector
void* gnod;
FILE* output;           //  output file

spm* spmalloc()
        {
        void * c;
        void * d;
        if(gcol == 0)
                {
                c = (void*)malloc(sizeof(spm));
                return(((spm*)c));
                }
        else
                {
                gcol--;
                c = ((void**)gnod)[0];
                d = gnod;
                gnod = c;
                return(((spm*)d));
                }
}

spfree(spm* nod)
        {
        void** b;
        b = (void**)nod;
        b[0]=gnod;
        gnod=(void*)b;
        gcol++;
}

int ind(int nod, int val)
{
int nos;
nos=2*(nod%2)-1;
if(val==1)
        {
        return((-1)*nos);
        }
if(val==2)
        {
        return(nos);
        }
if(val>2)
        {
        return((val-1)*nos);
        }
}

int rdd(spm* a, spm* b)
        {
        if((*a).row>(*b).row)
                {
                return(1);
                }
        if((*a).row<(*b).row)
                {
                return(0);
                }
        if((*a).col>(*b).col)
                {
                return(1);
                }
        if((*a).col<(*b).col)
                {
                return(0);
                }
        return(0); // resultativity conition
}

int sparprint(spm* root, int row, int col)
{
        if((*root).row==row&&(*root).col==col)
                {
                return((*root).indx);
                }
        if((*root).indx!=0)
        {
        if((*root).row>row)
                {
                return(sparprint((*root).left,row,col));
                }
        if((*root).row<row)
                {
                return(sparprint((*root).right,row,col));
                }
        if((*root).col>col)
                {
                return(sparprint((*root).left,row,col));
                }
        if((*root).col<col)
                {
                return(sparprint((*root).right,row,col));
                }
        }
        else
        {
        return(0);
        }
}

void spt(spm* root,int mmax)
        {
        int i,j;
        printf("\n");
        for(i=0;i<mmax;i++)
                {
                for(j=0;j<mmax;j++)
                        {
                        printf(" %i",sparprint(root,i,j));
                        }
                printf("\n");
                }
}

void sds(spm* root)   // destructor
{
if((*root).indx!=0)
        {
        sds((*root).right);
        sds((*root).left);
        }
spfree(root);
}

spm* smk(int row, int col, int indx) // structure make
{
```

7 Appendix B: Circuit determinant computation code

```
spm* nod;
nod=spmalloc();
(*nod).row=row;
(*nod).col=col;
(*nod).indx=indx;
(*nod).left=spmalloc();
(*nod).right=spmalloc();
(*((*nod).right)).indx=0;
(*((*nod).left)).indx=0;
return(nod);
}

spm* sdc(spm* infile)   // copy
{
spm* outfile;
outfile = smk(0,0,((*infile).indx));
if((*infile).indx!=0)
        {
        (*outfile).row=(*infile).row;
        (*outfile).col=(*infile).col;
        (*outfile).right=sdc((*infile).right);
        (*outfile).left=sdc((*infile).left);
        }
return(outfile);
}

void ldd(spm* root, spm* onenod) // one member add
        {
        if((*root).indx==0)
                {
                (*root).left=smk(0,0,0); // structure make
                (*root).right=smk(0,0,0);
                (*root).indx=(*onenod).indx;
                (*root).row=(*onenod).row;
                (*root).col=(*onenod).col;
                }
                else
                {
                if(rdd(root,onenod))
                        {
                        ldd((*root).left,onenod);
                        }
                        else
                        {
                        ldd((*root).right,onenod);
                        }
                }
}

// one member add with condition
void mdd(spm* root, spm* onenod, int row, int col)
        {
        if((*root).indx==0)
                {
                (*root).left=smk(0,0,0); // structure make
                (*root).right=smk(0,0,0);
                (*root).indx=(*onenod).indx;
                (*root).row=((*onenod).row>row) ?
((*onenod).row)-1:((*onenod).row) ;
                (*root).col=((*onenod).col>col) ?
((*onenod).col)-1:((*onenod).col) ;
                }
                else
                {
                if(rdd(root,onenod))
                        {
                        ldd((*root).left,onenod);
                        }
                        else
                        {
                        ldd((*root).right,onenod);
                        }
                }
}

// add two arbitrary structures together
void kdd(spm* root, spm* anex)
{
if((*anex).indx==0)
        {
        ;
        }
        else
        {
        ldd(root,anex);
        kdd(root,(*anex).right);
        kdd(root,(*anex).left);
        }
}

// add element to structure
void sad(spm* root,int row, int col, int indx)
{
kdd(root,smk(row,col,indx));
}

// removes and returns the last element of tree
spm* gle(spm* root)
{
if(((*root).indx!=0)&&((*((*root).right)).indx==0))
        {
        spm* tmp;
        spm* rest;
        tmp=sdc(root);   // copy
        sds((*root).right);
        rest = (*root).left; // left annex of last
        (*root).indx=(*((*root).left)).indx;
        if((*root).indx!=0)
                {
                (*root).row=(*rest).row;
                (*root).col=(*rest).col;
                (*root).right=(*rest).right;
                (*root).left=(*rest).left;
                }
        return(tmp);
        }
        else if(((*root).indx!=0)&&
((*((*root).right)).indx!=0))
        {
        return(gle(((*root).right)));
        }
        else
        {
        return(smk(0,0,0));
        }
}

// get minor - analogic to copy
spm* gmn(spm* infile, int row, int col)
{
spm* out1;
out1 = smk(0,0,0); // structure make
if(((*infile).row!=row)&&((*infile).col!=col))
        {
        if((*infile).indx!=0)
                {
                mdd(out1,infile,row,col);
                kdd(out1,gmn((*infile).left,row,col));
                kdd(out1,gmn((*infile).right,row,col));
                }
        }
        else
        {
        if((*infile).indx!=0)
                {
                kdd(out1,gmn((*infile).left,row,col));
                kdd(out1,gmn((*infile).right,row,col));
                }
        }
return(out1);
}

// add value to output tree
spm* adv(spm* lastnod, int value)
        {
        spm* tmp;
        tmp=spmalloc();
        (*tmp).indx = value;
        (*tmp).left = lastnod;
        return(tmp);
}

// trace output tree
void ttr(spm* lastnod, int sgn)
{
if((*lastnod).indx!=0)
        {
        if((*lastnod).indx==-1) ttr((*lastnod).left,-sgn);
        if((*lastnod).indx==1) ttr((*lastnod).left,sgn);
        if((*lastnod).indx<-1)
         {
         fprintf(output,"z%i*",(-1)*((*lastnod).indx)-1);
         ttr((*lastnod).left,-sgn);
         }
        if((*lastnod).indx>1)
         {
         fprintf(output,"z%i*",(*lastnod).indx-1);
         ttr((*lastnod).left,sgn);
         }
        }
        else
         {
         fprintf(output,"(%i)+",sgn);
         }
}

spm* dnd(spm* lastnod)
        {
```

```
        spm* tmp;
        tmp = (*lastnod).left;                          //
        spfree(lastnod);
        return(tmp);
}
// det. comp.
void dct(spm* infile, spm* lastnod, spm* lastinf, int nmax)
{
spm* a;
spm* b;
spm* c;
spm* d;
spm* e;
spm* f;
a = infile;
//spt(lastinf,nmax);
b = gle(lastinf);    // This element will be operated.
//printf(" -%i-, %i, %i ",(*b).indx,(*b).row,(*b).col);
//fprintf(output," -%i- ",(*b).indx);
//ttr(lastnod,1);
if((*b).row==nmax-1) // matrix have some valid element
        {
        if((*b).row==0)
                {
                if((*b).row==0&&(*b).col==0&&
(nmax-1)==0&&(*b).indx>0)
                        {
                        d=adv(lastnod,ind((*b).col,(*b).indx));
// zero det
//printf("trace %i %i ",(*b).row,(*b).col);
                        ttr(d,1); // trace output tree
                        }
                        else
                        {
// zero det
//printf("bad reminder %i %i ",(*b).row,(*b).col);
                        }
                }
                else
                {
                e=adv(lastnod,ind((*b).col,(*b).indx));
                c=gmn(a,(*b).row,(*b).col); //get minor
                f = sdc(c);
                dct(c,e,f,nmax-1); // computes minors determinant
                sds(c);
                sds(f);
                //blb;
                d = sdc(lastinf);
                b = gle(lastinf);
                if((*b).row==nmax-1)
                        {
//e=adv(lastnod,ind((*b).col,(*b).indx));
                        dct(a,lastnod,d,nmax); // computes rest
                        sds(b);
                        sds(d);
                        }
                }
        }

}

main(int argv,char**argc)
        {
        spm* root; // root of structure
        spm* rt;
        spm* rd;
        int i,j,k,l,a,b,c,d;
// nullators, norators, regulars, totals
        int nul, nor, reg, tot;
// maximal number of nodes, dimension of matrix
        int nmax, mmax;
        FILE * inf;
        printf(" %i \n",argv);
        if(argv<2)
        {
        printf("Extened sparse tableau analysis\n");
        printf("usage sta.exe infile\n");
        printf("input file struct: node node number\n");
        printf("\n");
        printf("when number is positive number,
symbol is regular imittance with that number\n");
        printf("nodes goes from 0 to NMAX, all node
No within interval must be used\n");
        printf("when number is 0, symbol is nullator\n");
        printf("when number is -8, symbol is norator\n");
        printf("outfile is symbolic formulla\n");
        printf("optimalised malloc\n");
        printf("output var: res\n");
        printf("After Braun, Vlach &t al. \n");
        printf("(c) Michal Vlk \n");
        printf("v. 1.0.2 14.01.2010\n");
        return(-1);
        }
        nul=0;nor=0;reg=0;nmax=0;
inf = fopen(argc[1],"rt");
outfile = fopen(argc[2],"wt");
output = fopen("output.txt","wt");
while(!feof(inf))
        {
        fscanf(inf,"%i",&a);
        fscanf(inf,"%i",&b);
        d=fscanf(inf,"%i",&c);
        if(d&&(!feof(inf)))
                {
                if(c==0){nul++;}
                if(c==-8){nor++;}
                if(c>0){reg++;}
                if(a>nmax){nmax=a;}
                if(b>nmax){nmax=b;}
        }
}
mmax=(nul+nor+reg)*2+nmax; // order of matrix
if(nul!=nor)
        {
        printf("no nullor pair");
        exit;
}
rewind(inf);
root=smk(0,0,0);
for(i=0,j=reg+2*(nul+nor)+nmax;i<reg;i++,j++)
        {
        // partial tree ballancing
        // giving -1 to place of lower unity matrix
        sad(root,j,i,1);
        // giving +1 to place of upper unity matrix
        sad(root,i,i,2);
        }

for(;i<(reg+nul+nor);i++)
        {
        //giving +1 to rest of upper unity matrix
        sad(root,i,i,2);
        }
for(i=reg,j=reg+nul+nor+nmax,k=0;k<nul;i++,j++,k++)
        {
        //givin +1 to I place of nullator
        sad(root,j,i,2);
        }
for(i=2*reg+nul+nor,j=reg+nul+nor+nmax+nor,k=0;k<nul;
                                        i++,j++,k++)
        {
        //givin +1 to U place of nullator
        sad(root,j,i,2);
        }
i=reg+nul+nor;j=reg+2*(nul+nor)+nmax;
while(!feof(inf))
        {
        fscanf(inf,"%i",&a);
        fscanf(inf,"%i",&b);
        d=fscanf(inf,"%i",&c);
        // impedance input
        if(d){if(c>0){sad(root,j,i,(2+c));j++;i++;}}
        }
rewind(inf);
i=2*(reg+nul+nor);j=0;k=reg+nor+nul;l=reg+nor+nul;
while(!feof(inf))
        {
        fscanf(inf,"%i",&a);
        fscanf(inf,"%i",&b);
        d=fscanf(inf,"%i",&c);
        if(d){if(c>0){
        if(a<b){c=a;a=b;b=c;}
                if(b==0)
                        {
                        sad(root,j,(i+a-1),1);
                        sad(root,(k+a-1),l,2);
                        }
                        else
                        {
                        sad(root,j,(i+a-1),1);
                        sad(root,(k+a-1),l,2);
                        sad(root,j,(i+b-1),2);
                        sad(root,(k+b-1),l,1);
                        }
        j++;l++;
        }}}   // regulars
        rewind(inf);

        while(!feof(inf))
        {
        fscanf(inf,"%i",&a);
        fscanf(inf,"%i",&b);
        d=fscanf(inf,"%i",&c);
        if(d){if(c==0){
        if(a<b){c=a;a=b;b=c;}
                if(b==0)
                        {
                        sad(root,j,(i+a-1),1);
```

```
                        sad(root,(k+a-1),1,2);
                        }
                        else
                        {
                        sad(root,j,(i+a-1),1);
                        sad(root,(k+a-1),1,2);
                        sad(root,j,(i+b-1),2);
                        sad(root,(k+b-1),1,1);
                        }
                j++;l++;
                }}}     // nullators
        rewind(inf);
                while(!feof(inf))
                {
                fscanf(inf,"%i",&a);
                fscanf(inf,"%i",&b);
                d=fscanf(inf,"%i",&c);
                if(d){if(c==-8){
                if(a<b){c=a;a=b;b=c;}
                        if(b==0)
                        {
                        sad(root,j,(i+a-1),1);
                        sad(root,(k+a-1),1,2);
                        }
                                        else
                                        {
                                        sad(root,j,(i+a-1),1);
                                        sad(root,(k+a-1),1,2);
                                        sad(root,j,(i+b-1),2);
                                        sad(root,(k+b-1),1,1);
                                        }
                                j++;l++;
                                }}}     // norators
                        rewind(inf);

        printf("\n.........................\n");
        spt(root,mmax);
        // computes determinant
        dct(root,smk(0,0,0),sdc(root),mmax);
        fprintf(output,"0"); // end of enum
        printf("\n recycle nodes: %i",gcol);
        //rt=gmn(root,mmax-1,0); //get minor
        //pmn(root,sdc(root),mmax);
        //spt(rt,mmax-1);
        close(output);
        return(0);
        }
```

8 Appendix C: Acquisition system code

```
/*
 * New Canmos main aquisition file
 * (c) vlk@ig.cas.cz\
 * 15.7.2012\
 */
#include <stdio.h>
#include <math.h>
#include <portaudio.h>
#include <conio.h>
#include <time.h>
#include <sys/time.h>
#include <string.h>
#define SAMPLE_RATE         (96000)
#define PA_SAMPLE_TYPE      paInt16
#define FRAMES_PER_BUFFER   (32768)
#define NUM_CHANNELS (2)
typedef float SAMPLE;
short int bufer[110];
double flta[]={0.0, 0.0, 0.0, 0.0, 0.0, 0.0, 0.0,
0.0, 0.0, 0.0, 0.0, 0.0, 0.0, 0.0, 0.0, 0.0, 0.0,
0.0, 0.0, 0.0, 0.0, 0.0, 0.0, 0.0, 0.0, 0.0, 0.0,
0.0, 0.0, 0.0};
double fltb[]={0.0, 0.0, 0.0, 0.0, 0.0, 0.0, 0.0,
0.0, 0.0, 0.0, 0.0, 0.0, 0.0, 0.0, 0.0, 0.0, 0.0,
0.0, 0.0, 0.0, 0.0, 0.0, 0.0, 0.0, 0.0, 0.0, 0.0,
0.0, 0.0, 0.0};

/* Structure init  */
void smpli(double* share)
{
int i;
for(i=0;i<4;i++){
((int*)((void*)(&(share[i])))[0]=0;}
for(i=4;i<1024;i++){
share[i]=0.0;}
}

/* Polyphase decimator   */
inline double dec(double* st, double in){
st[3]=st[7];
st[7]=st[2];
st[2]=st[1]-0.85*(st[1]+st[3]);
st[5]=st[8];
st[8]=st[4];
st[4]=in-0.4*(st[5]+in);
st[6]=st[3]+0.85*(st[3]+st[1])+st[5]+0.4*(st[5]+in);
st[1]=in;
return(st[6]);}

/* Videofilter   */
inline double vdflt(double* xv, double in){
xv[0] = xv[1]; xv[1] = xv[2]; xv[2] = xv[3];
xv[3] = xv[4]; xv[4] = in / 3.733668216e+05;
xv[10] = xv[11]; xv[11] = xv[12];
xv[12] = xv[13]; xv[13] = xv[14];  xv[14] =
(xv[0] + xv[4]) + 4.0 * (xv[1] + xv[3]) + 6.0 * xv[2]
+ ( -0.8821677565 * xv[10]) + (  3.6293675000 * xv[11])
+ ( -5.6111685256 * xv[12]) + (  3.8639259288 * xv[13]);
return(xv[14]);}

/* input filter */
inline double iir(double* yv,double in){
yv[7] = yv[8]; yv[8] = yv[9]; yv[9] = yv[10];
yv[10] = yv[11]; yv[11] = yv[12]; yv[12] = yv[13];
yv[13] = in/3.043185715e+04;
yv[0] = yv[1]; yv[1] = yv[2]; yv[2] = yv[3];
yv[3] = yv[4]; yv[4] = yv[5]; yv[5] = yv[6];
yv[6] =   (yv[13] - yv[7]) + 3 * (yv[9] - yv[11])
+ ( -0.8772852502 * yv[0]) + ( -2.9897505069 * yv[1])
+ ( -6.1437972631 * yv[2]) + ( -7.5302698407 * yv[3])
+ ( -6.4178379677 * yv[4]) + ( -3.2624571165 * yv[5]);
return(yv[6]);}


/* Allpass of the first order Here par is parameter,
st[3] is internal status and in is input */
inline double alp(double* st, double in) {
st[1]=(st[2]-in)*(-0.30)+st[0];
st[2]=st[1]; st[0]=in; return(st[1]);}

/* Filter returns -1 when out is not */
inline double smpf(double* share, double in){
double a,b,c,d; // intermediate results
int i; // phase of decimator
i=((int*)((void*)(&(share[0])))[0];//phase of dec
((int*)((void*)(&(share[0])))[0]=(i+1)>1023 ? 0:(i+1);
b=iir((&(share[50])),in); // input bandpass
c=alp((&(share[100])),b); // Dome appr
d=sqrt(b*b+c*c);
a=dec((&(share[150])),d); // 1-st
if((i%2)==0){
    b=dec((&(share[200])),a);} // 2-nd
if((i%4)==0){\
    a=vdflt((&(share[300])),b); b=vdflt((&(share[350])),a);
    a=dec((&(share[250])),b);} // 3-rd
if((i%8)==0){
    b=dec((&(share[400])),a);} // 4-th
if((i%16)==0){
    a=dec((&(share[450])),b);} // 5-th
if((i%32)==0){
    b=dec((&(share[500])),a);} // 6-th
if((i%64)==0){
    a=dec((&(share[550])),b);} // 7-th
if((i%128)==0){
    b=dec((&(share[600])),a);} // 8-th
if((i%256)==0){
    a=dec((&(share[650])),b);} // 9-th
if((i%512)==0){ // 187.5 Hz: for off-line flt
return(a);} return(-1.0);}

/* This routine will be called by the PortAudio
engine when audio is needed. It may be called
at interrupt level on some machines so don't
do anything that could mess up the system like
calling malloc() or free().
*/
```

```
static int fuzzCallback(
const void *inputBuffer, void *outputBuffer,
          unsigned long framesPerBuffer,
          const PaStreamCallbackTimeInfo* timeInfo,
          PaStreamCallbackFlags statusFlags,
          void *userData ){
(void*)outputBuffer;
(void*) inputBuffer; /* Prevent unused variable warnings.
SAMPLE *in = (SAMPLE*)inputBuffer;
(void) timeInfo; /* Prevent unused variable warnings. */
(void) statusFlags;
(void) userData;
(((void**) (&(bufer[16])) ) )[0]=inputBuffer; // Data
bufer[10]=1;   // semaphore
if(bufer[30]==1) \{
   struct timeval tv;
   gettimeofday(&tv, NULL);
   ((float*)((void*)(&(bufer[40])))[0]=
-1.0*((float)(tv.tv_sec % 3600 +
(tv.tv_usec+1)/1000000.0));
   bufer[30]=2;}
return paContinue;}

/*********************************************/

int main(void){
PaStreamParameters inputParameters, outputParameters;
PaStream *stream;
PaError err;
SAMPLE* aa;
int j, k, l, m;
char ac=' ';
time_t now, shifted, start;
struct tm ts;
struct tm tu;
struct timeval tv;
FILE* f1;
FILE* f2;
char fil1[200];
char fil2[200];
char filebuf[200];
char* filebuff;
char vocasout[]="C:\\\\data\\\\";
int nex; //next inspection in 100 msec
int i;
double fa[1024];
double fb[1024];
double corr = 0.5;
short int cp[70000];
float ff[1800];
float fta,ftb;
double a,b,c;
err = Pa_Initialize();
if( err != paNoError ) goto error;
inputParameters.device = Pa_GetDefaultInputDevice();
if (inputParameters.device == paNoDevice){
    fprintf(stderr,"Error: No default input device.\\n");
    goto error;}
inputParameters.channelCount = 2;    /* stereo input */
inputParameters.sampleFormat = PA_SAMPLE_TYPE;
inputParameters.suggestedLatency = Pa_GetDeviceInfo(
inputParameters.device )->defaultHighInputLatency;
inputParameters.hostApiSpecificStreamInfo = NULL;
err = Pa_OpenStream(&stream,&inputParameters,NULL,
SAMPLE_RATE,FRAMES_PER_BUFFER, 0, /* paClipOff, */
,fuzzCallback,NULL ); if( err != paNoError ) goto error;
time(&now); ts=*gmtime(&now); strcpy(filebuf,vocasout);
filebuff=&(filebuf[strlen(filebuf)]);
strftime(filebuff,sizeof(filebuf),
"%Y%m\\\\%Y%m%d%H.dat",&ts);
f1=fopen(filebuf,"ab"); gettimeofday(&tv, NULL);ftb=
-1.0*((float)(tv.tv_sec%3600 +
(tv.tv_usec+1)/1000000.0));
printf("_time: %f corr: %f\\n",ftb, ((float)corr));
fta=ftb; nex=(int)(-1000.0*corr*(ftb));
bufer[10]=0; bufer[5]=0; // Semaphore
smpli(fa); smpli(fb);  // Decimators init
bufer[30]=0;
err = Pa_StartStream( stream );
if( err != paNoError ) goto error;
printf("Hit 'a' to stop program.\\n");
fflush(stdout);
for(;ac!='a';){
    if(bufer[10]==1){
        memcpy(((void*)cp),
( (((void**) (&(bufer[16])) ) )[0]),(4*32768));
        bufer[10]=0;
        for(i=0, j=0;i<32768;i++){
        a=smpf(fa,((double)(cp[2*i]+cp[2*i+1])));
        if(a>0.0)\{ff[j]=a;j++;} }
    bufer[5]=1;
    if(bufer[30]==2){bufer[30]=3;}
    }
    else if(bufer[5]==1){
    bufer[5]=0; printf("%f  %f   %i\\n",ff[0],corr,nex);
    fwrite((void*)ff,sizeof(float),(j),f1);} //2*32768/512
    else if(bufer[30]==3){
    bufer[30]=0; fta = ftb;
    ftb = (((float*)((void*)(&(bufer[40]))))[0]);
    if(ftb<-1800.0) ftb+=3600.0;
    corr *= (3600.0+fta)/(3600.0+(fta-ftb)); // real/mach time
    nex=(int)(-1000.0*corr*(ftb)); // phase +1/2h in float
    printf("_time: %f corr: %f\\n",ftb,((float)corr));
    fwrite( (((void*)(&(bufer[40])))) ,sizeof(float),1,f1);
    fclose(f1); time(&now); ts=*gmtime(&now);
    now+=1800; tu=*gmtime(&now); strcpy(filebuf,vocasout);
    filebuff=&(filebuf[strlen(filebuf)]);
    strftime(filebuff,sizeof(filebuf),
"%Y%m\\\\%Y%m%d%H.dat",&tu);
    f1=fopen(filebuf,"ab");}
    else{
    Pa_Sleep(50); nex+=50;
    if(((float)nex)>(3600.0*1000.0*corr)){
       nex=0; bufer[30]=1;}
    if(kbhit()){ac=getche();}}
}
fclose(f1); err = Pa_CloseStream( stream );
if( err != paNoError ) goto error;
printf("Finished." );
Pa_Terminate();
return(0);
error: Pa_Terminate();
fprintf( stderr, "An error occured while
using the portaudio stream\\n" );
fprintf( stderr, "Error number: %d\\n", err );
fprintf( stderr, "Error message: %s\\n",
Pa_GetErrorText( err ) );
return(-1); }
```

9 Code D: Postprocessing system code

```
/* ********************************
*       Extract files from list of
*       hourly files & computes second IAGA files
*       from AMOS channell datas
*       Must be computed after 01 clock next day
*       29.10.2012
*       (c) vlk@ig.cas.cz, rev. 2.0 20.1.2013
********************************** */
#include <stdio.h>
#include <math.h>
#include <string.h>
#include <time.h>

//decimator
inline double dec(double* st, double in)
{
st[3]=st[7];
st[7]=st[2];
st[2]=st[1]-0.85*(st[1]+st[3]);
st[5]=st[8];
st[8]=st[4];
st[4]=in-0.4*(st[5]+in);
st[6]=st[3]+0.85*(st[3]+st[1])+st[5]+0.4*(st[5]+in);
st[1]=in;
return(st[6]);
}

// init of decimator structure
void smpli(double* share)
{
int i;
for(i=0;i<4;i++){
((int*)((void*)(&(share[i]))))[0]=0;}
for(i=4;i<1024;i++){share[i]=0.0;}}

inline double smpl(double* share, double in)
```

```
{
double a,b,c,d; // intermediate results
int i; // phase of decimator
i=((int*)((void*)(&(share[0])))[0];
((int*)((void*)(&(share[0])))[0]=((i+1)>1023)?0:(i+1);
a=dec((&(share[50])),in); // 10-th
if((i%2)==0){
b=dec((&(share[100])),a);} // 11-th
if((i%4)==0){
a=dec((&(share[150])),b);} // 12-th
if((i%8)==0){
b=dec((&(share[200])),a);} // 13-th
if((i%16)==0){return(b);}
return(-1.0);}

//five second to minute intermagnet filter
double fivesecflt[]={ 0.12578865, 0.11972085,
0.10321785, 0.08061140, 0.05702885, 0.03654680,
0.02121585, 0.01115655, 0.00531440, 0.00229315};

// one value of filter - len is half-length
inline double knev(double* infeld,double* coefs,
int len){ int i,j,k,l;
double a[len];
  {
  a[0]=infeld[0]*coefs[0]; for(i=1,j=-1;i<len;i++,j--)
a[i]=(infeld[j]+infeld[i])*coefs[i];
  for(i=1;i<len;i<<=1) for(j=0;j<(len-i);j+=i<<1)
a[j]+=a[j+i]; return(a[0]);
  }
}

// Plesiochronous interpolation
double interp(double* a, double where){
int i,j,k,l,m;
double bb=0.907; // filter roll-of
int wh;
double instp;
double whd;
int N = 128; // Length of filter
double c[128];
wh = (int)where; // integer part
whd = where - (double)wh; // fractional part
wh -=N/2; // start of the filter
instp = whd;
for(i=0;i<N;i++){
  if((i+instp)!=((double)(N/2))){
  c[i]=a[wh+i]*(0.42-0.5*cos(2.0*PI*(i+instp)/N)+0.08*
cos(4.0*PI*(i+instp)/N))*sin(PI*bb*(i-N/2+instp))
/(PI*(i-N/2+instp));}   else {
  c[i]=a[wh+i]*(0.42-0.5*cos(2.0*PI*(i+instp)/N)+0.08*
cos(4.0*PI*(i+instp)/N))*bb;}} //next - RDX2sum
for(l=1;l<N;l<<=1) for(m=0;m<(N-l);m+=l<<1) c[m]+=c[m+l];
 return(c[0]);
}

// Header of YAGA2002
void baba(FILE* outf)
{
fprintf(outf,"%s\n"," Format                  IAGA-2002
                          |\0");
fprintf(outf,"%s\n"," Source of Data  NAROD core CZE00001,
proprietar electronics     |\0");
fprintf(outf,"%s\n"," Station Name             Budkov
                          |\0");
fprintf(outf,"%s\n"," Geodetic Latitude        49.072
                          |\0");
fprintf(outf,"%s\n"," Geodetic Longitude       14.019
                          |\0");
fprintf(outf,"%s\n"," Elevation                496
                          |\0");
fprintf(outf,"%s\n"," Reported
                          |\0");
fprintf(outf,"%s\n"," Sensor orientation       DIF
                          |\0");
fprintf(outf,"%s\n"," Digital Sampling         1 Hz
                          |\0");
fprintf(outf,"%s\n"," Data Interval Type       1-second
                          |\0");
fprintf(outf,"%s\n"," Data type                variation
                          |\0");
fprintf(outf,"%s\n","DATE       TIME      DOY    BDVF      BD
VT      BDVE     BDVI      |\0");
}

inline double hp() { return(20396.957);}

// Parametrised Gaussian filter
void gsn(int n, double a, double* fl)
{
int i;
double b,c,e,f;
e=((double)n);
f=3.141592653/((double)n);
for(i=0;i<n;i++)
        {
        c=(double)i;
fl[i]=exp(((c*c)/(-2*a)))*(1.0-
(0.35875-0.48829*cos(f*(e+c))+
0.14128*cos(2.0*f*(e+c))-
0.01168*cos(3.0*f*(e+c))));
}}

// RMS Line fit computation
rms(int i,double* x,double* y,double* a, double* b){
double xm,ym,sx,sxy;
double pom[i];
int j,k,l,m;
for(j=0;j<i;j++) pom[j]=x[j]/((double)i); // preprocessing
for(l=1;l<i;l<<=1) for(m=0;m<(i-l);m+=l<<1) pom[m]+=pom[m+l];
xm=pom[0]; // mean of x
for(j=0;j<i;j++) pom[j]=y[j]/((double)i); // preprocessing
for(l=1;l<i;l<<=1) for(m=0;m<(i-l);m+=l<<1)
pom[m]+=pom[m+l]; ym=pom[0]; // mean of y
for(j=0;j<i;j++) pom[j]=(x[j]-xm)*(x[j]-xm);
for(l=1;l<i;l<<=1) for(m=0;m<(i-l);m+=l<<1)
pom[m]+=pom[m+l]; sx=pom[0];
for(j=0;j<i;j++) pom[j]=(x[j]-xm)*(y[j]-ym);
for(l=1;l<i;l<<=1) for(m=0;m<(i-l);m+=l<<1)
pom[m]+=pom[m+l]; sxy=pom[0];
*b=sxy/sx;
*a=ym-(sxy/sx)*xm;}

int main(int argc, char** argv)
{
//double res1[(60*60*10)]; // second output datas
//double res2[(60*60*10)];
double *res1;
double *res2;
double *res3;
double *res4;
double *res5;


int i,j,k,l,m,n,o,p;

float g[4];
float h[2];
double a,b,c,d,e,f; // buffer variables
FILE *in;    // output variables
FILE *outf;
double fa[1024]; // filter termporalies
double fb[1024];
double fc[1024];
double fd[1024];

double gs[1024]; // Gaussian filter approx.

double amid[27];
int acnt[27];
double bmid[27];
int bcnt[27];
double rx[27];
double ry[27];
double rc[4]; // regression coefficients a1,b1,a2,b2
time_t tme, start, now;
struct tm ts;
// infile name parts.
char *inf[]={"                                                                                ",
"                                                                                ",
"                                                                               "} ;\
char anf[2000];
char actfn[800];
char actfm[800];
char actfo[800];
char dock[20];
char *vock;

char vocasin[]="\0";
char vocasout[]="\0";
char filout[800];
char filerow[500];
char datestamp[200];
char year[200];
a = atoi(argv[1]);
//return(0);
anf[1900]='\0';
time(&now);
now+=60*60*24*(a-1);
now/=(60*60*24);
now*=(60*60*24);
start = now;
//return(0);

for(i=0;i<3;i++,start+=60*60*24)
        {
```

```
        ts=*gmtime(&start);
        strftime(&(anf[200*i]),50,"%Y%m/%Y%m%d\0",&ts);
        }
start = now;
start+=60*60*24;
ts=*gmtime(&start);
strftime(&(anf[600]),50,"%Y/%Y%m%d\0",&ts);
sprintf(filout,"%s%s.txt",vocasin,&(anf[600]));

smpli(fa);
smpli(fb);
smpli(fc);
smpli(fd);

res1=malloc((60*60*28*40)*sizeof(double));
res2=malloc((60*60*28*40)*sizeof(double));
res3=malloc((60*60*28*40)*sizeof(double));
res4=malloc((60*60*28*40)*sizeof(double));
res5=malloc((60*60*28*40)*sizeof(double));

// day, file, sampleA, sampleB
for(i=0,l=0,o=0,p=0;i<3;i++)
        {
        if(i==0)
                {
                j=23;k=24;
                vock=&(anf[0]);
                }
        if(i==1)
                {
                j=0;k=24;
                vock=&(anf[200]);
                }
        if(i==2)
                {
                j=0;k=1;
                vock=&(anf[400]);
                }
        for(;j<k;j++,l++){
         m=sizeof(vocasin);
         dock[0]=48+j/10;
         dock[1]=48+j%10;
         dock[2]='\0';
         sprintf(actfn,"%sd/%s%s.dat",vocasin,vock,dock);
         sprintf(actfm,"%sf/%s%s.dat",vocasin,vock,dock);
         printf("%s %i\n",actfn,l);
         if((in=fopen(actfn,"rb"))==NULL) return(-1);
         n=0;
         for(m=0;m<4;m++) ((char*)((void*)g))[m]=getc(in);
          for(;g[0]>=0.0;n++)
            {
            for(m=0;m<4;m++) ((char*)((void*)h))[m]=getc(in);
            a=(double)(g[0]); b=(double)(h[0]);
            c=smpl(fa,a);d=smpl(fb,b);
            if(c>0.0){
             res1[o]=c; res2[o]=d;o++;}
            for(m=0;m<4;m++) ((char*)((void*)g))[m]=getc(in);
            }
          amid[l]=(double)(g[0]);acnt[l]=n;fclose(in);
          if((in=fopen(actfm,"rb"))==NULL) return(1);
          n=0;
          for(m=0;m<4;m++) ((char*)((void*)g))[m]=getc(in);
          for(;g[0]>0.0;n++)
            {
            for(m=0;m<4;m++) ((char*)((void*)h))[m]=getc(in);
            a=(double)(g[0]); b=(double)(h[0]);
            c=smpl(fc,a);d=smpl(fd,b);
            if(c>0.0) {
             res3[p]=c; res4[p]=d;p++;}
            for(m=0;m<4;m++) ((char*)((void*)g))[m]=
getc(in);}
           bmid[l]=(double)(g[0]); bcnt[l]=n;fclose(in);
           } // end of one day
        } // end of three days
// *****************PROCESSING********************
for(l=0;l<26;l++) ry[l]=(l>0)?(ry[l-1]+(double)acnt[l]):
((double)acnt[l]);
for(l=0;l<26;l++) rx[l]=(3600.0*((double)l))+
((amid[l]<-1500.0)?(-(amid[l]+3600.0)):(-amid[l]));
rms(26,rx,ry,(&(rc[0])),(&(rc[1]))); // regresion of d,e
for(l=0;l<26;l++) ry[l]=(l>0)?(ry[l-1]+(double)bcnt[l]):
((double)bcnt[l]);
for(l=0;l<26;l++) rx[l]=(3600.0*((double)l))+
((bmid[l]<-1500.0)?(-(bmid[l]+3600.0)):(-bmid[l]));
for(l=0;l<26;l++) printf("%f ",((float)rx[l]));
for(l=0;l<26;l++) printf("%f ",((float)ry[l]));
rms(26,rx,ry,(&(rc[2])),(&(rc[3]))); // regression of f
a=rc[1]/16.0/12.0; // step of d,i
b=rc[0]/16.0; // position of zero time in irr. smpl)
printf("%f %f\n",((float)a),((float)b));
for(i=0,b-=20*a;i<(12*60*60*25);i++,b+=a) res5[i]=
interp(res1,b);
for(i=0,j=20;i<(60*60*24);i++,j+=12) res1[i]=0.000004*
knev(&(res5[j]),fivesecflt,10);
b=rc[0]/16.0;
for(i=0,b-=1300*a;i<(12*60*60*25);i++,b+=a) res5[i]=
interp(res2,b);
for(i=0,j=20;i<(60*60*25);i++,j+=12) res2[i]=0.000004*
knev(&(res5[j]),fivesecflt,10); // Temperature filtering
gsn(1200,10000.0,gs); for(i=0,j=1201;i<(60*60*25);i++,j++)
res5[i]=knev(&(res2[j]),gs,1200);
for(i=0,j=1300-1201-20;i<(60*60*25);i++,j++) res2[i]=
0.1*res5[j];
a=rc[3]/16.0/12.0; // step of f
b=rc[2]/16.0; // position of f
printf("%f %f\n",((float)a),((float)b));
for(i=0,b-=20*a;i<(12*60*60*25);i++,b+=a) res5[i]=
interp(res3,b);
for(i=0,j=20;i<(60*60*24);i++,j+=12) res3[i]=
0.000004*knev(&(res5[j]),fivesecflt,10); b=rc[2]/16.0;
for(i=0,b-=20*a;i<(12*60*60*25);i++,b+=a) res5[i]=
interp(res4,b);
for(i=0,j=20;i<(60*60*24);i++,j+=12) res4[i]=
0.000004*knev(&(res5[j]),fivesecflt,10);
// ********** OUTPUT ROUTINE**********************
//
 strftime(datestamp,sizeof(datestamp),"%Y-%m-%d",&ts);
 strftime(year,sizeof(year),"%j",&ts);
 outf=fopen(filout,"wt");
 baba(outf);
 for(j=0;j<60*60*24;j++)
        {
        // clock
        datestamp[10]=' ';
        datestamp[11]=48+((j/60)/60)/10;
        datestamp[12]=48+((j/60)/60)%10;
        datestamp[13]=':';
        datestamp[14]=48+((j/60)%60)/10;
        datestamp[15]=48+((j/60)%60)%10;
        datestamp[16]=':';
        datestamp[17]=48+(j%60)/10;
        datestamp[18]=48+(j%60)%10;
        datestamp[19]='.';
        datestamp[20]='0';
        datestamp[21]='0';
        datestamp[22]='0';
        datestamp[23]=' ';
        sprintf(&(datestamp[24]),"%s",year);
        // Blank fill
        for(k=27;k<70;k++) datestamp[k]=' ';
        datestamp[k+1]='\0';
        // processing
        for(k=0;k<4;k++){
sprintf(filerow,"%5.3f\0",((k==0)?((float)res1[j]):
((k==1)?((float)res2[j]):((k==2)?((float)res3[j]):
((float)res4[j])))));
i=(k==0)?30:((k==1)?40:((k==2)?50:60));
sprintf(&(datestamp[i]),"%s",filerow);
        datestamp[(i+strlen(filerow))]=' ';}
datestamp[70]='\0';
fprintf(outf,"%s\n",datestamp);
 }
 fclose(outf);
 return(0);
}
```